



**Margarida Henriques Custódio**

BSc in Biochemistry

**Bioprivileged Fluorinated Ionic Liquids in  
the Purification of Proteins: Towards  
Enhanced Tunability of Aqueous Biphasic  
Systems**

Dissertation to obtain a Master's Degree in Biochemistry

**Supervisor:** Doutor João Miguel Mendes de Araújo,  
Investigador Auxiliar, Faculdade de Ciências e Tecnologia,  
Universidade NOVA de Lisboa

**Co-Supervisor:** Doutora Ana Belén Pereiro Estévez,  
Investigador Auxiliar, Faculdade de Ciências e Tecnologia,  
Universidade NOVA de Lisboa

**Juri Constitution:**

**Presidente:** Prof. Doutor José Ricardo Ramos Franco Tavares, Professor  
Associado com Agregação, Faculdade de Ciências e Tecnologia, Universidade  
Nova de Lisboa

**Arguente:** Prof. Doutora Teresa Sacadura Santos Silva, Professor Auxiliar,  
Faculdade de Ciências e Tecnologia, Universidade Nova de Lisboa

**Vogal:** Doutor João Miguel Mendes de Araújo, Investigador Auxiliar,  
Faculdade de Ciências e Tecnologia, Universidade NOVA de Lisboa



FACULDADE DE  
CIÊNCIAS E TECNOLOGIA  
UNIVERSIDADE NOVA DE LISBOA

April 2021





**Margarida Henriques Custódio**

BSc in Biochemistry

# **Bioprivileged Fluorinated Ionic Liquids in the Purification of Proteins: Towards Enhanced Tunability of Aqueous Biphasic Systems**

Dissertation to obtain a Master's Degree in Biochemistry

**Supervisor:** Doutor João Miguel Mendes de Araújo, Investigador Auxiliar, Faculdade de Ciências e Tecnologia, Universidade NOVA de Lisboa

**Co-Supervisor:** Doutora Ana Belén Pereiro Estévez, Investigadora Auxiliar, Faculdade de Ciências e Tecnologia, Universidade NOVA de Lisboa

**Juri Constitution:**

Presidente: Prof. Doutor José Ricardo Ramos Franco Tavares, Professor Associado com Agregação, Faculdade de Ciências e Tecnologia, Universidade Nova de Lisboa

Arguente(s): Prof. Doutora Teresa Sacadura Santos Silva, Professor Auxiliar, Faculdade de Ciências e Tecnologia, Universidade Nova de Lisboa

Vogal(ais): Doutor João Miguel Mendes de Araújo, Investigador Auxiliar, Faculdade de Ciências e Tecnologia, Universidade NOVA de Lisboa

**April 2021**

## **Bioprivileged Fluorinated Ionic Liquids in the Purification of Proteins: Towards Enhanced Tunability of Aqueous Biphasic Systems**

Copyright © Margarida Henriques Custódio, Faculdade de Ciências e Tecnologia, Universidade Nova de Lisboa.

A Faculdade de Ciências e Tecnologia e a Universidade Nova de Lisboa têm o direito, perpétuo e sem limites geográficos, de arquivar e publicar esta dissertação através de exemplares impressos reproduzidos em papel ou de forma digital, ou por qualquer outro meio conhecido ou que venha a ser inventado, e de a divulgar através de repositórios científicos e de admitir a sua cópia e distribuição com objetivos educacionais ou de investigação, não comerciais, desde que seja dado crédito ao autor e editor

## **Acknowledgements**

Em primeiro lugar, quero agradecer aos meus orientadores Doutor João Araújo e à Doutora Ana Pereiro, por me terem proporcionado esta oportunidade, além de toda a paciência, orientação e partilha de conhecimento ao longo de todo o trabalho.

Ao Doutor Nuno Basílio, pela disponibilidade de realização dos ensaios de Fluorescência no seu laboratório e partilha de conhecimento sobre a área.

Quero agradecer também aos meus colegas do laboratório de Fluidos Alternativos para a Química Verde, por todo o companheirismo e ajuda nos momentos mais complicados. Em particular, quero agradecer à Sara Carvalho, por todo o apoio, palavras amigas e partilha de conhecimento.

Aos meus amigos, em particular à Ana Luísa Oliveira, por todo o apoio incondicional, carinho, paciência e acima de tudo acreditar em mim. Sem ti, teria sido impossível. Agradeço também à Marta Furtado, que mesmo estando longe sempre me acompanhou com toda a paciência e compreensão.

Estou grata pela minha família pelo apoio e ouvirem os meus queixumes. Em particular, quero agradecer à Filipa e ao Pedro por todo o apoio e motivação constantes.

## **Funding**

The present work was supported by FCT/MCTES through the projects PTDC/QEQ-FTT/3289/2014, IF/00210/2014/CP1244/CT0003 and PTDC/EQU-EQU/29737/2017.



## Abstract

Proteins are high value biomolecules with application in several fields, therefore the study of novel extraction methods using more biocompatible techniques is in large extent. Aqueous Biphasic Systems are increasingly being studied for that purpose, due to presenting two aqueous phases, usually protein-friendly. Fluorinated Ionic Liquids (FILs) are an emerging category of Ionic Liquids due to their unique properties, namely self-aggregation behavior, and already showing protein benign behavior.

In this work, Lysozyme was used as model protein, and used to be partitioned by systems composed by IL and FIL, besides several salting-out agents, specifically inorganic salt, carbohydrates and a dihydrogen phosphate choline ( $[N_{1112OH}][H_2PO_4]$ ). These studies revealed favored partition to FIL-aqueous rich phase comparing with IL-rich phase. Lysozyme activity was tested for each component and after partition protocol, and maintained for most cases. Turbidimetry was used to infer the presence of some interactions between the protein and some systems elements; Tryptophan Intrinsic Fluorescence studies were carried to verify some conformation changes in the presence of IL, FIL and  $N_{1112OH}[H_2PO_4]$ . Then, nano-Differential Scanning Calorimetry (nano-DSC) was used to confer the maintenance of thermal stability of Lysozyme, and determination of melting temperature ( $T_m$ ). These studies have revealed the presence of some interaction between IL/FIL and protein, besides different conformational changes in Lysozyme provoked by these compounds compared to reference. Also, was observed a decrease on  $T_m$  with increasing IL and FIL concentration, however at partition conditions, FIL presented more  $T_m$  conservation than IL.

This work permitted a higher insight on FIL application in ABS for protein extraction, and revealed their promising assets for this end; however more studies relatively to Lysozyme structure and thermodynamic parameters in the presence of IL/FIL are needed.

**Keywords:** Aqueous Biphasic Systems, Fluorinated Ionic Liquids, Ionic Liquids, Lysozyme, Extraction Efficiency.





## Resumo

As proteínas são biomoléculas de elevado valor e aplicabilidade em diversas áreas, desta forma o estudo de novas formas para a sua extração usando metodologias mais biocompatíveis é cada vez mais aprofundado. Os Sistemas Aquosos Bifásicos são cada vez mais estudados para este efeito, por apresentarem duas fases aquosas, tornando-os sistemas de extração mais biocompatíveis. Os Líquidos Iônicos Fluorados (FIL) são uma categoria de Líquidos Iônicos (IL) emergente devido às suas características únicas, nomeadamente a sua capacidade de fazerem “self-aggregations” e demonstrarem propriedades compatíveis com as proteínas.

Neste trabalho, a Lisozima foi usada como modelo e usada para estudo da partição em sistemas aquosos bifásicos compostos por IL, para além de uma variedade de agentes de “salting-out”, especificamente sais inorgânicos, carboidratos e colina dihidrogenofostato ( $[N_{11120H}][H_2PO_4]$ ). Estes estudos revelaram uma partição maioritária para as fases ricas em FIL, em comparação com as fases ricas em IL. A atividade enzimática foi também testada para cada componente e após o procedimento de partição, e mantida para a maioria dos casos. Turbidimetria foi usada para aferir a presença de interações entre a proteína e alguns compostos usados na partição; Fluorescência Intrínseca do Triptofano foi usado para verificar algumas alterações conformacionais na presença de IL, FIL e  $[N_{11120H}][H_2PO_4]$ . Em seguida, nano-Calorimetria de Varredura Diferencial (nano-DSC) foi usada para conferir a manutenção da estabilidade térmica da Lisozima provocada por estes componentes e determinação da Temperatura de Fusão ( $T_m$ ). Estes estudos revelaram a presença de interações entre o IL/FIL e a proteína, para além de diferentes alterações na conformação provocados por estes compostos, comparando com a referência em água. Foi também verificada uma diminuição de  $T_m$  com o aumento da concentração de IL e FIL, contudo às condições de partição, o FIL apresentava maior conservação da  $T_m$ .

Este trabalho permitiu uma maior análise da aplicação de FILs em ABS para extração das proteínas, e revelou características únicas para este fim; contudo são necessários mais estudos relativamente à estrutura da Lisozima e aos parâmetros termodinâmicos na presença de IL e FIL.

**Palavras-Chave:** Sistemas Aquosos Bifásicos, Líquidos Iônicos Fluorados, Líquidos Iônicos, Lisozima, Eficiência de Extração.



# Table of Contents

1. Introduction.....	1
1.1. Protein Purification .....	1
1.2. Aqueous Biphasic Systems.....	3
1.3. Ionic Liquids .....	6
1.4. Fluorinated Ionic Liquids .....	8
1.5. Lysozyme .....	12
2. Materials and Methods .....	13
2.1. Reagents .....	13
2.2. Aqueous Biphasic System determination - Cloud Point Titration, Diagrams and Tie-Lines .....	15
2.3. Lysozyme Extraction.....	15
2.4. Phase Characterization .....	16
2.5. Solute Detection Procedures.....	17
BCA and $\mu$ BCA assays .....	17
Bradford Assay.....	17
UV-Vis.....	18
2.6. Extraction Efficiency.....	18
2.7. Lysozyme Activity .....	18
2.8. IL/FIL-Protein Interaction Studies .....	19
Turbidimetry .....	19
Fluorescence.....	19
Nano-DSC .....	20
3. Results and Discussion.....	21
3.1. Phase Diagrams .....	21
3.2. Phase Identification: NMR .....	25
3.3. Lysozyme Activity - Screening .....	28
3.4. Extraction Efficiency.....	29
3.5. Lysozyme Activity – Partitioned Lysozyme.....	35

3.6. IL/FIL-Protein Interaction Studies .....	39
Turbidimetry .....	39
Fluorescence.....	43
4. Conclusions.....	57
5. References .....	59
6. Appendix.....	63
6.1. Aqueous Biphasic Systems.....	63
6.2. NMR <sup>1</sup> H and <sup>17</sup> F Spectra .....	76
6.3. Phase Identification and pH.....	81
6.4. Lys Enzymatic Activity Screening .....	83
6.5. UV-VIS Calibration .....	89
6.6. Extraction Efficiency.....	91
6.7. Nano-DSC.....	94

## List of Figures

Figure 1. 1 Protein purification protocol complexity effects on the cost (C), purity (P) and yield (Y) of the overall process .....	2
Figure 1. 2 Orthogonal ternary phase diagram of a hypothetical system composed by compound 1 + compound 2 + water (concentration on weight percentage - wt%).....	3
Figure 1. 3 Salting-out mechanism representation of non-polar solutes. ....	4
Figure 1. 4 Representation of common cation cores in ILs. ....	6
Figure 1. 5 Ionic Liquids Application in several fields.....	6
Figure 1. 6 TEM images of [C <sub>2</sub> C <sub>1</sub> Im][C <sub>4</sub> F <sub>9</sub> SO <sub>3</sub> ] aggregates at FIL concentration in aqueous solution 2.5 times the first CAC (a, b) and 2 times the second CAC (c, d).....	9
Figure 3. 1 Phase diagrams for ternary systems composed of IL + K <sub>3</sub> PO <sub>4</sub> + H <sub>2</sub> O at 25°C: [C <sub>2</sub> C <sub>1</sub> Im]Cl; [C <sub>2</sub> C <sub>1</sub> Im]Cl from literature and [C <sub>4</sub> C <sub>1</sub> Im]Cl from literature.....	21
Figure 3. 2 Phase diagrams for ternary systems composed of IL + K <sub>3</sub> PO <sub>4</sub> + H <sub>2</sub> O at 25°C: [N <sub>11120H</sub> ][CF <sub>3</sub> SO <sub>3</sub> ]; .....	22
Figure 3. 3 Phase diagrams for ternary systems composed of IL + [N <sub>11120H</sub> ][H <sub>2</sub> PO <sub>4</sub> ] + H <sub>2</sub> O at 25°C: .....	22
Figure 3. 4 Phase diagrams for ternary systems composed of [C <sub>4</sub> C <sub>1</sub> Im][CF <sub>3</sub> SO <sub>3</sub> ], [C <sub>2</sub> C <sub>1</sub> Im][C <sub>4</sub> F <sub>9</sub> SO <sub>3</sub> ] and [C <sub>2</sub> C <sub>1</sub> Py][C <sub>4</sub> F <sub>9</sub> SO <sub>3</sub> ] + carbohydrate + H <sub>2</sub> O at 25°C: Sucrose (darker color); D-(+)-Glucose (lighter color).....	23
Figure 3. 5 <sup>19</sup> F NMR spectra of Top (up) and Bottom phase (down) of system 30% [C <sub>2</sub> C <sub>1</sub> Im][C <sub>4</sub> F <sub>9</sub> SO <sub>3</sub> ] + 20% [N <sub>11120H</sub> ][H <sub>2</sub> PO <sub>4</sub> ]; 30% [C <sub>2</sub> C <sub>1</sub> Im][C <sub>4</sub> F <sub>9</sub> SO <sub>3</sub> ] + 10% [N <sub>11120H</sub> ][H <sub>2</sub> PO <sub>4</sub> ] and 30% [C <sub>2</sub> C <sub>1</sub> Im][C <sub>4</sub> F <sub>9</sub> SO <sub>3</sub> ] + 6% [N <sub>11120H</sub> ][H <sub>2</sub> PO <sub>4</sub> ] (left to right) in D <sub>2</sub> O. ....	25
Figure 3. 6 <sup>1</sup> H NMR spectra of Top phase of systems 30% [C <sub>2</sub> C <sub>1</sub> Im][C <sub>4</sub> F <sub>9</sub> SO <sub>3</sub> ] + 20% [N <sub>11120H</sub> ][H <sub>2</sub> PO <sub>4</sub> ]; 30% [C <sub>2</sub> C <sub>1</sub> Im][C <sub>4</sub> F <sub>9</sub> SO <sub>3</sub> ] + 10% [N <sub>11120H</sub> ][H <sub>2</sub> PO <sub>4</sub> ] and 30% [C <sub>2</sub> C <sub>1</sub> Im][C <sub>4</sub> F <sub>9</sub> SO <sub>3</sub> ] + 6% [N <sub>11120H</sub> ][H <sub>2</sub> PO <sub>4</sub> ] in D <sub>2</sub> O superimposed.....	26
Figure 3. 7 <sup>1</sup> H NMR spectra of Bottom phase of systems 30% [C <sub>2</sub> C <sub>1</sub> Im][C <sub>4</sub> F <sub>9</sub> SO <sub>3</sub> ] + 20% [N <sub>11120H</sub> ][H <sub>2</sub> PO <sub>4</sub> ]; 30% [C <sub>2</sub> C <sub>1</sub> Im][C <sub>4</sub> F <sub>9</sub> SO <sub>3</sub> ] + 10% [N <sub>11120H</sub> ][H <sub>2</sub> PO <sub>4</sub> ] and 30% [C <sub>2</sub> C <sub>1</sub> Im][C <sub>4</sub> F <sub>9</sub> SO <sub>3</sub> ] + 6% [N <sub>11120H</sub> ][H <sub>2</sub> PO <sub>4</sub> ] in D <sub>2</sub> O superimposed.....	26
Figure 3. 8 Relative Lys Enzymatic Activity for 0.2 mg/mL Lys for 5% (w/w), 10% (w/w), 15% (w/w), 25% (w/w) and 35% (w/w) of [C <sub>2</sub> C <sub>1</sub> Im][CF <sub>3</sub> SO <sub>3</sub> ], [C <sub>2</sub> C <sub>1</sub> Im][C <sub>4</sub> F <sub>9</sub> SO <sub>3</sub> ] and Sucrose. ....	28
Figure 3. 9 Extraction Efficiencies of Lysozyme for each system containing K <sub>3</sub> PO <sub>4</sub> and respective extraction point at 25°C, and several detection methods. UV-Vis; BCA; μBCA; Coomassie ....	30

Figure 3. 10 Extraction Efficiencies of Lysozyme for each system of [C <sub>4</sub> C <sub>1</sub> Im][CF <sub>3</sub> SO <sub>3</sub> ] and [C <sub>2</sub> C <sub>1</sub> Im][C <sub>4</sub> F <sub>9</sub> SO <sub>3</sub> ] using Sucrose and Glucose as salting-out agent at 25°C, using several detection methods: UV-Vis; BCA; μBCA; .....	31
Figure 3. 11 Extraction Efficiencies of Lysozyme for each system containing [N <sub>11120H</sub> ][H <sub>2</sub> PO <sub>4</sub> ] and respective extraction point at 25°C, using several detection methods: UV-Vis; BCA; μBCA; Coomassie .....	32
Figure 3. 12 Extraction Efficiencies of Lysozyme for systems 30% wt [C <sub>2</sub> C <sub>1</sub> Im][C <sub>4</sub> F <sub>9</sub> SO <sub>3</sub> ] + 6, 10 and 20% wt [N <sub>11120H</sub> ][H <sub>2</sub> PO <sub>4</sub> ] and 30% [N <sub>11120H</sub> ][C <sub>4</sub> F <sub>9</sub> SO <sub>3</sub> ] + 30% [N <sub>11120H</sub> ][H <sub>2</sub> PO <sub>4</sub> ] at 25°C, and the several detection method: UV-Vis; BCA; μBCA; Coomassie .....	33
Figure 3. 13 Lysozyme relative enzymatic activity of 30% [C <sub>4</sub> C <sub>1</sub> Im][CF <sub>3</sub> SO <sub>3</sub> ] + 20% [N <sub>11120H</sub> ][H <sub>2</sub> PO <sub>4</sub> ] for each phase. ....	35
Figure 3. 14 Lysozyme relative enzymatic activity of 30% [C <sub>2</sub> C <sub>1</sub> Im][C <sub>4</sub> F <sub>9</sub> SO <sub>3</sub> ] + 6% [N <sub>11120H</sub> ][H <sub>2</sub> PO <sub>4</sub> ].....	35
Figure 3. 15 Lysozyme relative enzymatic activity of 30% [C <sub>2</sub> C <sub>1</sub> Im][C <sub>4</sub> F <sub>9</sub> SO <sub>3</sub> ]+25% Glucose. .	36
Figure 3. 16 Lysozyme relative enzymatic activity of 30% [C <sub>2</sub> C <sub>1</sub> Im][C <sub>4</sub> F <sub>9</sub> SO <sub>3</sub> ]+25% Sucrose ...	36
Figure 3. 17 Lysozyme relative enzymatic activity of 30% [C <sub>4</sub> C <sub>1</sub> Im][CF <sub>3</sub> SO <sub>3</sub> ]+25% Glucose....	37
Figure 3. 18 Lysozyme relative enzymatic activity of 30% [C <sub>4</sub> C <sub>1</sub> Im][CF <sub>3</sub> SO <sub>3</sub> ]+25% Sucrose. ....	37
Figure 3. 19 Lysozyme relative enzymatic activity of 30% [C <sub>2</sub> C <sub>1</sub> Im][C <sub>4</sub> F <sub>9</sub> SO <sub>3</sub> ]+2% K <sub>3</sub> PO <sub>4</sub> .....	38
Figure 3. 20 Turbidity of Lysozyme (0.2mg/mL) as a function of IL [C <sub>4</sub> C <sub>1</sub> Im][CF <sub>3</sub> SO <sub>3</sub> ] concentration at 25°C.....	40
Figure 3. 21 Turbidity of Lysozyme (0.2mg/mL) as a function of IL [C <sub>2</sub> C <sub>1</sub> Im][C <sub>4</sub> F <sub>9</sub> SO <sub>3</sub> ] concentration at 25°C.....	40
Figure 3. 22 UV-Vis absorption spectra of Lysozyme in the different concentrations of [C <sub>4</sub> C <sub>1</sub> Im][CF <sub>3</sub> SO <sub>3</sub> ] studied in this work (0-120mM).....	42
Figure 3. 23 UV-Vis absorption spectra of Lysozyme in the different concentrations of [C <sub>2</sub> C <sub>1</sub> Im][C <sub>4</sub> F <sub>9</sub> SO <sub>3</sub> ] studied in this work (0-120mM).....	42
Figure 3. 24 Lysozyme structure: a) completed; b) zoom at dominant fluorophores (Trp 62 and 108). Adapted from Balme et al. <sup>50</sup> .....	44
Figure 3. 25 Fluorescence spectra of Lysozyme acquired at 25°C for [C <sub>4</sub> C <sub>1</sub> Im][CF <sub>3</sub> SO <sub>3</sub> ] concentrations (0-800mM).....	44
Figure 3. 26 Emission intensity of Lysozyme at 0.2mg/mL recorded at each maxima wavelength for [C <sub>4</sub> C <sub>1</sub> Im][CF <sub>3</sub> SO <sub>3</sub> ].....	45
Figure 3. 27 Fluorescence spectra of Lysozyme acquired at 25°C for [C <sub>2</sub> C <sub>1</sub> Im][C <sub>4</sub> F <sub>9</sub> SO <sub>3</sub> ].....	46
Figure 3. 28 Emission intensity of Lysozyme at 0.2mg/mL recorded at each maxima wavelength for [C <sub>2</sub> C <sub>1</sub> Im][C <sub>4</sub> F <sub>9</sub> SO <sub>3</sub> ].....	46
Figure 3. 29 Fluorescence spectra of Lysozyme acquired at 25°C for [N <sub>11120H</sub> ][H <sub>2</sub> PO <sub>4</sub> ].....	47

Figure 3. 30 Emission intensity of Lysozyme at 0.2mg/mL recorded at 343nm for [N <sub>11120H</sub> ][H <sub>2</sub> PO <sub>4</sub> ].	48
Figure 3. 31 Stern-Volmer curves for fluorescence quenching of Lys in presence of [C <sub>2</sub> C <sub>1</sub> Im][C <sub>4</sub> F <sub>9</sub> SO <sub>3</sub> ].	49
Figure 3. 32 Stern-Volmer curves for fluorescence quenching of Lys in presence of [N <sub>11120H</sub> ][H <sub>2</sub> PO <sub>4</sub> ].	50
Figure 3. 33 Melting Temperature of Lysozyme in water and in presence of different concentration of [C <sub>4</sub> C <sub>1</sub> Im][CF <sub>3</sub> SO <sub>3</sub> ] and [C <sub>2</sub> C <sub>1</sub> Im][C <sub>4</sub> F <sub>9</sub> SO <sub>3</sub> ] (0.1-10mM).	51
Figure 3. 34 Melting Temperature of Lysozyme in water and in presence of [C <sub>4</sub> C <sub>1</sub> Im][CF <sub>3</sub> SO <sub>3</sub> ]-rich phase (30% IL+25% Glucose) and [C <sub>2</sub> C <sub>1</sub> Im][C <sub>4</sub> F <sub>9</sub> SO <sub>3</sub> ]-rich phase (30% FIL+25% Glucose) with stirring and without stirring.	52
Figure 3. 35 Melting Temperature of Lysozyme in water (1 and 3 mg/mL) and partitioned for [C <sub>4</sub> C <sub>1</sub> Im][CF <sub>3</sub> SO <sub>3</sub> ]-rich phase (30% IL+25% Glucose) and [C <sub>2</sub> C <sub>1</sub> Im][C <sub>4</sub> F <sub>9</sub> SO <sub>3</sub> ]-rich phase (30% FIL+25% Glucose). Glucose Sucrose.	53
Figure 6. 1 <sup>1</sup> H NMR spectra of Top (up) and Bottom (down) phase of system 30% [N <sub>11120H</sub> ]Cl + 20% K <sub>3</sub> PO <sub>4</sub> in D <sub>2</sub> O.	76
Figure 6. 2 <sup>1</sup> H NMR spectra of Top (up) and Bottom (down) phase of system 30% [N <sub>11120H</sub> ][C <sub>4</sub> F <sub>9</sub> SO <sub>3</sub> ] + 30% [N <sub>11120H</sub> ][H <sub>2</sub> PO <sub>4</sub> ] in D <sub>2</sub> O.	76
Figure 6. 3 <sup>19</sup> F NMR spectra of Top (up) and Bottom (down) phase of system 30% [N <sub>11120H</sub> ][C <sub>4</sub> F <sub>9</sub> SO <sub>3</sub> ] + 30% [N <sub>11120H</sub> ][H <sub>2</sub> PO <sub>4</sub> ] in D <sub>2</sub> O.	76
Figure 6. 4 <sup>1</sup> H NMR spectra of Top (up) and Bottom (down) phase of system 30% [C <sub>2</sub> C <sub>1</sub> Im][C <sub>4</sub> F <sub>9</sub> SO <sub>3</sub> ] + 25% Glucose in D <sub>2</sub> O.	77
Figure 6. 5 <sup>19</sup> F NMR spectra of Top (up) and Bottom (down) phase of system 30% [C <sub>2</sub> C <sub>1</sub> Im][C <sub>4</sub> F <sub>9</sub> SO <sub>3</sub> ] + 25% Glucose in D <sub>2</sub> O.	77
Figure 6. 6 <sup>1</sup> H NMR spectra of Top (up) and Bottom (down) phase of system 30% [C <sub>2</sub> C <sub>1</sub> Im][C <sub>4</sub> F <sub>9</sub> SO <sub>3</sub> ] + 25% Sucrose in D <sub>2</sub> O.	77
Figure 6. 7 <sup>19</sup> F NMR spectra of Top (up) and Bottom (down) phase of system 30% [C <sub>2</sub> C <sub>1</sub> Im][C <sub>4</sub> F <sub>9</sub> SO <sub>3</sub> ] + 25% Sucrose in D <sub>2</sub> O.	78
Figure 6. 8 <sup>1</sup> H NMR spectra of Top (up) and Bottom (down) phase of system 30% [C <sub>4</sub> C <sub>1</sub> Im][CF <sub>3</sub> SO <sub>3</sub> ] + 5% K <sub>3</sub> PO <sub>4</sub> in D <sub>2</sub> O.	78
Figure 6. 9 <sup>19</sup> F NMR spectra of Top (up) and Bottom (down) phase of system 30% [C <sub>4</sub> C <sub>1</sub> Im][CF <sub>3</sub> SO <sub>3</sub> ] + 5% K <sub>3</sub> PO <sub>4</sub> in D <sub>2</sub> O.	78
Figure 6. 10 <sup>1</sup> H NMR spectra of Top (up) and Bottom (down) phase of system 30% [C <sub>4</sub> C <sub>1</sub> Im][CF <sub>3</sub> SO <sub>3</sub> ] + 20% [N <sub>11120H</sub> ][H <sub>2</sub> PO <sub>4</sub> ] in D <sub>2</sub> O.	79
Figure 6. 11 <sup>19</sup> F NMR spectra of Top (up) and Bottom (down) phase of system 30% [C <sub>4</sub> C <sub>1</sub> Im][CF <sub>3</sub> SO <sub>3</sub> ] + 20% [N <sub>11120H</sub> ][H <sub>2</sub> PO <sub>4</sub> ] in D <sub>2</sub> O.	79

Figure 6. 12 <sup>1</sup> H NMR spectra of Top (up) and Bottom (down) phase of system 30% [C <sub>4</sub> C <sub>1</sub> Im][CF <sub>3</sub> SO <sub>3</sub> ] + 25% Glucose in D <sub>2</sub> O. ....	79
Figure 6. 13 <sup>19</sup> F NMR spectra of Top (up) and Bottom (down) phase of system 30% [C <sub>4</sub> C <sub>1</sub> Im][CF <sub>3</sub> SO <sub>3</sub> ] + 25% Glucose in D <sub>2</sub> O. ....	80
Figure 6. 14 <sup>1</sup> H NMR spectra of Top (up) and Bottom (down) phase of system 30% [C <sub>4</sub> C <sub>1</sub> Im][CF <sub>3</sub> SO <sub>3</sub> ] + 25% Sucrose in D <sub>2</sub> O. ....	80
Figure 6. 15 <sup>19</sup> F NMR spectra of Top (up) and Bottom (down) phase of system 30% [C <sub>4</sub> C <sub>1</sub> Im][CF <sub>3</sub> SO <sub>3</sub> ] + 25% Sucrose in D <sub>2</sub> O. ....	80
Figure 6. 16 Calibration curve for Lysozyme in water at 280 nm for 0.4mL Quartz cuvette. ....	89
Figure 6. 17 Calibration curve for Lysozyme in water at 280 nm for 4mL Quartz cuvette. ....	89
Figure 6. 18 Calibration curve for Lysozyme in 0.1% K <sub>3</sub> PO <sub>4</sub> at 280 nm for 0.4 mL Quartz cuvette. ....	90
Figure 6. 19 Calibration curve for Lysozyme in 0.1% K <sub>3</sub> PO <sub>4</sub> at 280nm for 4.0 mL Quartz cuvette. ....	90
Figure 6. 20 Thermogram of Lys 1mg/mL in water. ....	94
Figure 6. 21 Thermogram of Lys 1mg/mL in 0.1mM [C <sub>4</sub> C <sub>1</sub> Im][CF <sub>3</sub> SO <sub>3</sub> ]. ....	94
Figure 6. 22 Thermogram of Lys 1mg/mL in 1.0 mM [C <sub>4</sub> C <sub>1</sub> Im][CF <sub>3</sub> SO <sub>3</sub> ]. ....	94
Figure 6. 23 Thermogram of Lys 1mg/mL in 5.0 mM [C <sub>4</sub> C <sub>1</sub> Im][CF <sub>3</sub> SO <sub>3</sub> ]. ....	95
Figure 6. 24 Thermogram of Lys 1mg/mL in 10.0 mM [C <sub>4</sub> C <sub>1</sub> Im][CF <sub>3</sub> SO <sub>3</sub> ]. ....	95
Figure 6. 25 Thermogram of Lys 1mg/mL in 0.1 mM [C <sub>2</sub> C <sub>1</sub> Im][C <sub>4</sub> F <sub>9</sub> SO <sub>3</sub> ]. ....	95
Figure 6. 26 Thermogram of Lys 1mg/mL in 1.0 mM [C <sub>2</sub> C <sub>1</sub> Im][C <sub>4</sub> F <sub>9</sub> SO <sub>3</sub> ]. ....	96
Figure 6. 27 Thermogram of Lys 1mg/mL in 5.0 mM [C <sub>2</sub> C <sub>1</sub> Im][C <sub>4</sub> F <sub>9</sub> SO <sub>3</sub> ]. ....	96
Figure 6. 28 Thermogram of Lys 1mg/mL in 10.0 mM [C <sub>2</sub> C <sub>1</sub> Im][C <sub>4</sub> F <sub>9</sub> SO <sub>3</sub> ]. ....	96
Figure 6. 29 Thermogram of Lys 1mg/mL in [C <sub>4</sub> C <sub>1</sub> Im][CF <sub>3</sub> SO <sub>3</sub> ]-rich phase (30% [C <sub>4</sub> C <sub>1</sub> Im][CF <sub>3</sub> SO <sub>3</sub> ]+25% Glucose) – with stirring. ....	97
Figure 6. 30 Thermogram of Lys 1mg/mL in [C <sub>4</sub> C <sub>1</sub> Im][CF <sub>3</sub> SO <sub>3</sub> ]-rich phase (30% [C <sub>4</sub> C <sub>1</sub> Im][CF <sub>3</sub> SO <sub>3</sub> ]+25% Glucose) – without stirring. ....	97
Figure 6. 31 Thermogram of Lys 1mg/mL in [C <sub>2</sub> C <sub>1</sub> Im][C <sub>4</sub> F <sub>9</sub> SO <sub>3</sub> ]-rich phase (30% [C <sub>2</sub> C <sub>1</sub> Im][C <sub>4</sub> F <sub>9</sub> SO <sub>3</sub> ]+25% Glucose) – with stirring. ....	97
Figure 6. 32 Thermogram of Lys 1mg/mL in [C <sub>2</sub> C <sub>1</sub> Im][C <sub>4</sub> F <sub>9</sub> SO <sub>3</sub> ]-rich phase (30% [C <sub>2</sub> C <sub>1</sub> Im][C <sub>4</sub> F <sub>9</sub> SO <sub>3</sub> ]+25% Glucose) – without stirring. ....	98
Figure 6. 33 Thermogram of partitioned Lys in [C <sub>4</sub> C <sub>1</sub> Im][CF <sub>3</sub> SO <sub>3</sub> ]-rich phase (30% [C <sub>4</sub> C <sub>1</sub> Im][CF <sub>3</sub> SO <sub>3</sub> ]+25% Glucose) – without stirring. ....	98
Figure 6. 34 Thermogram of partitioned Lys in [C <sub>4</sub> C <sub>1</sub> Im][CF <sub>3</sub> SO <sub>3</sub> ]-rich phase (30% [C <sub>4</sub> C <sub>1</sub> Im][CF <sub>3</sub> SO <sub>3</sub> ]+25% Sucrose) – without stirring. ....	98
Figure 6. 35 Thermogram of Lys 3mg/mL in water. ....	99



Figure 6. 36 Thermogram of partitioned Lys in [C<sub>2</sub>C<sub>1</sub>Im][C<sub>4</sub>F<sub>9</sub>SO<sub>3</sub>]-rich phase (30% [C<sub>2</sub>C<sub>1</sub>Im][C<sub>4</sub>F<sub>9</sub>SO<sub>3</sub>]+25% Glucose) – without stirring.....99

Figure 6. 37 Thermogram of partitioned Lys in [C<sub>2</sub>C<sub>1</sub>Im][C<sub>4</sub>F<sub>9</sub>SO<sub>3</sub>]-rich phase (30% [C<sub>2</sub>C<sub>1</sub>Im][C<sub>4</sub>F<sub>9</sub>SO<sub>3</sub>]+25% Sucrose) – without stirring. ....99



## List of Tables

Table 2. 1 Designation and chemical structure of the compound used in this work. ....	13
Table 2. 2 Ionic Liquid/Fluorinated Ionic Liquid ABS and different Salting-Out Agents system composition used for Lysozyme partition experiments at 25°C.....	16
Table 3. 1 Critical aggregation concentrations (CACs) of [C <sub>2</sub> C <sub>1</sub> Im][C <sub>4</sub> F <sub>9</sub> SO <sub>3</sub> ] in aqueous solutions determined by Isothermal Calorimetry at 25°C. ....	39
Table 3. 2 Melting Temperature (T <sub>m</sub> ) of Lysozyme in water and in phase, either simulated (left) and partitioned (right).....	54
Table 6. 1 Experimental weight fraction data for [N <sub>11120H</sub> ]Cl + K <sub>3</sub> PO <sub>4</sub> and [C <sub>2</sub> C <sub>1</sub> Py]Br + K <sub>3</sub> PO <sub>4</sub> at 25°C.....	63
Table 6. 2 Experimental weight fraction data for [C <sub>2</sub> C <sub>1</sub> Im]Cl + K <sub>3</sub> PO <sub>4</sub> and [C <sub>2</sub> C <sub>1</sub> Im][C <sub>1</sub> CO <sub>2</sub> ] + K <sub>3</sub> PO <sub>4</sub> at 25°C. ....	64
Table 6. 3 Experimental weight fraction data for [C <sub>2</sub> C <sub>1</sub> Im][CF <sub>3</sub> SO <sub>3</sub> ] + K <sub>3</sub> PO <sub>4</sub> at 25°C.....	65
Table 6. 4 Experimental weight fraction data for [C <sub>4</sub> C <sub>1</sub> Im][CF <sub>3</sub> SO <sub>3</sub> ] + K <sub>3</sub> PO <sub>4</sub> and [C <sub>2</sub> C <sub>1</sub> im][C <sub>4</sub> F <sub>9</sub> SO <sub>3</sub> ] + K <sub>3</sub> PO <sub>4</sub> at 25°C.....	66
Table 6. 5 Experimental weight fraction data for [C <sub>2</sub> C <sub>1</sub> Py][C <sub>4</sub> F <sub>9</sub> SO <sub>3</sub> ] + K <sub>3</sub> PO <sub>4</sub> at 25°C. ....	67
Table 6. 6 Experimental weight fraction data for [N <sub>11120H</sub> ][C <sub>4</sub> F <sub>9</sub> SO <sub>3</sub> ] + [N <sub>11120H</sub> ][H <sub>2</sub> PO <sub>4</sub> ] and [C <sub>4</sub> C <sub>1</sub> Im][CF <sub>3</sub> SO <sub>3</sub> ] + [N <sub>11120H</sub> ][H <sub>2</sub> PO <sub>4</sub> ] at 25°C.....	68
Table 6. 7 Experimental weight fraction data for [C <sub>2</sub> C <sub>1</sub> Im][C <sub>4</sub> F <sub>9</sub> SO <sub>3</sub> ] + [N <sub>11120H</sub> ][H <sub>2</sub> PO <sub>4</sub> ] + and [C <sub>2</sub> C <sub>1</sub> Py][C <sub>4</sub> F <sub>9</sub> SO <sub>3</sub> ] + [N <sub>11120H</sub> ][H <sub>2</sub> PO <sub>4</sub> ] at 25°C.....	69
Table 6. 8 Experimental weight fraction data for [C <sub>2</sub> C <sub>1</sub> Im]Cl + K <sub>2</sub> HPO + and [C <sub>4</sub> C <sub>1</sub> Im][CF <sub>3</sub> SO <sub>3</sub> ] + Sucrose at 25°C.....	70
Table 6. 9 Experimental weight fraction data for [C <sub>2</sub> C <sub>1</sub> im][C <sub>4</sub> F <sub>9</sub> SO <sub>3</sub> ] + Sucrose at 25°C. ....	71
Table 6. 10 Experimental weight fraction data for [C <sub>2</sub> C <sub>1</sub> Py][C <sub>4</sub> F <sub>9</sub> SO <sub>3</sub> ] + Sucrose at 25°C. ....	72
Table 6. 11 Experimental weight fraction data for [C <sub>4</sub> C <sub>1</sub> im][CF <sub>3</sub> SO <sub>3</sub> ] + Glucose and [C <sub>2</sub> C <sub>1</sub> im][C <sub>4</sub> F <sub>9</sub> SO <sub>3</sub> ] + Glucose at 25°C.....	73
Table 6. 12 Experimental weight fraction data for [C <sub>2</sub> C <sub>1</sub> Py][C <sub>4</sub> F <sub>9</sub> SO <sub>3</sub> ] + Glucose at 25°C.....	74
Table 6. 13 Fitted parameters for experimental binodal data for the systems by Equation 1. ....	75
Table 6. 14 Characterization of Top and Bottom phases in terms of volume and pH.....	81
Table 6. 15 Phase identification for each system in terms of FIL/IL-rp and respective Salting-Out Agent (IS, Salt or CH) and respective identification methods. ....	82
Table 6. 16 Relative Enzymatic Activity of Lysozyme in 0.2, 0.5 and 1.0 mg/mL at 5% -35% (w/w) of K <sub>3</sub> PO <sub>4</sub> in water. ....	83
Table 6. 17 Relative Enzymatic Activity of Lysozyme in 0.2, 0.5 and 1.0 mg/mL at 5% -35% (w/w) of K <sub>2</sub> HPO <sub>4</sub> in water.....	83

Table 6. 18 Relative Enzymatic Activity of Lysozyme in 0.2, 0.5 and 1.0 mg/mL at 5%-35% (w/w) of K <sub>3</sub> Citrate in water. ....	84
Table 6. 19 Relative Enzymatic Activity of Lysozyme in 0.2, 0.5 and 1.0 mg/mL at 5%-35% (w/w) of Sucrose in water. ....	84
Table 6. 20 Relative Enzymatic Activity of Lysozyme in 0.2, 0.5 and 1.0 mg/mL at 5%-35% (w/w) of [C <sub>2</sub> C <sub>1</sub> Im]Cl in water. ....	85
Table 6. 21 Relative Enzymatic Activity of Lysozyme in 0.2, 0.5 and 1.0 mg/mL at 5%-35% (w/w) of [C <sub>2</sub> C <sub>1</sub> Im][C <sub>1</sub> CO <sub>2</sub> ] in water. ....	85
Table 6. 22 Relative Enzymatic Activity of Lysozyme in 0.2, 0.5 and 1.0 mg/mL at 5%-35% (w/w) of [C <sub>2</sub> C <sub>1</sub> Im][CF <sub>3</sub> SO <sub>3</sub> ] in water. ....	86
Table 6. 23 Relative Enzymatic Activity of Lysozyme in 0.2, 0.5 and 1.0 mg/mL at 5%-35% (w/w) of [C <sub>2</sub> C <sub>1</sub> Im][C <sub>4</sub> F <sub>9</sub> SO <sub>3</sub> ] in water. ....	86
Table 6. 24 Relative Enzymatic Activity of Lysozyme in 0.2, 0.5 and 1.0 mg/mL at 5%-35% (w/w) of [C <sub>4</sub> C <sub>1</sub> Im]Cl in water. ....	87
Table 6. 25 Relative Enzymatic Activity of Lysozyme in 0.2, 0.5 and 1.0 mg/mL at 5%-35% (w/w) of [C <sub>2</sub> C <sub>1</sub> Py]Br in water. ....	87
Table 6. 26 Relative Enzymatic Activity of Lysozyme in 0.2, 0.5 and 1.0 mg/mL at 5%-35% (w/w) of [N <sub>11120H</sub> ][H <sub>2</sub> PO <sub>4</sub> ] in water. ....	88
Table 6. 27 Extraction efficiency by UV-Vis spectroscopy detection methodology for all systems available. ....	91
Table 6. 28 Extraction efficiency by BCA assay detection methodology for all systems available. ....	92
Table 6. 29 Extraction efficiency by μBCA assay detection methodology for all systems available. ....	93
Table 6. 30 Extraction efficiency by Coomassie assay detection methodology for all systems available. ....	93

## Abbreviations

ABS	Aqueous Biphasic System
BCA	Bicinchoninic Acid
BSA	Bovine Serum Albumin
CAC	Critical Aggregation Concentration
CD	Circular Dichroism
CMC	Critical Micellar Concentration
DDS	Drug Delivery Systems
DSC	Differential Scanning Calorimetry
EE%	Extraction Efficiency (%)
FIL	Fluorinated Ionic Liquids
GHS	Globally Harmonized System of Classification and Labeling of Chemicals
IL	Ionic Liquids
ITC	Isothermal Calorimetry
LLE	Liquid-Liquids Extraction
Lys	Lysozyme
NMR	Nuclear magnetic resonance
PFC	Perfluorcarbon Compounds
pH	Potential of Hydrogen
SAIL	Surface Active Ionic Liquid
TEM	Transmission electron microscopy
T <sub>m</sub>	Melting Temperature
Trp	Tryptophan
UV-Vis	Ultraviolet visible
Wt%	Weight percentage



## Symbols

Y and X	Mass fraction percentage of the IL/FIL and Salting-Out Agents
A, B and C	Fitting parameters by least squares regression
$w_{IL}^{Calc}$	Ionic Liquid weight fraction calculated
$w_{IL}^{Exp}$	Ionic Liquid experimental weight fraction
n	Number of binodal points
$F_0$	Fluorescence intensities of the fluorophore in the absence of Quencher
F	Fluorescence intensities of the fluorophore in the presence of Quencher
[Q]	Concentration of the quencher
$K_{SV}$	Stern-Volmer constant
$k_q$	Bimolecular quenching constant
$\tau_0$	Lifetime of the fluorophore in the absence of the quencher





# 1. Introduction

## 1.1. Protein Purification

Proteins are applied in several fields in industry, namely food and biopharmaceutical industry, and in this way, it is important the development of the best protocol for its production and purification. The purification procedures have been pointed out as the most important step in proteins production, however they are difficult to optimize. It is vital to consider aspects as the scale-up level of difficulty, purity and yield achieved in the end of the production.

Protein purification follows several steps, beginning in initial recovery from the solid phase, usually cell debris; followed by purification step, where contaminants are removed; and then purification polishing step, where more specific contaminants are removed and removal of undesirable protein structures, allowing to achieve higher levels of purity.

Proteins and peptides are widely used in the biopharmaceutical industry as substitutes of the defective protein in the patient or the case of inexistence of the target protein due to genetic defect. The level of purity depends on the proteins' final purpose, and in this case may reach the 99% of purity, in order to ensure safety to the patient. In this sense, the number of steps and process complexity, affects both the final product yield and the purity (and the overall cost of production).<sup>1</sup>

Besides purity, isolating protein from its matrix with its structure and activity is also a critical aspect for the success of the extraction. Depending on the purity and concentration of the protein acquired, several steps are needed, which leads to higher process cost, in some cases can reach to 90% of the overall production cost, which is one major drawbacks of protein purification.<sup>2,3</sup> After purification steps, in cases of downstream processing of recombinant proteins for example, the final product usually results in less than 50% of the initial product.<sup>4</sup> As verified in Figure 1.1, the more complex the protein purification protocol, the more costly is the overall process and also the yield is more reduced. Therefore, the decreased number of purification step helps on the protein activity maintenance and reduced final product loss.<sup>2</sup>

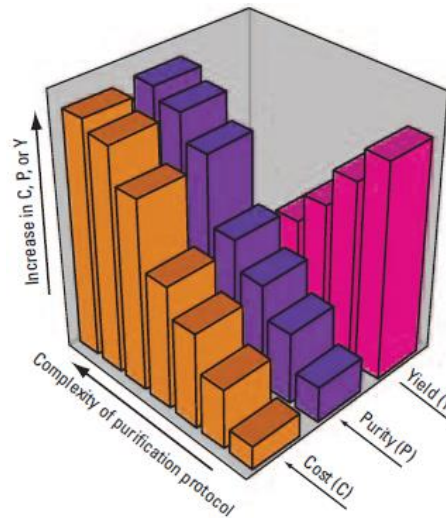


Figure 1. 1 Protein purification protocol complexity effects on the cost (C), purity (P) and yield (Y) of the overall process. Adapted from Mondal et al<sup>1</sup>

Liquid-Liquid Extraction may be a good choice to protein extraction due to their simplicity on operating, high yields and low time consuming.<sup>5</sup> In addition, it does not need pre-purification steps and it is easy to scale-up.<sup>1</sup>

Liquid-Liquid extraction is a separation method used for the removal of a solute from a liquid solution. A second solvent, insoluble or partially soluble in the first solvent, is added to the solution and the formation of two immiscible phases occur, to which the solutes partition, according to its distribution coefficient.<sup>6</sup> Some advantages rely on the good selectivity and two-in-one step of recovery and purification of the product.<sup>3</sup> However, one of the major drawbacks of conventional LLE are related to the usage of organic solvents that besides non-environmentally friendly may lead to protein structure and activity damage, due to low protein solubility in these solvents.<sup>5</sup>

## 1.2. Aqueous Biphasic Systems

Ever since Albertson et al suggested Aqueous Biphasic Systems for the separation of biologically active products in 1958,<sup>7</sup> studies focused on the development of several polymer-based ABS.

ABS are formed by mixing two water soluble compounds above a given concentration, in order to separate on two aqueous-rich phases, each one rich in one of the compounds. Therefore, ABS are ternary systems composed by water and two solutes.<sup>8</sup> Due to the co-existing of two aqueous-rich phases, extraction process becomes more biocompatible than traditional liquid-liquid extraction, based on organic solvents.<sup>9,10</sup>

Although they are ternary systems, in order to facilitate the interpretation of the diagrams, they are represented orthogonally, omitting the composition in water. Binodal curves are representative of weight percentage (wt%) of compound 1 (referred as “Top phase constituent” in Figure 1.2) versus wt% of compound 2 (“Bottom phase constituent”) in each axis. Above the binodal curve constitutes the biphasic region and undergo liquid-liquid demixing, and below the monophasic region.

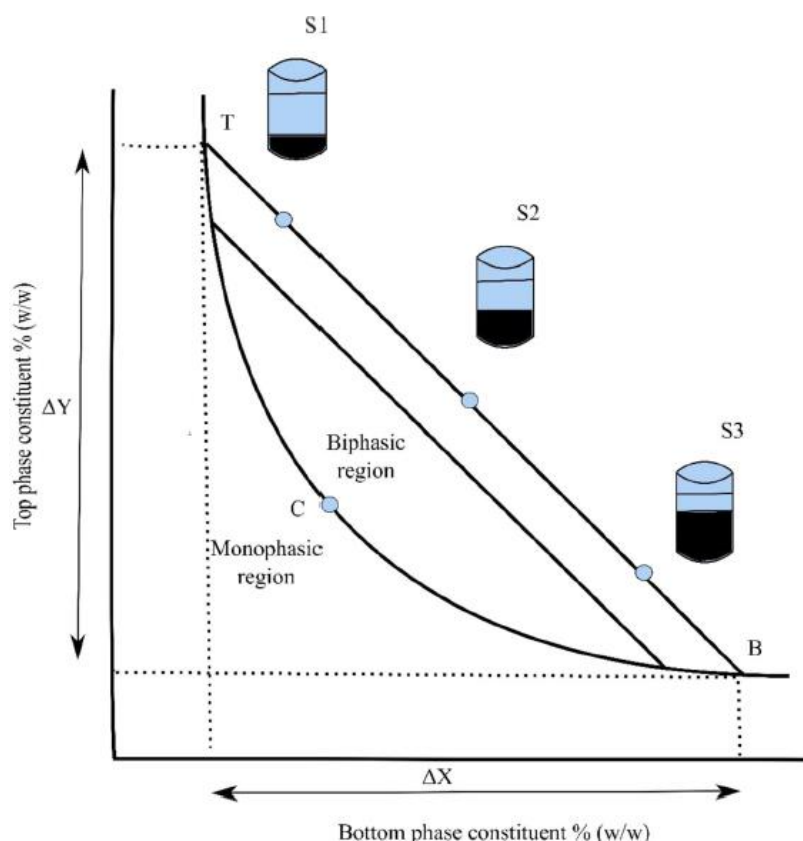


Figure 1. 2 Orthogonal ternary phase diagram of a hypothetical system composed by compound 1 + compound 2 + water (concentration on weight percentage - wt%). Adapted from Iqbal et al.<sup>10</sup>

In Figure 1.2 is represented several tie-lines. Mixtures with compositions at the same tie-line have the same composition of compound 1 and compound 2 in each phase, however different relative phase volumes, as represented in S1 to S3. The composition of each mixture is obtained by the end points of the tie line (T and B, for Top phase and Bottom phase constituent, respectively). The Critical Point (indicated as C in Figure 1.2) indicates the terminal point of immiscibility, at which both phases present the same composition and the compounds are miscible at all proportions.<sup>1,10,11</sup>

In the year of 1888, Franz Hofmeister studied the salts effect on precipitation of egg proteins. Therefore, the Hofmeister series are an empirical order of salts by their salting-out strength, from kosmotropic and chaotropic. Chaotropic species are “water structure breakers”, are poorly hydrated and are responsible for salting-in processes, on the other hand, a kosmotropic salt are “order-making” species. These species are highly hydrated and able to salt-out proteins and biomolecules. So far, the exact mechanism of salting-out is not fully comprehended, but it is accepted the salt competes with the solute for water molecules. Due to its high affinity to water, salt attracts water molecules, the solute aggregates and is expelled from this phase, forming a salt-rich phase and a solute-rich phase as it is represented in Figure 1.3.<sup>12, 13,14</sup>

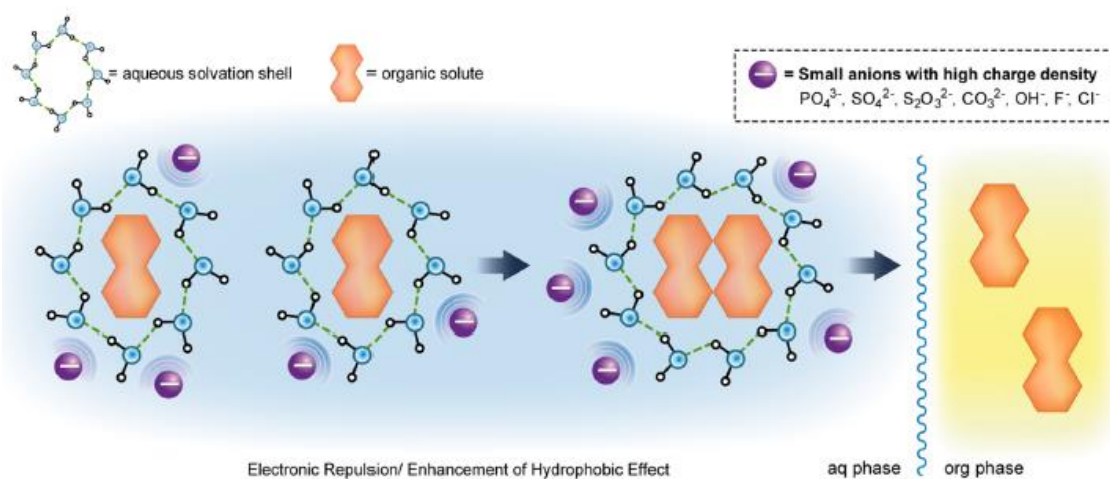


Figure 1. 3 Salting-out mechanism representation of non-polar solutes.

The salting effects follows the tendency of Hofmeister series, which orders salts from Kosmotropic to Chaotropic, as followed: citrates >  $\text{SO}_4^{2-}$  >  $\text{HPO}_4^{2-}$  >  $\text{F}^-$  >  $\text{Cl}^-$  >  $\text{Br}^-$  >  $\text{I}^-$  >  $\text{NO}_3^-$  >  $\text{ClO}_4^-$  >  $\text{N}(\text{CH}_3)^{4+}$  >  $\text{NH}_4^+$  >  $\text{Cs}^+$  >  $\text{Rb}^+$  >  $\text{K}^+$  >  $\text{Na}^+$  >  $\text{H}^+$  >  $\text{Ca}^{2+}$  >  $\text{Mg}^{2+}$  >  $\text{Al}^{3+}$ .<sup>14</sup>

Aqueous Biphasic Systems, as are composed by 70-80% weight/weight of water allows a safer environment to biomolecules extraction, due to a diminished interfacial tension between

the two aqueous phases. Besides, due to diminished number of separation steps and minimized energy cost, overall costs are reduced.<sup>15</sup>

Traditional polymer-based ABS are studied ever since the 1980's and are constituted by polymer-polymer or co-used with salt. The use of polymer-polymer based-systems take the advantage of avoidance of strong salting-out agents, as are inorganic salts, and so are more friendly for protein separation. However, polymer-polymer based systems are usually composed by two phases with very similar properties, this way displays low hydrophilicity-hydrophobicity range. To overcome this problem would be necessary polymer derivatization process which are hard to accomplish and turns the extraction procedure costly.<sup>8,11</sup> On the other hand, polymer-based systems are known to have high viscous phases, which is a downside to its application in separation systems, due to its slow phase separation.<sup>8</sup> The lack of selectivity and difficulty of remove proteins from the polymer phase is also a problem that needs solving for more applicability of ABS in industry.<sup>1</sup>

In this sense, exploring different components for ABS application consists in a great advantage, not only to overcome traditional ABS drawbacks, but also to improve the physical and chemical properties that suits best to the desired solute to extract. Besides, biocompatibility is also a characteristic that has to be fulfilled in order to these systems to be applied to proteins.

### 1.3. Ionic Liquids

Ionic liquids (ILs) are salts which consist in a combination of organic cation and organic or inorganic anion. By definition, this mixture results in a compound with a melting temperature below 100°C. The asymmetry between the cation and the anion leads a lower melting point, when compared to other salts.<sup>16</sup> In Figure 1.4 are represented the most common cations core used in these combinations.

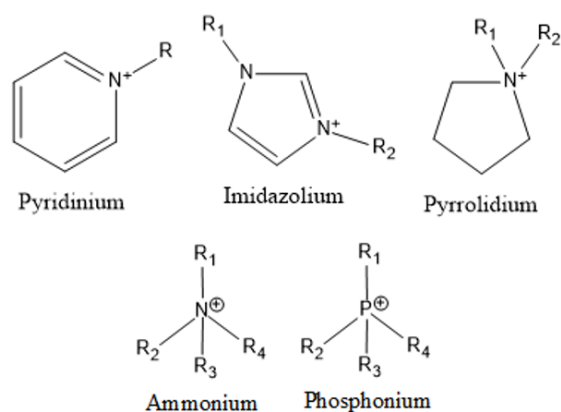


Figure 1. 4 Representation of common cation cores in ILs.

Due to the number of combinations between cation and anion, the main advantage of Ionic Liquids is they are “tailored solvents”. Besides, they have low flammability and volatility, and present chemically, physically and thermal stability, and as they have ionic nature, present high conductivity. In that sense, it is possible to design the solvent with the physical and chemical properties desired for a particular purpose. Due to their unique properties, ILs can be used for several applications, namely organic synthesis, electrochemistry, separation technology, among other applications, as summarized in Figure 1.5.<sup>17</sup>

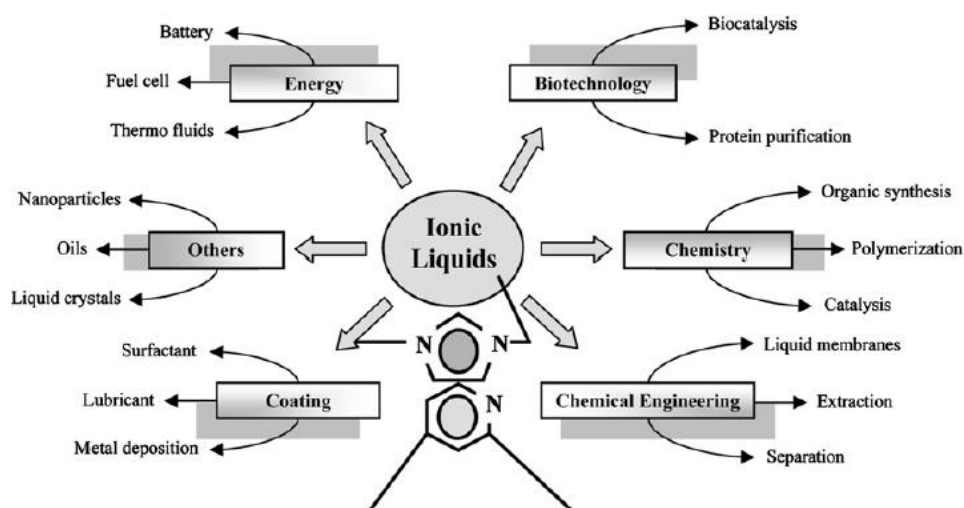


Figure 1. 5 Ionic Liquids Application in several fields. Adapted from Yeoung-Sang Yun et al.<sup>18</sup>

Ionic Liquids' toxicity is widely studied in order to evaluate the possibility of application in industry. Due to its high solubility in water, can be released into the environment through accidental discharges. Due to its high stability, either chemical and physical and non-volubility, hard degradation and persistence in the environment may become some drawbacks in its application. Therefore, it is important to access its toxicity in several organism models of different complexities. In general, the nature of the cation and the alkyl side length seem to have a major impact in ILs' toxicity than anion component. In particular, it is pointed out hydrophobicity of the IL provokes cell membrane physical changes, leading to membrane disruption as the mechanism of action for cytotoxicity. Also, the same IL have demonstrated to trigger different responses in different species, namely in invertebrates.<sup>18</sup>

Therefore, even though there are some evidences of some toxicity in some cases, as ILs are "design-solvents", it is possible to design solvents that are less hazardous and present low toxicity to the environment.

The work of Rogers et al (2003)<sup>19</sup> with concentrated solutions of kosmotropic salt ( $K_3PO_4$ ) in the formation of ABS, and in the following years the focus on this systems have been increasing.

Several studies have focused their attention in the characterization either on IL-salt based ABS, or IL-polymer and IL-carbohydrate systems. Others have put a step forward, and already applied this systems in extraction of molecules, such as alkaloids,<sup>20</sup> antioxidants,<sup>5</sup> amino acids,<sup>21</sup> or even proteins.<sup>22</sup>

## 1.4. Fluorinated Ionic Liquids

Fluorinated Ionic Liquids (FILs) have arrived as alternative solvents with peculiar properties. Is considered FIL an Ionic Liquid with long fluoroalkyl chain, usually longer than four carbon atoms.<sup>23</sup>

These solvents have been proposed as common perfluorocarbon compounds (PFC) replacers, mainly in biological applications as in vivo gas carriers, due to fluorocarbons' low solubility in water and biological fluids. FILs bring together the best properties of fluorocarbons compounds and ILs, namely enhanced surface activity and surfactant power, besides total miscibility in water and have small volatility under atmospheric conditions, are easily recovered and recycled and their toxicity is tuneable.<sup>24,25</sup>

These solvents are able to self-aggregate and form structures with three domains: one polar and two nonpolar (one aliphatic/hydrogenated and other perfluorinated), becoming very tunable and exceptional solvents compared to conventional Ionic Liquids. Different combinations of these domains and their relative size control the properties of the FILs, such as solubility, polarity and hydrophobicity/hydrophilicity.<sup>23,24</sup>

Different Critical Aggregation Concentration (CAC) were determined for FILs, and was observed the similar CAC values for FILs and water immiscible 7-8 carbon atoms perfluorinated anionic surfactants. Also, the size of the fluorinated alkyl chain in FILs controls the CAC, where longer chains lead to lower CAC; and also controls the shape of the aggregate. Therefore, FILs are solvents with tunable properties, miscible in water (applicable in biological systems) and also tunable aggregation behavior, which permits its application in several areas. The FIL [C<sub>2</sub>C<sub>1</sub>Im][C<sub>4</sub>F<sub>9</sub>SO<sub>3</sub>] was used for several analysis, namely the type of self-assembly structure acquired in its three CAC, as it is illustrated in Figure 1.6. As was possible to verify, at FIL concentrations higher than the first CAC, aggregates take the shape of spherical micelles (Figure 1.6 a and b) and at concentrations higher than the second CAC, they take shape of globular micelles (Figures 1.6 c and d). Above third CAC was not possible to analyze the aggregate structure by Transmission Electronic Microscopy (TEM).<sup>25</sup>



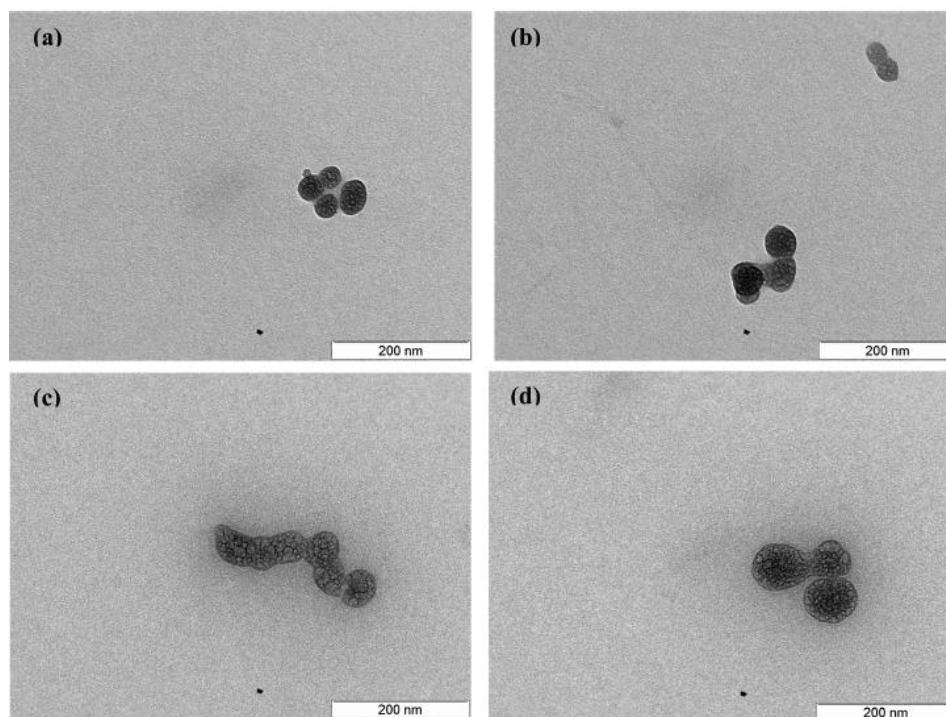


Figure 1. 6 TEM images of  $[C_2C_1Im][C_4F_9SO_3]$  aggregates at FIL concentration in aqueous solution 2.5 times the first CAC (a, b) and 2 times the second CAC (c, d). Adapted from Pereira et al.<sup>25</sup>

Due to Ionic Liquids application in biological systems, namely protein dissolution, extraction and purification, it is important to access its polarity. In particular, its Hydrogen-bonding acceptance ability or hydrogen-bond basicity,  $\beta$  value. This parameter is mainly important for biomaterial dissolution in ILs aqueous solutions. On the other hand, adding water to ILs solutions, as occurs when dealing with biological systems, usually leads to a decrease on this parameter, a may become a drawback in biomaterial dissolution in these solvent solutions. It was showed the addition of water to FILs, namely  $[C_2C_1Im][C_4F_9SO_3]$  and  $[C_2C_1Im][C_8F_{17}SO_3]$  did not change the hydrogen-bond basicity parameter ( $\beta$  value), contrarily to hydrogenated ILs or fluoro-containing ILs, possibly due to the nanosegregation behavior of FILs.<sup>24</sup>

As mentioned, this category of Ionic Liquids has very interesting properties for several areas. Some of these properties are high thermal and electrochemical stability, high ionic conductivity, null flammability and low surface tension.<sup>23</sup> Investigations stand out separation methods using this FILs to separate perfluoroalkyl acid contaminants from industrial residues and biomedical applications, as perfluoro components alternatives in oxygen carriers, currently used in therapeutic emulsions.<sup>26</sup>

Besides FILs studies on solvent properties, it is important to study the environmental impact of these FILs and cytotoxicity on human cells, however, information is still scarce about this matter.

It was pointed out the fully miscibility in water of perfluorobutanesulphonate anion based-FILs, and also good surfactant behavior. Plus, it was verified the maintenance of Lysozyme's activity, stability and secondary structure. Overall, FILs showed lower toxicity and bioaccumulation when shorter fluorinated chains of the anions were used. However, this factor needs to be more accessed to be more conclusive.

In order to determine the acute toxicity in aquatic organisms, several FILs was tested in *Vibrio fischeri*, *Daphnia magna* and *Lemna minor*, a gram-negative bacteria, a freshwater crustacean and an aquatic plant, respectively. *Vibrio fischeri* showed to be the less sensitive organism to the FILs, and both EC<sub>50</sub> values of *Daphnia magna* and *Lemna minor* are located above the upper limit of "Category acute 3" level from Globally Harmonized System of Classification and Labelling of Chemicals (GHS), which represents the category with lowest risk in terms of acute toxicity. However, chronic toxicity needs to be evaluated for these FILs.

Despite their negligible acute toxicity, their biodegradability seems to depend on cation nature, where Cholinium and Pyridinium-based FILs cations are more likely to be degraded, however fluorinated anions seem to be more resistant to degradation, which is still one of the drawbacks of FILs.<sup>27</sup>

Cytotoxicity is also an important parameter to assess the biocompatibility, although there are not many studies related to this parameter. FILs containing Imidazolium, Pyridinium, Pyrrolidinium, Cholinium and Tetraalkylammonium cations with short hydrogenated alkyl chain coupled with [C<sub>4</sub>F<sub>9</sub>SO<sub>3</sub>] anion did not affect the viability of four cell lines, CaCo, HepG2, HaCaT and EA.hy926, representative of several human tissues, such as intestine, liver, skin and blood vessels, respectively. Overall, the more hydrophobic the FIL, more toxicity is associated. However, based on this study, it is possible to tune the toxicological properties by changing the cationic hydrogenated alkyl-side chain and the anionic fluorinated chain length for the best application of these compounds as biomolecules solvent.<sup>28</sup>

Therefore, taking in account FILs properties, they are promising solvents for application in biomedical and biomolecules extraction application, due to their biocompatibility and low cytotoxicity.

Moreover, FILs are proposed as Drug Delivery Systems (DDS) due to their ability to encapsulate solutes. Specifically, lysozyme in the presence of surfactant FILs, namely [N<sub>11120H</sub>][C<sub>4</sub>F<sub>9</sub>SO<sub>3</sub>], [C<sub>2</sub>C<sub>1</sub>Im][C<sub>4</sub>F<sub>9</sub>SO<sub>3</sub>], [C<sub>2</sub>C<sub>1</sub>Py][C<sub>4</sub>F<sub>9</sub>SO<sub>3</sub>] and [C<sub>2</sub>C<sub>1</sub>Py][C<sub>4</sub>F<sub>9</sub>CO<sub>2</sub>] did not show loss of stability (measured by melting temperature - T<sub>m</sub>). These FILs were able to encapsulate the protein with maintenance of the protein's activity, and in some cases, the addition of FIL increased the protein activity (most noticeable effect in [C<sub>2</sub>C<sub>1</sub>Im][C<sub>4</sub>F<sub>9</sub>SO<sub>3</sub>]). After protein encapsulation in FIL micelle, Lysozyme seems to retain its activity. FILs did not change significantly protein structure, either before or after encapsulation.<sup>29</sup>

Another study was carried to understand the effect of FILs on the stability, structure and encapsulation of Bovine Serum Albumin.  $[\text{C}_2\text{C}_1\text{Im}][\text{C}_4\text{F}_9\text{SO}_3]$  and  $[\text{N}_{11120\text{H}}][\text{C}_4\text{F}_9\text{SO}_3]$  caused a significant increase on protein's  $T_m$  at concentrations below the Critical Micelle Concentration (CMC) when compared to non-surfactant IL,  $[\text{N}_{11120\text{H}}][\text{H}_2\text{PO}_4]$ . Namely,  $[\text{N}_{11120\text{H}}][\text{C}_4\text{F}_9\text{SO}_3]$  led to protein stabilization in a more compact shape (increase of  $\alpha$ -helical content).<sup>30</sup>

In both studies, protein did not denature in the presence of FILs at concentration above CMC, in this way, at least the FILs under study, are considered biomolecule friendly.

Carbohydrates are polyhydroxy aldehydes and ketones. These molecules have hydroxyl (-OH) groups able to perform either acceptance or donation of electrons, and capable of forming hydrogen bonding with water. In this sense, carbohydrates may be used as salting-out agents in ABS. However, as are weak salting-out agents, the number of possibilities in ABS formation is more limited, therefore have few studies for this end. Usually, these studies comprise ILs with lower capability to hydrogen-bonding with water molecules are able to form ABS.<sup>8,16</sup> Nevertheless, carbohydrates exhibit good properties for their application in ABS, due to their low toxicity and origin from biomass.<sup>8</sup>

Carbohydrates have great potential for its application in biological systems, however its low range of applicable ILs limits its application in ABS. However, FILs  $[\text{C}_2\text{C}_1\text{Im}][\text{C}_4\text{F}_9\text{SO}_3]$ ,  $[\text{C}_2\text{C}_1\text{Py}][\text{C}_4\text{F}_9\text{SO}_3]$ ,  $[\text{N}_{11120\text{H}}][\text{C}_4\text{F}_9\text{SO}_3]$ ,  $[\text{C}_2\text{C}_1\text{Im}][\text{CF}_3\text{SO}_3]$  and  $[\text{C}_2\text{C}_1\text{Pyr}][\text{CF}_3\text{SO}_3]$  were tested in terms of ABS formation with several carbohydrates; also, a system composed by  $[\text{C}_2\text{C}_1\text{Py}][\text{C}_4\text{F}_9\text{SO}_3]$  and D-(+)-maltose was applied in ABS for the extraction of four azo dyes Brilliant Blue FCF (E133), Green S (E142), tartrazine (E102) and Ponceau 4R (E124). For most of the dyes, partition occur favorably for carbohydrate-rich phase; however, for Brilliant Blue FCF, E133, partition occurred for FIL-rich phase.<sup>16</sup>

This study demonstrated the possibility of applying FILs, with its numberless advantages mentioned earlier, in systems composed with weak salting-out agents and low toxicity as carbohydrates are, improving the range of ABS possibilities composed by these fluorinated alternative solvents.

## 1.5. Lysozyme

Lysozyme (muramidase, EC 3.2.1.17) is one natural mechanism of defense against bacterial infection present in mammalian, and is produced by several tissues and fluids. This protein hydrolyze Gram-positive bacterial wall, by the hydrolysis of the  $\beta$  (1-4) glycosidic bonds of the peptidoglycan present on the bacterial cell wall.<sup>31</sup> Nowadays can be used as food conservative in food industry and is also considered a therapeutic protein due to its ability in the defense against bacterial infections and control immune responses on the hostage body.<sup>32</sup> Lysozyme is largely investigated and characterized, besides often used as a protein model in several studies. This protein has also intrinsic fluorescence, given by the Trp 62 and Trp 108, from which it is possible to take advantage to perform several studies based on this characteristic, namely by Fluorescence Spectroscopy.<sup>29,33</sup>

In this work, novel ABS were tested, including more benign and biocompatible salting-out agents, such as choline dihydrogenphosphate ( $[N_{1112OH}][H_2PO_4]$ ) and carbohydrates (Glucose and Sucrose), besides the traditional inorganic salt Potassium Phosphate Tribasic ( $K_3PO_4$ ). On the other hand, besides ILs, FILs were also tested for ABS formation with these salting-out agents. FILs used in this work present undeniable promising features as presented previously in Introduction section. FILs have the ability to maintain their hydrogen-bond basicity in water; this fact does not occur with ILs, which decrease the ability to donate hydrogen-bonds in water, decreasing the ability to solubilize solutes. On the other hand, FILs used are biocompatible to human cells<sup>28</sup> and do not show toxicity effects to aquatic organisms,<sup>27</sup> besides maintaining Lysozyme activity, stability and secondary structure.<sup>29</sup> These systems were applied for Lysozyme partition studies and tested Lysozyme activity in the presence of these components using *Micrococcus lysodeikticus* as substrate. IL and FIL-Protein Interaction Studies were carried through Turbidity method and Fluorescence Spectroscopy, measuring intrinsic fluorescence of this protein in the presence of  $[C_4C_1Im][CF_3SO_3]$ ,  $[C_2C_1Im][C_4F_9SO_3]$  and  $[N_{1112OH}][H_2PO_4]$ . Also, thermal stability was measured in the presence of  $[C_4C_1Im][CF_3SO_3]$  and  $[C_2C_1Im][C_4F_9SO_3]$  aqueous solutions and in the presence of extraction phases of one system.

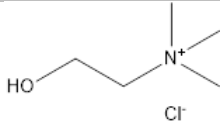
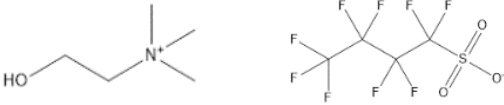
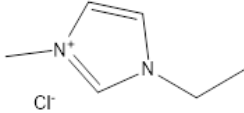
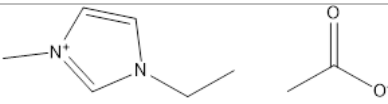
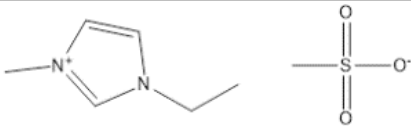
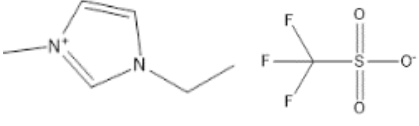
## 2. Materials and Methods

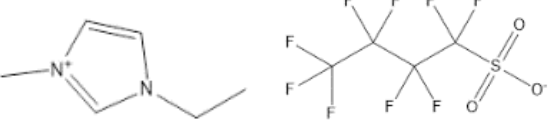
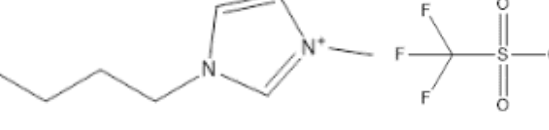
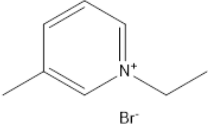
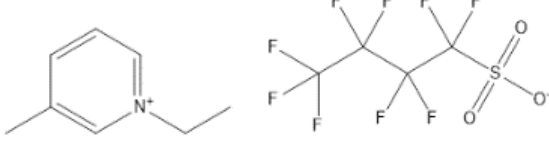
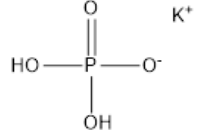
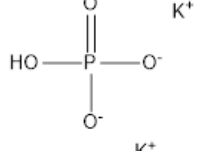
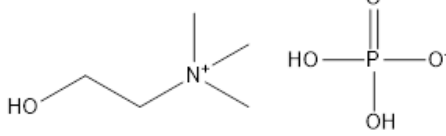
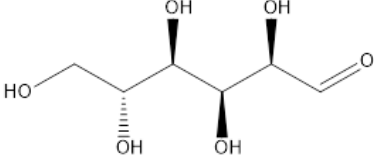
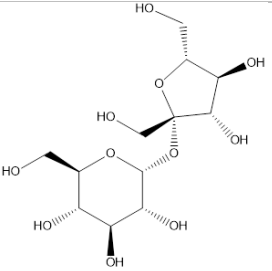
### 2.1. Reagents

1-ethyl-3-methylimidazolium chloride,  $\geq 98\%$  mass fraction purity; 1-ethyl-3-methylimidazolium acetate,  $\geq 95\%$  mass fraction purity; 1-Ethyl-3-Methylimidazolium-Methylsulfonate,  $\geq 95\%$  mass fraction purity; 1-Ethyl-3-Methylimidazolium trifluoromethanesulfonate,  $\geq 99\%$  mass fraction purity; 1-Ethyl-3-Methylimidazolium Perfluorobutanesulfonate,  $\geq 97\%$  mass fraction purity; 1-Butyl-3-Methylimidazolium Trifluoromethanesulfonate,  $\geq 99\%$  mass fraction purity; 1-Ethyl-3-Methylpyridinium Bromide, 99% mass fraction purity and 1-Ethyl-3-Methylpyridinium Perfluorobutane-sulfonate, 99% mass fraction purity and Choline Perfluorobutanesulfonate, 97% mass fraction purity were acquired from IoLiTec.

Sucrose, D-(+)-glucose, choline chloride, potassium phosphate dibasic and lyophilized powder of lysozyme from chicken egg white ( $\geq 90\%$ ) and *Micrococcus lysodeikticus* were acquired from Sigma Aldrich. Potassium dihydrogen phosphate was acquired from Fluka. Potassium hydroxide was acquired from Merck.

Table 2. 1 Designation and chemical structure of the compound used in this work.

Compound Designation	Chemical Structure
Choline Chloride [N <sub>11120H</sub> ]Cl	
Choline Perfluorobutanesulfonate [N <sub>11120H</sub> ][C <sub>4</sub> F <sub>9</sub> SO <sub>3</sub> ]	
1-Ethyl-3-Methylimidazolium Chloride [C <sub>2</sub> C <sub>1</sub> Im]Cl	
1-Ethyl-3-Methylimidazolium Acetate [C <sub>2</sub> C <sub>1</sub> Im][C <sub>1</sub> CO <sub>2</sub> ]	
1-Ethyl-3-Methylimidazolium-Methylsulfonate [C <sub>2</sub> C <sub>1</sub> Im][CH <sub>3</sub> SO <sub>3</sub> ]	
1-Ethyl-3-Methylimidazolium Trifluoromethanesulfonate [C <sub>2</sub> C <sub>1</sub> Im][CF <sub>3</sub> SO <sub>3</sub> ]	

<p>1-Ethyl-3-Methylimidazolium Perfluorobutanesulfonate <b>[C<sub>2</sub>C<sub>1</sub>Im][C<sub>4</sub>F<sub>9</sub>SO<sub>3</sub>]</b></p>	
<p>1-Butyl-3-Methylimidazolium Trifluoromethanesulfonate <b>[C<sub>4</sub>C<sub>1</sub>Im][CF<sub>3</sub>SO<sub>3</sub>]</b></p>	
<p>1-Ethyl-3-Methylpyridinium Bromide <b>[C<sub>2</sub>C<sub>1</sub>Py]Br</b></p>	
<p>1-Ethyl-3-Methylpyridinium Perfluorobutane Sulfonate <b>[C<sub>2</sub>C<sub>1</sub>Py][C<sub>4</sub>F<sub>9</sub>SO<sub>3</sub>]</b></p>	
<p>Potassium Phosphate Tribasic <b>K<sub>3</sub>PO<sub>4</sub></b></p>	
<p>Potassium Phosphate Dibasic <b>K<sub>2</sub>HPO<sub>4</sub></b></p>	
<p>Choline Dihydrogen Phosphate <b>[N<sub>1112OH</sub>][H<sub>2</sub>PO<sub>4</sub>]</b></p>	
<p>Glucose <b>C<sub>6</sub>H<sub>12</sub>O<sub>6</sub></b></p>	
<p>Sucrose <b>C<sub>12</sub>H<sub>22</sub>O<sub>11</sub></b></p>	

## 2.2. Aqueous Biphasic System determination - Cloud Point Titration, Diagrams and Tie-Lines

Ionic Liquids/Fluorinated Ionic Liquids and salting-out agents' aqueous solutions were prepared by weight using an analytical balance Sartorius CPA 225D.

The binodal curves were determined at 25°C and at atmospheric pressure through the cloud point titration method. This method consists on drop-wise addition of the IL/FIL aqueous solution to the salting-out agent aqueous solution, which is under stirring, until the cloud point is reached. After this stage, water is drop-wise added to the turbid mixture, until a clear solution is visually confirmed. The weight fractions were determined gravimetrically.

The binodal curves Tie Lines were determined by gravimetric method proposed initially by Merchuck et al.<sup>34</sup> A biphasic point is selected from the binodal and the system components are weighted, mixed using Vortex Mixer Labnet International for 30 seconds and then centrifuged for 3 minutes at 10000 rpm. The two phases are separated and weighted.

The binodal curves were fitted to three-parameter equation (Equation 1)

$$Y = A \exp[(B \times X^{0.5}) - C \times X^3] \quad \text{Equation 1}$$

where Y and X represent the mass fraction percentage of the IL/FIL and Salting-Out Agents, respectively. A, B and C are the fitting parameters by least squares regression.

Each tie lines were determined by the solution of the system of four unknown constants,

$$Y_T = A \exp[(B \times X_T^{0.5}) - (C \times X_T^3)] \quad \text{Equation 2}$$

$$Y_B = A \exp[(B \times X_B^{0.5}) - (C \times X_B^3)] \quad \text{Equation 3}$$

$$Y_T = \frac{Y_M}{\alpha} - \frac{1-\alpha}{\alpha} \times Y_B \quad \text{Equation 4}$$

$$X_T = \frac{X_M}{\alpha} - \frac{1-\alpha}{\alpha} \times X_B \quad \text{Equation 5}$$

where T, B and M are Top phase, bottom phase and the mixture, respectively; X and Y are the weight fraction percentage of the IL/FIL and Salting-Out Agent, respectively; and  $\alpha$  is the ration between the mass of the Top phase and the total mass of the mixture. A, B and C are the fitted constants determined by Equation 1.

## 2.3. Lysozyme Extraction

Each sample and control were prepared in a total mass of 2 g in 2 ml microtube, mixed at vortex and centrifuged 10 000 rpm for 3 minutes in order to phase separation occur. Lysozyme

final concentration in sample ampoules was 1mg/mL. After extraction, phase approximate volume was measured.

*Table 2. 2 Ionic Liquid/Fluorinated Ionic Liquid ABS and different Salting-Out Agents system composition used for Lysozyme partition experiments at 25°C.*

N°	Ionic Liquid/Fluorinated Ionic Liquid wt%	Salting-Out Agent wt%
1	30% wt [N <sub>11120H</sub> ]Cl	20% wt K <sub>3</sub> PO <sub>4</sub>
2	30% wt [N <sub>11120H</sub> ][C <sub>4</sub> F <sub>9</sub> SO <sub>3</sub> ]	30% wt [N <sub>11120H</sub> ][H <sub>2</sub> PO <sub>4</sub> ]
3	30% wt [C <sub>2</sub> C <sub>1</sub> Im]Cl	15% wt K <sub>3</sub> PO <sub>4</sub>
4	30% wt [C <sub>2</sub> C <sub>1</sub> Py]Br	15% wt K <sub>3</sub> PO <sub>4</sub>
5	30% wt [C <sub>2</sub> C <sub>1</sub> Im][CF <sub>3</sub> SO <sub>3</sub> ]	10% wt K <sub>3</sub> PO <sub>4</sub>
6	30% wt [C <sub>4</sub> C <sub>1</sub> Im][CF <sub>3</sub> SO <sub>3</sub> ]	5% wt K <sub>3</sub> PO <sub>4</sub>
7		20% wt [N <sub>11120H</sub> ][H <sub>2</sub> PO <sub>4</sub> ]
8		25% wt Glucose
9		25% wt Sucrose
10	30% wt [C <sub>2</sub> C <sub>1</sub> Im][C <sub>4</sub> F <sub>9</sub> SO <sub>3</sub> ]	2% wt K <sub>3</sub> PO <sub>4</sub>
11		6% wt [N <sub>11120H</sub> ][H <sub>2</sub> PO <sub>4</sub> ]
12		10% wt [N <sub>11120H</sub> ][H <sub>2</sub> PO <sub>4</sub> ]
13		20% wt [N <sub>11120H</sub> ][H <sub>2</sub> PO <sub>4</sub> ]
14		25% wt Glucose
15		25% wt Sucrose
16	30% wt [C <sub>2</sub> C <sub>1</sub> Py][C <sub>4</sub> F <sub>9</sub> SO <sub>3</sub> ]	2% wt K <sub>3</sub> PO <sub>4</sub>
17		6% wt [N <sub>11120H</sub> ][H <sub>2</sub> PO <sub>4</sub> ]
18		25% wt glucose
19		25% wt sucrose

#### 2.4. Phase Characterization

Was measured pH of each phase, using color-fixed 0-14 indicator strips Macherey-Nagel. Also, ampoule total volume and each phase volume was measured with an error of ± 0.05mL. These values are registered in Appendix Table 6.14.

In order to identify Top and Bottom phase composition, either is IL/FIL-rich phase or Salting-Out Agent-rich phase, NMR <sup>1</sup>H and <sup>17</sup>F spectra were carried. In that sense, 70uL of phase and 690uL of D<sub>2</sub>O is added to the NMR tube. Resume table of phase identification is in Appendix Table 6.15.



## **2.5. Solute Detection Procedures**

### **BCA and $\mu$ BCA assays**

Protein concentration was determined by Bicinchoninic Acid (BCA) assays reagent kits (Pierce<sup>TM</sup> and Micro BCA Thermo Scientific). In both assays, known concentrations of Lysozyme were used as standards.

#### BCA Protein Assay Kit

The total protein concentration of FIL-rp of each extraction system was determined according to Pierce<sup>TM</sup> BCA Protein Assay Kit microplate procedure protocol. Working reagent is prepared by mixing 50 parts of BCA reagent A with 1 part of BCA reagent B. 100  $\mu$ L of sample is pipetted to the microplate and added 100 $\mu$ L of working reagent. Microplate is sealed with SecureSeal Thermal Adhesive Sealing Film and mixed on a plate shaker for 30 seconds and incubated at 37°C for 30 minutes. Absorbance at 562 nm is measured after this time using Thermo Scientific Multiskan Go.

#### Micro BCA Protein Assay Kit

The total protein concentration of IL/FIL-rich phase of each extraction system was determined according to Micro BCA Protein Assay Kit microplate procedure protocol. Working reagent is prepared by mixing 25 parts of Micro BCA reagent MA, 24 part of BCA reagent MB and 1 part of BCA reagent MC. 100  $\mu$ L of sample is pipetted to the microplate and added 100 $\mu$ L of working reagent. Microplate is sealed with SecureSeal Thermal Adhesive Sealing Film and mixed on a plate shaker for 30 seconds and incubated at 37°C for 2 hours. Absorbance at 562 nm is measured after this time using Thermo Scientific Multiskan Go.

### **Bradford Assay**

The total protein concentration of FIL-rich phase of each extraction system was determined according to Coomassie Plus Kit microplate procedure protocol. 100  $\mu$ L of sample is pipetted to the microplate and added 100 $\mu$ L of Coomassie Plus Reagent. Microplate is mixed manually for 30 seconds and incubated at room temperature for 10 minutes. Absorbance at 595 nm is measured after this time using Thermo Scientific Multiskan Go.

## UV-Vis

UV-Vis Spectrophotometry was also used for protein detection on both phases. For this technique, a UV6300PL Double Beam UV spectrophotometer was used.

Firstly, calibrations with Lysozyme were performed in 0.1% K<sub>3</sub>PO<sub>4</sub>, 1% K<sub>3</sub>PO<sub>4</sub> and water and maximum absorbance peak was determined at 280 nm, for both 0.4 mL and 4.0 mL cuvette. Calibration curves are represented in Index.

Lysozyme presence in IL/FIL-aqueous rich phase and Salting-Out Agent-aqueous rich phase was determined by UV-Vis Spectrophotometry in 4 mL cuvette whenever possible. Phases were diluted at the minimum concentration possible to despise the phase components interference and 280 nm peak profile was analyzed.

## 2.6. Extraction Efficiency

After protein detection procedures were carried, Extraction Efficiency (% EE) was determined for each system and for each procedure. Extraction Efficiency is defined as the ratio between the mass of protein in the IL/FIL-aqueous rich phase ( $m_{Lys\ IL/FIL-rp}$ ) and the total mass of protein in the ampoule ( $m_{Lys\ total}$ ), as described in Equation 1:

$$\% EE = \frac{m_{Lys\ IL/FIL-rp}}{m_{Lys\ Total}} \times 100 \quad \text{Equation 6}$$

Biphasic points prepared for each system are represented in Table 2.2.

## 2.7. Lysozyme Activity

A lysozyme stock solution was prepared with a concentration of 4mg/mL and diluted to a concentration of 0.2, 0.5 and 1.0 mg/mL in 5%, 10%, 15%, 25% or 35% (w/w) of each compound under analysis. The list of tested compounds are represented in Appendix Tables 6.15-6.25. These solutions were allowed to settle for 30 minutes at room temperature. Substrate solution was prepared in a concentration of 0.30 mg/mL in KH<sub>2</sub>PO<sub>4</sub> buffer pH 6.2 and also settled for 30 minutes at room temperature.

After this time, 100 $\mu$ L of substrate were added to 10 $\mu$ L aliquot of Lysozyme solution in a round-bottomed 96-well plate. Absorbance at 450 nm was measured immediately after substrate addition at 25°C using Thermo Scientific Multiskan GO. A<sub>450</sub> was controlled for 5 minutes, with 30 seconds between each measurement. Lys plate's concentration was 0.05mg/mL. Each measurement was done in triplicate.

To ensure the protein activity after extraction procedure, *Micrococcus lysodeikticus* turbidity method was used. This procedure was carried after Lysozyme quantification in each phase for every system.

This procedure was prepared in a 96-well microplate U-shaped. A lysozyme solution was prepared with the concentration of 4.0 mg/mL in water. Blanks were prepared diluting this solution to 0.2 mg/mL in well. Only a few systems were tested in terms of Lysozyme activity and are as follow: 30% [C<sub>2</sub>C<sub>1</sub>Im][CF<sub>3</sub>SO<sub>3</sub>] + 10% K<sub>3</sub>PO<sub>4</sub>, 30% [C<sub>4</sub>C<sub>1</sub>Im][CF<sub>3</sub>SO<sub>3</sub>] + 20% [N<sub>11120H</sub>][H<sub>2</sub>PO<sub>4</sub>], 30% [C<sub>4</sub>C<sub>1</sub>Im][CF<sub>3</sub>SO<sub>3</sub>] + 25% Glucose, 30% [C<sub>4</sub>C<sub>1</sub>Im][CF<sub>3</sub>SO<sub>3</sub>] + 25% Sucrose, 30% [C<sub>2</sub>C<sub>1</sub>Im][C<sub>4</sub>F<sub>9</sub>SO<sub>3</sub>] + 2% K<sub>3</sub>PO<sub>4</sub>, 30% [C<sub>2</sub>C<sub>1</sub>Im][C<sub>4</sub>F<sub>9</sub>SO<sub>3</sub>] + 6% [N<sub>11120H</sub>][H<sub>2</sub>PO<sub>4</sub>], 30% [C<sub>2</sub>C<sub>1</sub>Im][C<sub>4</sub>F<sub>9</sub>SO<sub>3</sub>] + 25% Glucose, 30% [C<sub>2</sub>C<sub>1</sub>Im][C<sub>4</sub>F<sub>9</sub>SO<sub>3</sub>] + 25% Sucrose. Each phase was diluted to a concentration of 0.2mg/mL Lysozyme in well.

Substrate solution was prepared at concentration 0.3 mg/mL in phosphate buffer 66mM KH<sub>2</sub>PO<sub>4</sub> pH 6.2. The final solution was incubated at 25°C for at least 30 minutes.

Lysozyme relative activity was determined considering the blank of Lysozyme 0.2mg/mL as 100% activity, and Lysozyme activity was determined comparatively.

## **2.8. IL/FIL-Protein Interaction Studies**

### Turbidimetry

Several solution with different concentrations were prepared using [C<sub>4</sub>C<sub>1</sub>Im][CF<sub>3</sub>SO<sub>3</sub>], [C<sub>2</sub>C<sub>1</sub>Im][C<sub>4</sub>F<sub>9</sub>SO<sub>3</sub>] and [N<sub>11120H</sub>][H<sub>2</sub>PO<sub>4</sub>] from 0.1 to 120mM, with a concentration of 0.2mg/mL Lysozyme. Turbidimetry studies were carried by UV6300PL Double Beam UV spectrophotometer and UV-Vis spectra from 190 to 650 nm were acquired.

### Fluorescence

Fluorescent measurements were carried by spectrofluorometer Spex Horiba Jobin-Yvon. Tryptophan residues from Lysozyme were used as intrinsic fluorophore. These residues were excited at 295 nm and fluorescence intensity was collected as function of wavelength (300-500nm). The width of the excitation and emission slit was set to 2 nm for both cases.

Several solution with different concentrations were prepared using [C<sub>4</sub>C<sub>1</sub>Im][CF<sub>3</sub>SO<sub>3</sub>], [C<sub>2</sub>C<sub>1</sub>Im][C<sub>4</sub>F<sub>9</sub>SO<sub>3</sub>] and [N<sub>11120H</sub>][H<sub>2</sub>PO<sub>4</sub>] from 0.1 to 800mM, with a concentration of 0.2mg/mL Lysozyme.

In order to understand the quenching mechanism, results for [C<sub>2</sub>C<sub>1</sub>Im][C<sub>4</sub>F<sub>9</sub>SO<sub>3</sub>] and [N<sub>11120H</sub>][H<sub>2</sub>PO<sub>4</sub>] were fitted to Stern-Volmer equation (Equation 7), and determined the K<sub>SV</sub> and k<sub>q</sub> constants for each case.

$$\frac{F_0}{F} = 1 + K_{SV}[Q] = 1 + k_q\tau_0[Q] \quad \text{Equation 7}$$

### Nano-DSC

Several solution were prepared using [C<sub>4</sub>C<sub>1</sub>Im][CF<sub>3</sub>SO<sub>3</sub>], [C<sub>2</sub>C<sub>1</sub>Im][C<sub>4</sub>F<sub>9</sub>SO<sub>3</sub>] from 0.1 to 10mM, with a concentration of 1.0 mg/mL Lysozyme for nano-DSC analysis. Were also prepared solutions of 1mg/mL in a blank partition phase of system 30% [C<sub>2</sub>C<sub>1</sub>Im][C<sub>4</sub>F<sub>9</sub>SO<sub>3</sub>]+25% Glucose and tested partitioned Lysozyme from systems 30% [C<sub>4</sub>C<sub>1</sub>Im][CF<sub>3</sub>SO<sub>3</sub>]+25% Carbohydrate and 30% [C<sub>2</sub>C<sub>1</sub>Im][C<sub>4</sub>F<sub>9</sub>SO<sub>3</sub>]+25% Carbohydrate, where carbohydrate are Glucose and Sucrose.

Thermograms were acquired by Nano DSC (TA instruments, New Castle, DE, USA) at a scanning rate of 1°C/min in the temperature range of 20 to 90°C. The baseline was acquired measuring a reference solution without Lysozyme before sample measurement. Samples and references were degassed for 7 minutes at 20°C, except for samples containing ABS phases, and software NanoAnalyze (TA instruments, New Castle, DE, USA) was used to obtain the T<sub>m</sub>.

### 3. Results and Discussion

#### 3.1. Phase Diagrams

This work focuses on the implementation of FILs in ABS design, where new features are achieved. In this section, it is assessed the possibility of the formation of a biphasic system and determine the binodal firstly in order to be later applied in extraction. Some of the determined binodals are represented and discussed the effect of IL anion fluorination effect.

All systems tested were able to form ABS, except for  $[\text{C}_2\text{C}_1\text{Im}][\text{CF}_3\text{SO}_3]$  with Glucose and Sucrose and  $[\text{N}_{1112}\text{OH}][\text{CF}_3\text{SO}_3]$  with  $[\text{N}_{1112}\text{OH}][\text{H}_2\text{PO}_4]$ . The experimental weight fractions of all the systems are represented in Appendix Tables 6.1-6.11.

From all 20 systems determined, 8 binodal curves were found in literature.<sup>16,35-39</sup> After comparison of the experimental binodal to literature, 6 were in agreement with literature. In that case, experimental method is validated and so it was applied a solid turbidity method for binodal determination.

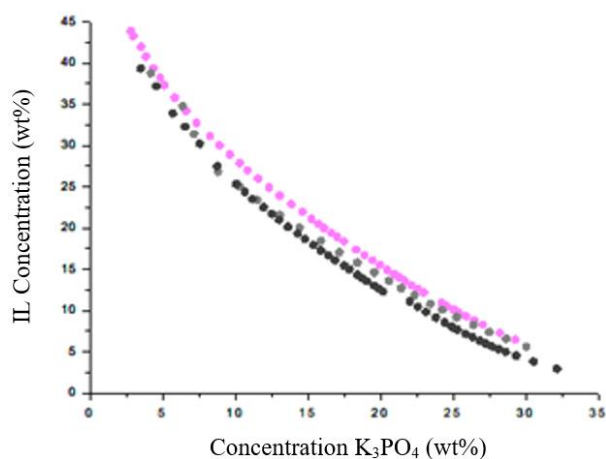


Figure 3. 1 Phase diagrams for ternary systems composed of IL +  $\text{K}_3\text{PO}_4$  +  $\text{H}_2\text{O}$  at  $25^\circ\text{C}$ :  $\bullet$   $[\text{C}_2\text{C}_1\text{Im}]\text{Cl}$ ;  $\circ$   $[\text{C}_2\text{C}_1\text{Im}]\text{Cl}$  from literature<sup>36</sup> and  $\bullet$   $[\text{C}_4\text{C}_1\text{Im}]\text{Cl}$  from literature.<sup>38</sup>

In order to compare the fluorination effect later on this work, it is necessary to access the influence of the alkylic chain in the cation on the binodal curves. In Figure 3.1 is represented the experimental binodal of  $[\text{C}_2\text{C}_1\text{Im}]\text{Cl}$  and literature binodal of  $[\text{C}_2\text{C}_1\text{Im}]\text{Cl}$  and  $[\text{C}_4\text{C}_1\text{Im}]\text{Cl}$ , using  $\text{K}_3\text{PO}_4$  as salting-out agent. Comparing both binodals, even though  $[\text{C}_4\text{C}_1\text{Im}]\text{Cl}$  has the binodal closer to the axis origin, there is no significant difference in terms of biphasic area. Also, literature  $[\text{C}_2\text{C}_1\text{Im}]\text{Cl}$  binodal is below experimental data and even closer to  $[\text{C}_4\text{C}_1\text{Im}]\text{Cl}$ , reinforcing this similarity. Therefore, it is possible to assume that the use of  $[\text{C}_4\text{C}_1\text{Im}]^+$  cation may be used for future comparison purposes, since cation does not seem to have a significant influence on the binodal.

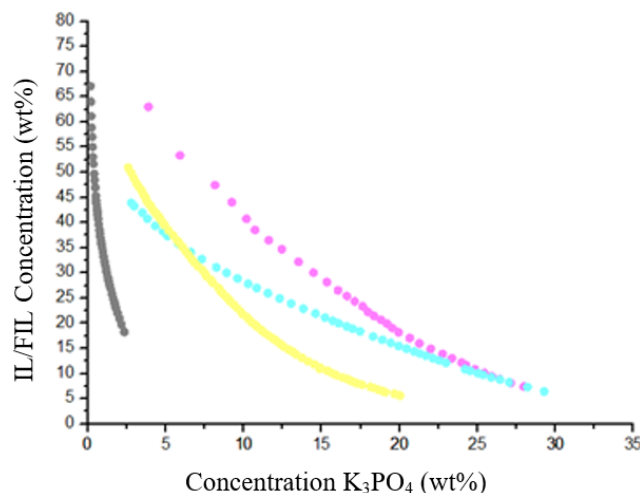


Figure 3. 2 Phase diagrams for ternary systems composed of IL +  $\text{K}_3\text{PO}_4$  +  $\text{H}_2\text{O}$  at  $25^\circ\text{C}$ : •  $[\text{N}_{1112\text{OH}}][\text{CF}_3\text{SO}_3]$ ; •  $[\text{C}_2\text{C}_1\text{Im}]\text{Cl}$ ; •  $[\text{C}_2\text{C}_1\text{Im}][\text{CF}_3\text{SO}_3]$ ; •  $[\text{C}_2\text{C}_1\text{Im}][\text{C}_4\text{F}_9\text{SO}_3]$ .

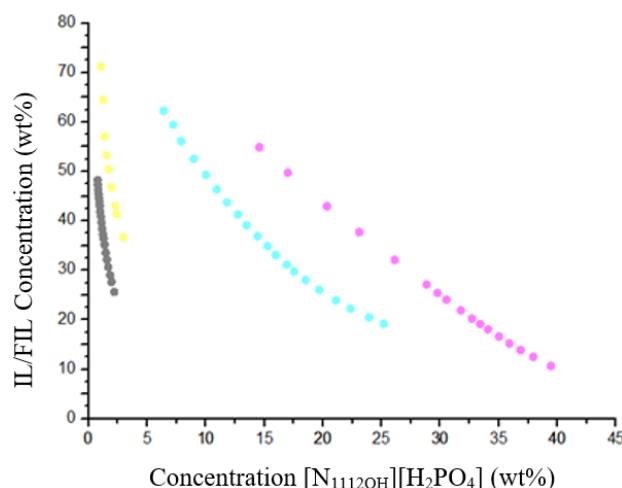


Figure 3. 3 Phase diagrams for ternary systems composed of IL +  $[\text{N}_{1112\text{OH}}][\text{H}_2\text{PO}_4]$  +  $\text{H}_2\text{O}$  at  $25^\circ\text{C}$ : •  $[\text{N}_{1112\text{OH}}][\text{C}_4\text{F}_9\text{SO}_3]$ ; •  $[\text{C}_4\text{C}_1\text{Im}][\text{CF}_3\text{SO}_3]$ ; •  $[\text{C}_2\text{C}_1\text{Im}][\text{C}_4\text{F}_9\text{SO}_3]$ ; •  $[\text{C}_2\text{C}_1\text{Py}][\text{C}_4\text{F}_9\text{SO}_3]$ .

Figure 3.2 represents the binodal curves of  $[\text{N}_{1112\text{OH}}][\text{CF}_3\text{SO}_3]$ ,  $[\text{C}_2\text{C}_1\text{Im}]\text{Cl}$ ,  $[\text{C}_2\text{C}_1\text{Im}][\text{CF}_3\text{SO}_3]$ ,  $[\text{C}_2\text{C}_1\text{Im}][\text{C}_4\text{F}_9\text{SO}_3]$ , using  $\text{K}_3\text{PO}_4$  as salting-out agent and Figure 3.3 represents the binodal curves of  $[\text{N}_{1112\text{OH}}][\text{C}_4\text{F}_9\text{SO}_3]$ ,  $[\text{C}_4\text{C}_1\text{Im}][\text{CF}_3\text{SO}_3]$ ,  $[\text{C}_2\text{C}_1\text{im}][\text{C}_4\text{F}_9\text{SO}_3]$  and  $[\text{C}_2\text{C}_1\text{Py}][\text{C}_4\text{F}_9\text{SO}_3]$  using  $[\text{N}_{1112\text{OH}}][\text{H}_2\text{PO}_4]$ .

Inorganic salts are strong salting-out agents, located in the most kosmotropic end of the Hofmeister series, while other salting-out agents may be weaker. The inorganic salt  $\text{K}_3\text{PO}_4$  was able to form demixing with all IL/FIL tested, meanwhile  $[\text{N}_{1112\text{OH}}][\text{H}_2\text{PO}_4]$  formed with all systems, except for  $[\text{N}_{1112\text{OH}}][\text{CF}_3\text{SO}_3]$  and  $[\text{C}_2\text{C}_1\text{Im}][\text{CF}_3\text{SO}_3]$ .

The ability of IL/FIL to form ABS follows the order:  $[\text{C}_2\text{C}_1\text{Im}][\text{C}_4\text{F}_9\text{SO}_3] > [\text{C}_2\text{C}_1\text{Im}][\text{CF}_3\text{SO}_3] > [\text{C}_2\text{C}_1\text{Im}]\text{Cl} > [\text{N}_{1112\text{OH}}][\text{CF}_3\text{SO}_3]$  for  $\text{K}_3\text{PO}_4$  as salting-out agent and

$[C_2C_1Py][C_4F_9SO_3] > [C_2C_1Im][C_4F_9SO_3] > [C_4C_1Im][CF_3SO_3] > [N_{1112OH}][C_4F_9SO_3]$  for  $[N_{1112OH}][H_2PO_4]$  as salting-out agent. Overall, this capability seems to be influenced by the fluor functionalization of the IL anion, since a longer fluorinated chain leads to closer binodal curve to the axis origin, leading to a higher biphasic area, therefore a higher ability in ABS formation for most FILs when compared to the respective ILs. However, although not the same salting-out agents, this behavior was observed in several ABS using ILs and FILs with carbohydrate, namely maltose.<sup>16</sup> In this paper,  $[CF_3SO_3]^-$  based ILs were not able to form phase separation in contrast with the respective FILs ( $[C_4F_9SO_3]$  based FIL). It was proposed that the increasing length of the fluorinated alkyl chain of the anion leads to a more hydrophobic FIL, diminishing the affinity to water molecules, therefore are more likely to be salted-out by the salting-out agent, favoring the phase separation. It is noticeable the higher ability of the  $[C_4F_9SO_3]^-$  anion to form demixing than the anion  $[CF_3SO_3]^-$  due to the increased hydrophobicity permitted by the longer fluorinated alkylic chain.

However,  $[N_{1112OH}][C_4F_9SO_3] + [N_{1112OH}][H_2PO_4]$  seems to be an exception to the fact that longer fluorinated alkylic chain favor the ABS formation, possibly due to the nature of the cation, since it is more hydrophilic than Imidazolium and Pyridinium based IL/FILs. Also, on this paper, this FIL was tested with maltose, and was unable to form a two-phase system, and may represent its lower ability due to cation more hydrophilic character.

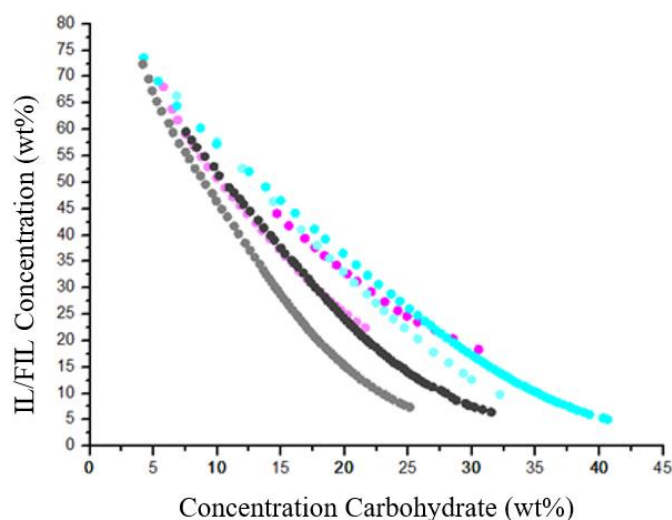


Figure 3.4 Phase diagrams for ternary systems composed of  $\bullet [C_4C_1Im][CF_3SO_3]$ ,  $\bullet [C_2C_1Im][C_4F_9SO_3]$  and  $\bullet [C_2C_1Py][C_4F_9SO_3]$  + carbohydrate +  $H_2O$  at  $25^\circ C$ : Sucrose (darker color); D-(+)-Glucose (lighter color).

This effect was also analyzed for carbohydrates systems. Figure 3.4 represent the binodal curves of  $[C_4C_1Im][CF_3SO_3]$ ,  $[C_2C_1Im][C_4F_9SO_3]$  and  $[C_2C_1Py][C_4F_9SO_3]$  with the monosaccharide D-(+)-glucose and the disaccharide Sucrose.

The carbohydrates Glucose and Sucrose were able to form two-phase systems with  $[\text{C}_4\text{C}_1\text{Im}][\text{CF}_3\text{SO}_3]$ ,  $[\text{C}_2\text{C}_1\text{Im}][\text{C}_4\text{F}_9\text{SO}_3]$  and  $[\text{C}_2\text{C}_1\text{Py}][\text{C}_4\text{F}_9\text{SO}_3]$ ;  $[\text{C}_2\text{C}_1\text{Im}][\text{CF}_3\text{SO}_3]$  was tested but did not form ABS, as was confirmed by literature.<sup>16</sup>

As mentioned before, carbohydrates are considered weaker salting-out agents than, for example, inorganic salts. For that reason, in order to form phase separation, ILs available for that end are more limited, since only more hydrophobic ILs form ABS. For that reason, and as happened for  $[\text{N}_{1112\text{OH}}][\text{H}_2\text{PO}_4]$  salt,  $[\text{C}_2\text{C}_1\text{Im}][\text{CF}_3\text{SO}_3]$  is not able to perform phase separation, and only  $[\text{C}_4\text{C}_1\text{Im}][\text{CF}_3\text{SO}_3]$  forms ABS with these carbohydrates. This behavior is due to longer alkylic chain, which gives the IL a more hydrophobic character.<sup>8</sup>

The implementation of FILs in ABS is an advantage over using IL. First, due to the increase of hydrophobicity relatively to IL, FILs permitted the usage of carbohydrates in separation systems to replacement of inorganic salts. These salts lead to alkaline solutions, which may present a drawback in separation of pH sensitive biomolecules. Carbohydrates, on the other hand are non-charged, and overcome this problem, showing a protein-friendly behavior, besides also present biodegradability and non-toxicity.<sup>39</sup> This was verified with  $[\text{C}_2\text{C}_1\text{Im}][\text{CF}_3\text{SO}_3]$ , which was unable to form ABS with  $[\text{N}_{1112\text{OH}}][\text{H}_2\text{PO}_4]$  and carbohydrates, and the fluorinated anion form  $[\text{C}_2\text{C}_1\text{Im}][\text{C}_4\text{F}_9\text{SO}_3]$  gained this ability. On the other hand, using FILs in these separation systems permit to decrease the amount of salting-out agent to form two-phase system, reflected by larger biphasic region in FILs compared to IL, favoring the biocompatibility of the IS aqueous-rich phase.

After the determination of the binodal for each system, the fitting constants A, B and C, the correlation coefficient (R) were determined using methodology presented in section 2.2, the gravimetric method proposed by Merchuck<sup>34</sup> and are represented at Table 6.13.



### 3.2. Phase Identification: NMR

In order to identify each phase, as either IL/FIL-rich phase or salting-out agent-rich phase,  $^1\text{H}$  and  $^{19}\text{F}$  NMR spectra in  $\text{D}_2\text{O}$  were done for whenever characterization by visual analysis or pH values were not conclusive. In this section will be presented results related to system  $30\%[\text{C}_2\text{C}_1\text{Im}][\text{C}_4\text{F}_9\text{SO}_3]+6\text{-}20\%[\text{N}_{11120\text{H}}][\text{H}_2\text{PO}_4]$ . The remaining NMR results are presented in Appendix Figures 6.1-6.15. Phases' identification is presented in Appendix Table 6.15.

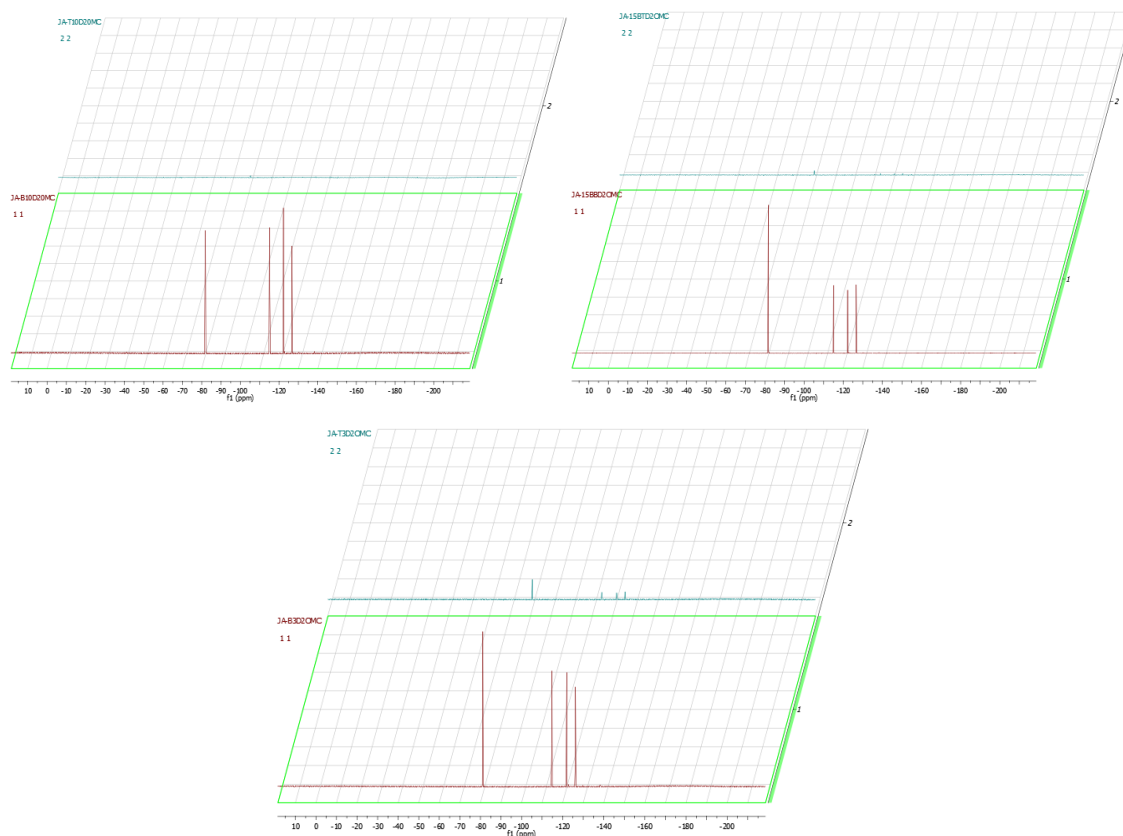


Figure 3. 5  $^{19}\text{F}$  NMR spectra of Top (up) and Bottom phase (down) of system  $30\%[\text{C}_2\text{C}_1\text{Im}][\text{C}_4\text{F}_9\text{SO}_3] + 20\%[\text{N}_{11120\text{H}}][\text{H}_2\text{PO}_4]$ ;  $30\%[\text{C}_2\text{C}_1\text{Im}][\text{C}_4\text{F}_9\text{SO}_3] + 10\%[\text{N}_{11120\text{H}}][\text{H}_2\text{PO}_4]$  and  $30\%[\text{C}_2\text{C}_1\text{Im}][\text{C}_4\text{F}_9\text{SO}_3] + 6\%[\text{N}_{11120\text{H}}][\text{H}_2\text{PO}_4]$ (left to right) in  $\text{D}_2\text{O}$ .

Figure 3.5 represents  $^{19}\text{F}$  NMR spectra of systems  $30\%[\text{C}_2\text{C}_1\text{Im}][\text{C}_4\text{F}_9\text{SO}_3] + 6\%[\text{N}_{11120\text{H}}][\text{H}_2\text{PO}_4]$ ,  $30\%[\text{C}_2\text{C}_1\text{Im}][\text{C}_4\text{F}_9\text{SO}_3] + 10\%[\text{N}_{11120\text{H}}][\text{H}_2\text{PO}_4]$  and  $30\%[\text{C}_2\text{C}_1\text{Im}][\text{C}_4\text{F}_9\text{SO}_3] + 20\%[\text{N}_{11120\text{H}}][\text{H}_2\text{PO}_4]$  of both Top and Bottom phases of this systems' blank ampoule.  $^{19}\text{F}$  NMR spectra comparison of both phases may provide evidences about phase identification, due to the identifying the fluorinated alkyl groups of FIL's anion. Therefore, more intense peaks in these spectra are associated to FIL-rich phase.

Comparing both  $^{19}\text{F}$  NMR spectra, it is possible to verify an increase in peaks intensity in Bottom phase. Thus, it is suggested that Bottom phase is FIL-rich phase for all systems presented in this section.

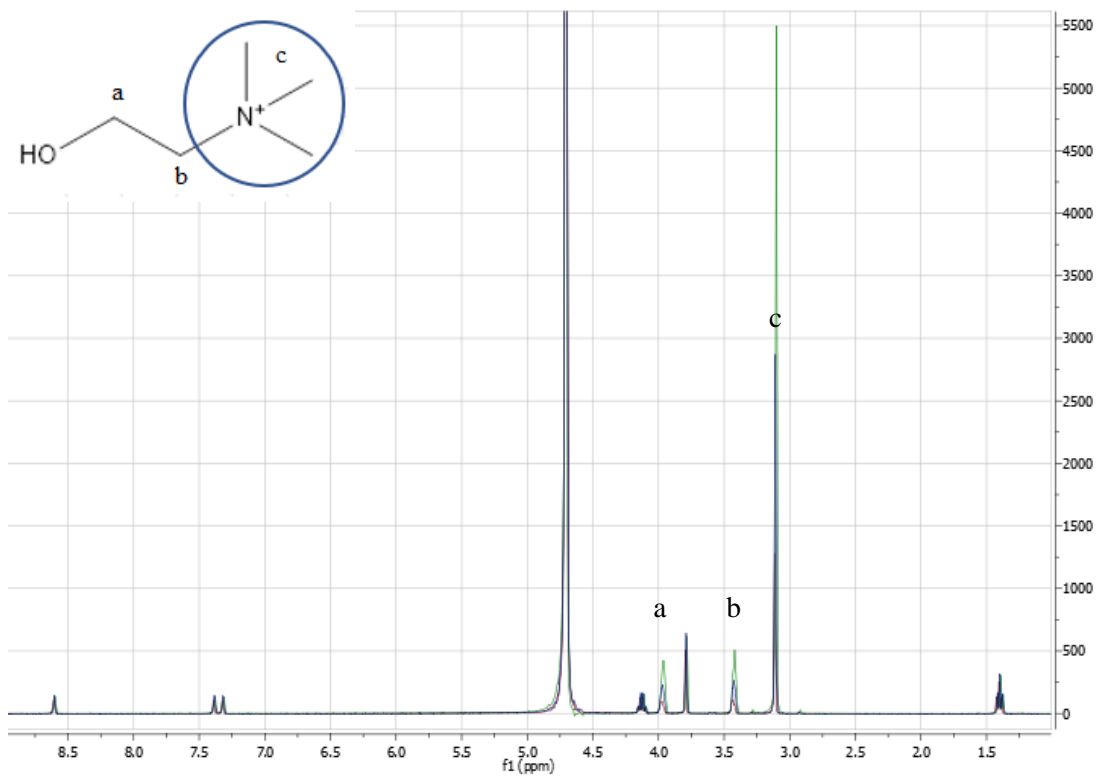


Figure 3.  $^6\text{H}$  NMR spectra of Top phase of systems  $30\%[\text{C}_2\text{C}_1\text{Im}][\text{C}_4\text{F}_9\text{SO}_3]+20\%[\text{N}_{11120\text{H}}][\text{H}_2\text{PO}_4]$ ;  $30\%[\text{C}_2\text{C}_1\text{Im}][\text{C}_4\text{F}_9\text{SO}_3]+10\%[\text{N}_{11120\text{H}}][\text{H}_2\text{PO}_4]$  and  $30\%[\text{C}_2\text{C}_1\text{Im}][\text{C}_4\text{F}_9\text{SO}_3]+6\%[\text{N}_{11120\text{H}}][\text{H}_2\text{PO}_4]$  in  $\text{D}_2\text{O}$  superimposed.

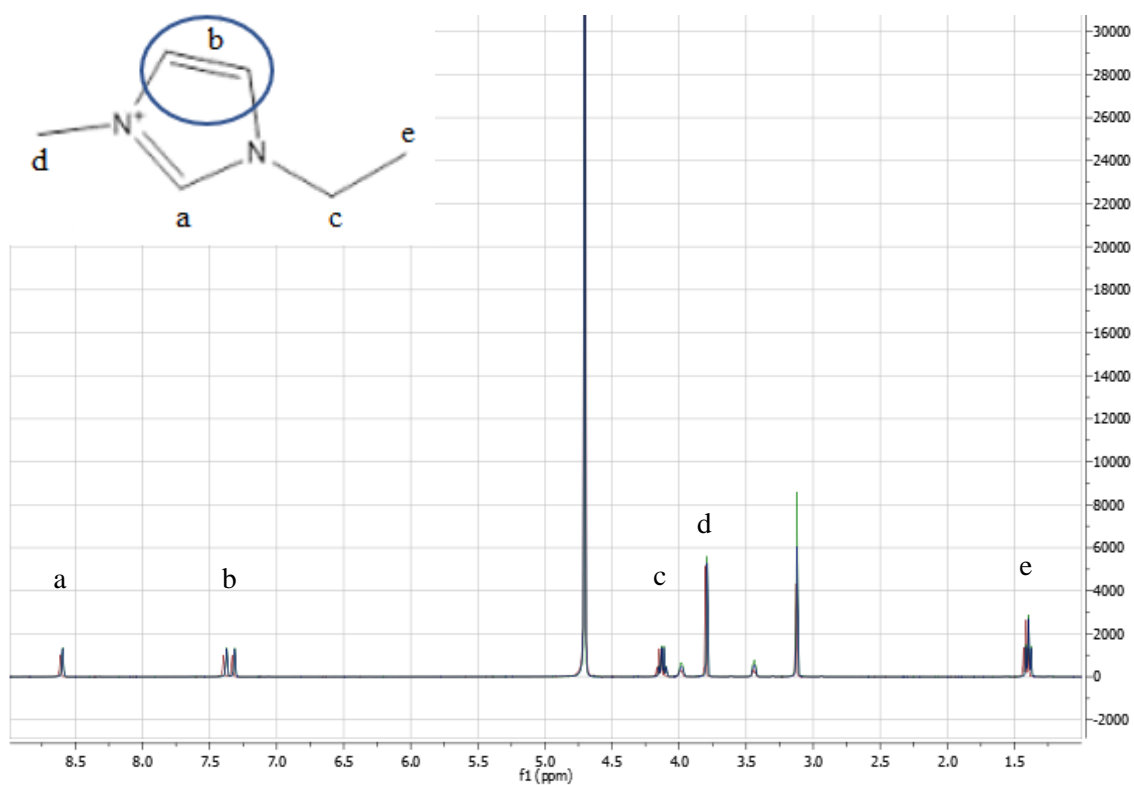


Figure 3.  $^7\text{H}$  NMR spectra of Bottom phase of systems  $30\%[\text{C}_2\text{C}_1\text{Im}][\text{C}_4\text{F}_9\text{SO}_3]+20\%[\text{N}_{11120\text{H}}][\text{H}_2\text{PO}_4]$ ;  $30\%[\text{C}_2\text{C}_1\text{Im}][\text{C}_4\text{F}_9\text{SO}_3]+10\%[\text{N}_{11120\text{H}}][\text{H}_2\text{PO}_4]$  and  $30\%[\text{C}_2\text{C}_1\text{Im}][\text{C}_4\text{F}_9\text{SO}_3]+6\%[\text{N}_{11120\text{H}}][\text{H}_2\text{PO}_4]$  in  $\text{D}_2\text{O}$  superimposed.

On the other hand,  $^1\text{H}$  NMR spectra were acquired to identification of compounds present in the phases and verify the phase identification done by  $^{19}\text{F}$  NMR spectra. Figures 3.6 and 3.7 represent the  $^1\text{H}$  NMR spectra of both Top and Bottom phases of this system's blank ampoule, respectively, for all three systems presented.

For top phase, identified as  $[\text{N}_{11120\text{H}}][\text{H}_2\text{PO}_4]$ -rich phase, are noticed the three alkyl groups bonded to N of  $[\text{N}_{11120\text{H}}]^+$  cation at 3.12 ppm and the protons from the alkyl chain at 3.44 and 3.97 ppm. On bottom phase  $^1\text{H}$  NMR spectra, identified earlier as  $[\text{C}_2\text{C}_1\text{Im}][\text{C}_4\text{F}_9\text{SO}_3]$ -rich phase, are recognized the triplet signal from the end alkyl chain methyl group at 1.41 ppm and the methyl group signal bonded directly to the N atom from the Imidazolium ring at 3.80 ppm; is also notorious the methylene group signal as a quartet signal at approximately 4.1 ppm. The protons of imidazolium's ring position 4 and 5 are detected at 7.40 and 7.33, and the proton in position 2 is at 8.6 ppm. Therefore, for salt-rich phase is identified the  $[\text{N}_{11120\text{H}}][\text{H}_2\text{PO}_4]$  and for FIL-rich phase the  $[\text{C}_2\text{C}_1\text{Im}][\text{C}_4\text{F}_9\text{SO}_3]$ , in higher intensity signals than the opposite phase.

### 3.3. Lysozyme Activity - Screening

In order to choose a system suitable for Lysozyme extraction to analyze, Lysozyme enzymatic activity was accessed in the presence of each component of the systems presented in Table 2.1 from Material and Methods section by *Micrococcus lysodeikticus* turbidimetric method at concentrations between 5 and 35% (w/w). These concentrations were selected based on the ABS biphasic region of overall systems.

Firstly, several concentrations of Lys were analyzed in order to understand the influence of the concentration of protein in the Lys activity at each concentration of compound. For this purpose, were studied the Lys concentrations of 0.2, 0.5 and 1.0 mg/mL. All results are presented in Appendix Tables 6.16-6.26. The results did not present a trend in the variation of enzyme activity at different concentrations, and so Lys enzymatic activity is independent of its concentration.

As mentioned, several compounds were analyzed in a concentration range in order to determine to primarily screen their biocompatibility with the protein. The tests were carried out in the range of concentrations of 5-35% (w/w) due to the biphasic region of ABS.

Figure 3.8 represents some of the screening assays performed in this work.

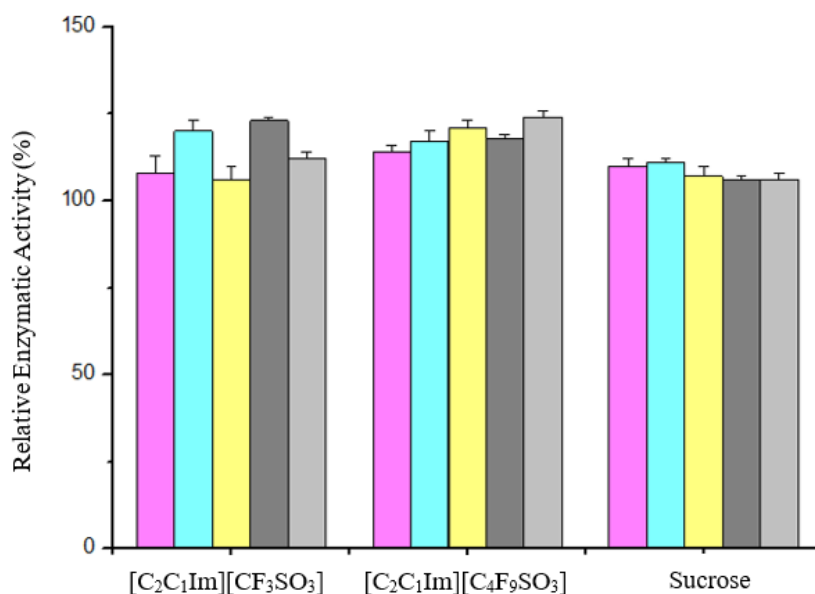


Figure 3. 8 Relative Lys Enzymatic Activity for 0.2 mg/mL Lys for • 5% (w/w), • 10% (w/w), • 15% (w/w), • 25% (w/w) and • 35% (w/w) of [C<sub>2</sub>C<sub>1</sub>Im][CF<sub>3</sub>SO<sub>3</sub>], [C<sub>2</sub>C<sub>1</sub>Im][C<sub>4</sub>F<sub>9</sub>SO<sub>3</sub>] and Sucrose.

Analyzing all results, it is possible to conclude compounds in the conditions tested do not lead to a lost of Lys enzymatic activity.

### 3.4. Extraction Efficiency

After performing assays to determine concentration range in which the protein maintains its function, these systems were tested in terms of Extraction Efficiency (% EE), which was calculated using Equation 6 in section 2.6 of Materials and Methods, that is considering IL/FIL-rich phase as target phase.

In this work, several factors were taken in account in evaluating extraction efficiency. All biphasic points were chosen considering the Lysozyme activity in each IL/FIL and salting-out agent concentration and all compositions are approximately at the same distance of the binodal for each system. It was analyzed the influence of different salting-out agents (using the same extraction composition for different systems) and analyzed the effect of composition in salting-out agent (same salting-out agent in different extraction concentrations).

Whenever possible, several detection methods were applied for protein detection: UV-Vis spectroscopy, BCA,  $\mu$ BCA and Coomassie colorimetric assays. Not all detection assays were suitable for quantification of Lys in both phases. UV-Vis spectroscopy failed in quantification of Lys in systems composed by Pyridinium-based IL/FIL, due to pyridinium ring characteristic absorption at 259 nm, which showed to interfere with Lys band at 280 nm.<sup>40</sup> Also, colorimetric assays, namely BCA,  $\mu$ BCA and Coomassie described particular sensibility to carbohydrate-based systems, more evident for Glucose, leading to usually overestimated Lys concentration determined by these assays. Therefore, a conjugated study with UV-Vis and colorimetric assays was done to a more reliable analysis, and considering each method sensibility, results are in agreement.

All results for each detection methodology are summarized in Appendix Figures 6.27-6.30.

Firstly, all systems with an inorganic salt ( $K_3PO_4$ ) were evaluated and results are represented in Figure 3.9.

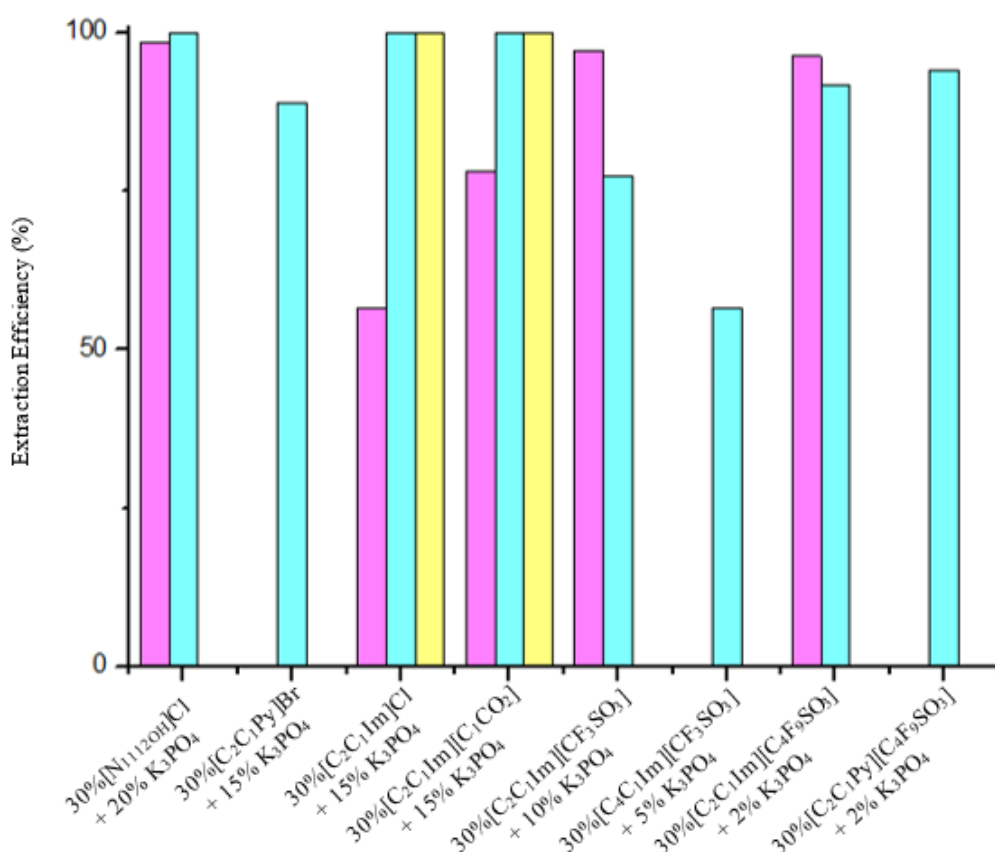


Figure 3. 9 Extraction Efficiencies of Lysozyme for each system containing  $K_3PO_4$  and respective extraction point at  $25^\circ C$ , and several detection methods. • UV-Vis; • BCA; •  $\mu$ BCA; • Coomassie. None of the results present replicates.

Considering all systems containing  $K_3PO_4$ , it is possible to conclude that all systems have majority partition to IL/FIL-rich phase, that is EE% higher than 50%, regardless the nature of the IL/FIL. Therefore, in this case, it may be suggested that it is not the nature of the IL/FIL cation that controls the partitions, but the nature of the salting-out agent, in a sense  $K_3PO_4$  does not seem to be a good component for concentrating Lys in a rich phase in this inorganic salt, and protein shows preference in the opposite phase of the system.

Inorganic salts are strong salting-out agents which can be an advantage due to its higher ability to form ABS. However, inorganic salts often originate basic aqueous solutions, as occurred in all  $K_3PO_4$ -based systems in this work, which may be a drawback for its application of biomolecules, as for example proteins, due to its sensibility to pH variations and result in a denaturated of desired product after separation.<sup>41</sup>

Due to this factor, partition is apparently favored to a more “protein-friendly” phase, as are IL/FIL’s phases.

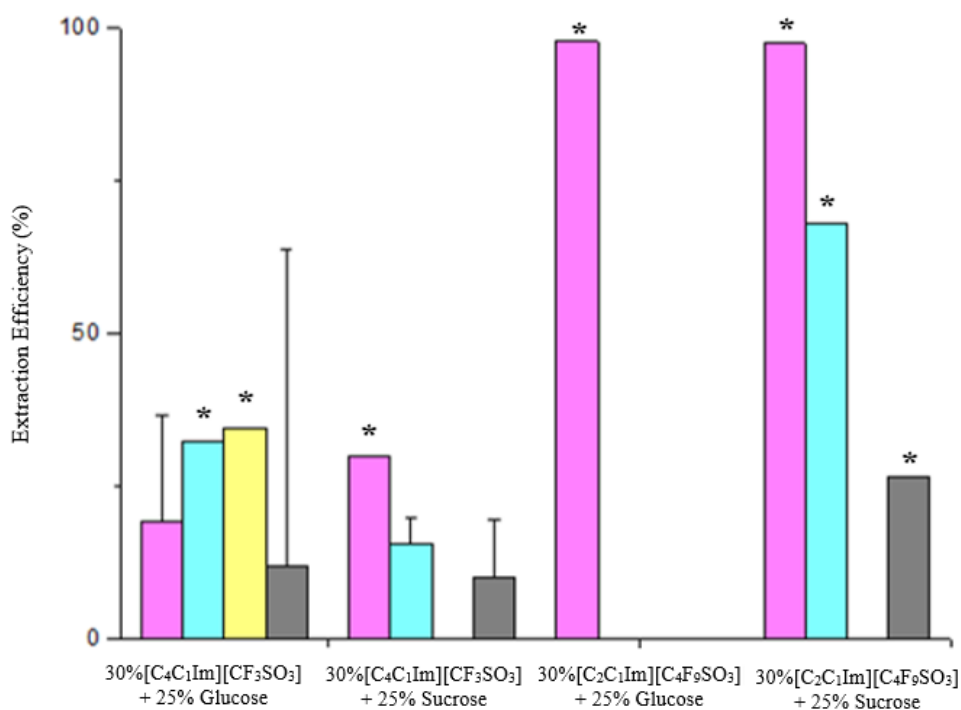


Figure 3. 10 Extraction Efficiencies of Lysozyme for each system of [C<sub>4</sub>C<sub>1</sub>Im][CF<sub>3</sub>SO<sub>3</sub>] and [C<sub>2</sub>C<sub>1</sub>Im][C<sub>4</sub>F<sub>9</sub>SO<sub>3</sub>] using Sucrose and Glucose as salting-out agent at 25°C, using several detection methods: • UV-Vis; • BCA; • μBCA; • Coomassie. \* Systems without replicates

On the other hand, carbohydrate-based systems were analyzed, using IL, [C<sub>4</sub>C<sub>1</sub>Im][CF<sub>3</sub>SO<sub>3</sub>], and the respective FIL, [C<sub>2</sub>C<sub>1</sub>Im][C<sub>4</sub>F<sub>9</sub>SO<sub>3</sub>]. Comparison of IL/FIL with the same cation would be ideal, however, due to the fact that [C<sub>2</sub>C<sub>1</sub>Im][CF<sub>3</sub>SO<sub>3</sub>] did not form demixing with carbohydrates tested and as was shown in previous section the negligible effect of alkylic chain in cation, [C<sub>4</sub>C<sub>1</sub>Im][CF<sub>3</sub>SO<sub>3</sub>] will be used for further analysis.

Figure 3.10 represents both [C<sub>4</sub>C<sub>1</sub>Im][CF<sub>3</sub>SO<sub>3</sub>] and [C<sub>2</sub>C<sub>1</sub>Im][C<sub>4</sub>F<sub>9</sub>SO<sub>3</sub>] EE% with carbohydrates D-(+)-Glucose and Sucrose.

As referred earlier, carbohydrate-based systems interfered with colorimetric assays and in that sense only UV-Vis spectroscopy results were taken in account for the quantitative analysis and colorimetric assays only prove the presence of Lys in the phases. In the case of [C<sub>2</sub>C<sub>1</sub>Im][C<sub>4</sub>F<sub>9</sub>SO<sub>3</sub>]-rich phase, a Lys spectrum overlapped with FIL spectrum was observed, possibly due to visual turbidity in the phase containing Lys, but not in the respective blank. Therefore, for the analysis of [C<sub>2</sub>C<sub>1</sub>Im][C<sub>4</sub>F<sub>9</sub>SO<sub>3</sub>]-based systems carbohydrate-rich phases were used for a quantitative analysis, and FIL-rich phase qualitatively.

Considering the data of both carbohydrates used, the fluorinated IL seems to favor partition to FIL-rich phase. Comparing the respective IL systems it is verified the increase of EE% from 19.21 and 29.99% to 98.68 and 98.83% for Glucose and Sucrose-based systems, respectively, as it is presented in Table 6.27. Since both binodal and phase characteristics (phase pH and size) are equivalent, there are no evidences that systems parameters other than the fluorination of the anion itself coordinate the partition.

Previous studies suggested fluorination as a key factor for the formation of self-assembled structures, and it was determined three critical aggregation concentrations (CACs) for  $[C_2C_1Im][C_4F_9SO_3]$  and was possible to demonstrate the formation of different structures associated to this concentrations.<sup>25</sup> Besides, above this FIL's CACs, the presence of  $[C_2C_1Im][C_4F_9SO_3]$  not only increased Lysozyme activity, but also enzyme activity analysis did not show signs of activity loss once protein is encapsulated inside the FIL micelles. Also, CD analysis showed protein structure was not significantly changed by FIL presence in either concentration above or below CAC.<sup>29</sup> In addition, these aggregates seem to be relatively stable up to 12h after incubation, where no significant protein was released from structures.<sup>42</sup>

Therefore,  $[C_2C_1Im][C_4F_9SO_3]$  is likely to encapsulate Lysozyme during extraction process, with maintenance of its activity and structure, permitting a higher partition to FIL-rich phase when compared to the respective IL, which is unable to form this type of structures. Consequently, it is possible to assume fluorination of the IL anion is a key factor for tailoring ABS systems partition. In this sense, designing ABS with FIL led to an abrupt change on partition phase preference, from CH-rich phase to FIL-rich phase.

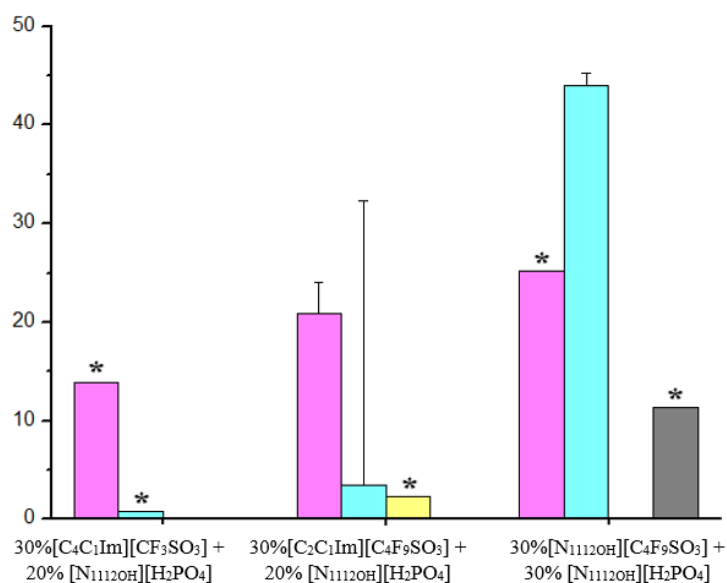


Figure 3.11 Extraction Efficiencies of Lysozyme for each system containing  $[N_{1112OH}][H_2PO_4]$  and respective extraction point at 25°C, using several detection methods: • UV-Vis; • BCA; • μBCA; • Coomassie. \* Systems without replicates

Figure 3.11 represents EE% for systems composed by the salt  $[N_{1112OH}][H_2PO_4]$  and  $[C_4C_1Im][CF_3SO_3]$ ,  $[C_2C_1Im][C_4F_9SO_3]$  and  $[N_{1112OH}][C_4F_9SO_3]$ . As occurred in previous analysis with carbohydrates, anion fluorination increased the partition to FIL-rich phase, comparing with  $[C_4C_1Im][CF_3SO_3]$  system. However, the effect is not as prominent as with carbohydrate-based systems extraction, with an increase of 13.84 to 20.82%,  $[C_4C_1Im][CF_3SO_3]$  and



[C<sub>2</sub>C<sub>1</sub>Im][C<sub>4</sub>F<sub>9</sub>SO<sub>3</sub>], respectively, considering UV-Vis spectroscopy detection methodology. Hence, as occurred for carbohydrate-based systems, the self-aggregation behavior may also be an EE% increasing factor when compared to IL system.

In the set of systems composed by [N<sub>1112OH</sub>][H<sub>2</sub>PO<sub>4</sub>], a choline-based FIL was also tested in terms of partition, [N<sub>1112OH</sub>][C<sub>4</sub>F<sub>9</sub>SO<sub>3</sub>]. Although this system presented some disparity between detection techniques, considering UV-Vis spectroscopy analysis, the EE% is 25.23%. It is important to highlight the similarity in partition capacity for [N<sub>1112OH</sub>][C<sub>4</sub>F<sub>9</sub>SO<sub>3</sub>] and [C<sub>2</sub>C<sub>1</sub>Im][C<sub>4</sub>F<sub>9</sub>SO<sub>3</sub>]-based systems, where both permitted the favored partition to FIL-rich phase, therefore fluorination of the anion, independent of the nature of the cation leads to similar extraction capacity.

In the past few years, choline-based molten salts have been investigated for their use as protein solvents, due to their biocompatibility and capability of solubilizing proteins. In particular, studies on [N<sub>1112OH</sub>][H<sub>2</sub>PO<sub>4</sub>] have showed their ability to stabilize proteins for longer periods of time, protection against chemical denaturants and high temperatures. Besides, for some proteins, namely Cytochrome C, [N<sub>1112OH</sub>][H<sub>2</sub>PO<sub>4</sub>] presence increased catalytic activity.<sup>43</sup> These kind of properties are very attractive for its application in extraction systems, because it is crucial the preservation of solute activity and structure after its extraction. On the other hand, as both phases stabilize protein, it is possible some competitive partition between FIL-rich phase and salt-rich phase, and may justify a decrease of %EE relatively to the carbohydrate-based systems.

As discussed in section 3.1 “Phase Diagrams”, [N<sub>1112OH</sub>][C<sub>4</sub>F<sub>9</sub>SO<sub>3</sub>] was the FIL-based system with minor biphasic region, and was not possible to test partition with lower concentrations of salt lesser than 30% wt. However, [C<sub>2</sub>C<sub>1</sub>Im][C<sub>4</sub>F<sub>9</sub>SO<sub>3</sub>] has a larger biphasic region than choline-based FIL, and [N<sub>1112OH</sub>][H<sub>2</sub>PO<sub>4</sub>] concentration effect is studied next.

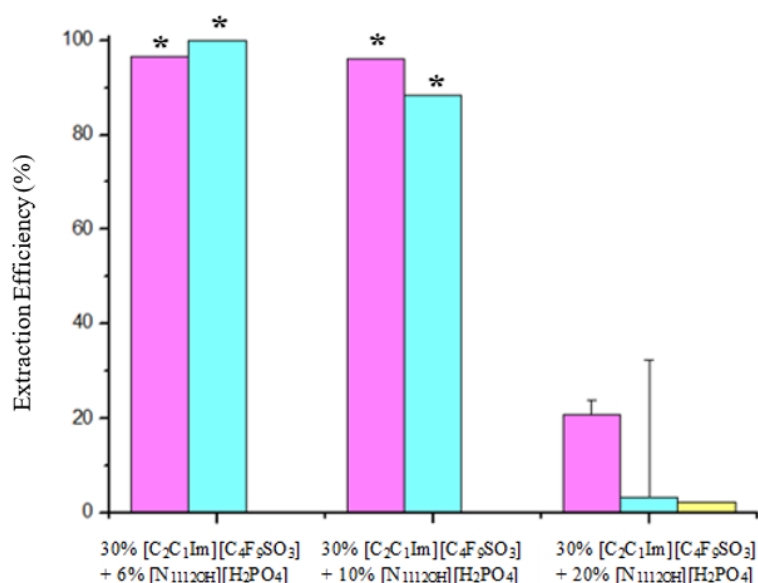


Figure 3. 12 Extraction Efficiencies of Lysozyme for systems 30%wt [C<sub>2</sub>C<sub>1</sub>Im][C<sub>4</sub>F<sub>9</sub>SO<sub>3</sub>] + 6, 10 and 20% wt [N<sub>1112OH</sub>][H<sub>2</sub>PO<sub>4</sub>] and 30% [N<sub>1112OH</sub>][C<sub>4</sub>F<sub>9</sub>SO<sub>3</sub>] + 30% [N<sub>1112OH</sub>][H<sub>2</sub>PO<sub>4</sub>] at 25°C, and the several detection method: • UV-Vis; • BCA; • μBCA; • Coomassie. \* Systems without replicates

In Figure 3.12 is represented the effect of the increasing concentration of  $[N_{11120H}][H_2PO_4]$  (6% to 20% wt) in fixed concentration of  $[C_2C_1Im][C_4F_9SO_3]$ . It is possible to notice total partition to FIL-rich phase for both 6% and 10% wt  $[N_{11120H}][H_2PO_4]$ . However, for 20%  $[N_{11120H}][H_2PO_4]$  an abrupt decrease on %EE is observed. It is verified almost 100% EE% at lower concentrations of  $[N_{11120H}][H_2PO_4]$ , and at 20%  $[N_{11120H}][H_2PO_4]$  it is obtained EE% of 20.82%, considering UV-Vis spectroscopy results. Due to  $[N_{11120H}][H_2PO_4]$  protein stabilizing character discussed earlier on this discussion, it is possible that protein structure is stable in both phases, and competitive partition occurs in both phases.

On the other hand, although was not found direct evidence of phosphate-based salts effect on surfactant FILs in terms of aggregation process, it is established that the increase of ionic strength on ionic surfactants solution change some aggregation properties, namely surfactant critical micelle concentration (CMC).<sup>44,45</sup> Since self-aggregation of the FIL was thought to control the partition, it is possible the higher concentration of the salt may have a more pronounced effect on formation of these aggregates, interfering with the encapsulation of the protein and hamper partition to FIL-rich phase.

Despite any possible influence  $[N_{11120H}][H_2PO_4]$  provokes on FIL aggregation behavior, it is undeniable the advantages on designing ABS with FILs and using this salt as salting-out agent. In this case,  $[C_2C_1Im][C_4F_9SO_3]$  allowed the design of an ABS with a more hydrophobic FIL (with maintained water solubility) and permitting a larger biphasic region than  $[C_4C_1Im][CF_3SO_3]$  and also  $[N_{11120H}][C_4F_9SO_3]$  (as verified earlier in Figure 3.3), which allowed a wider range of  $[N_{11120H}][H_2PO_4]$  concentrations with different partition behavior, from major partition to FIL-rich phase to major partition to salt-rich phase. Therefore, functionalization of either the cation (from  $[N_{11120H}]$ - to  $[C_2C_1Im]$ -based FIL) or either the anion (from  $[CF_3SO_3]$ - to  $[C_4F_9SO_3]$ -based IL) permitted different behaviors in partition, giving rise a more versatile extraction system.

### 3.5. Lysozyme Activity – Partitioned Lysozyme

In this section, partitioned Lys enzymatic activity was analyzed for 7 systems. Lysozyme concentration in each phase was estimated by detection methodologies presented earlier in this work and the Lys enzymatic activity was applied in each phase after partition procedure. Besides quantification of the partitioned Lys, it is important to access if protein maintains its activity after partitioned to target phase.

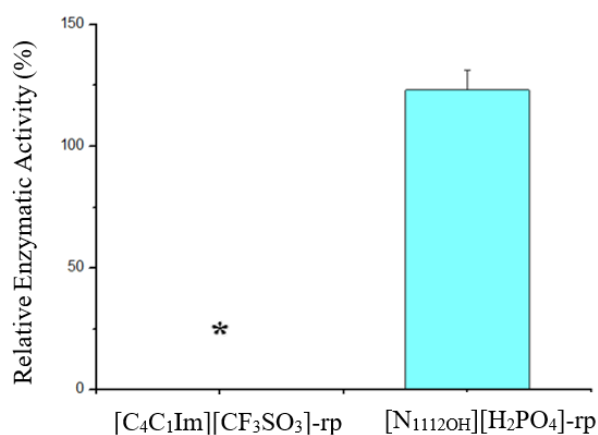


Figure 3. 13 Lysozyme relative enzymatic activity of 30%[C<sub>4</sub>C<sub>1</sub>Im][CF<sub>3</sub>SO<sub>3</sub>]+20%[N<sub>1112</sub>OH][H<sub>2</sub>PO<sub>4</sub>] for each phase. \* not possible to quantify enzymatic activity in this phase.

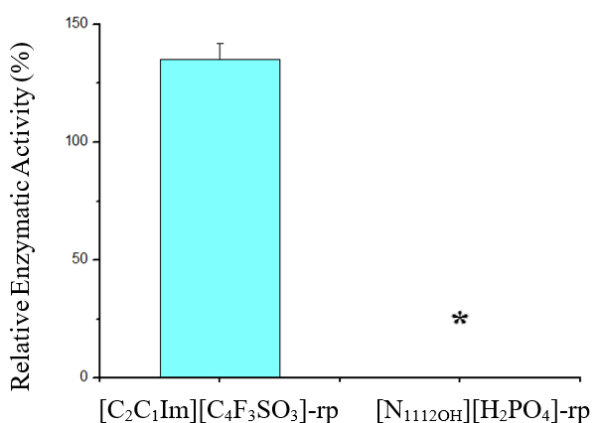


Figure 3. 14 Lysozyme relative enzymatic activity of 30%[C<sub>2</sub>C<sub>1</sub>Im][C<sub>4</sub>F<sub>3</sub>SO<sub>3</sub>]+6%[N<sub>1112</sub>OH][H<sub>2</sub>PO<sub>4</sub>]. \* not possible to quantify enzymatic activity in this phase (below assay detection limit).

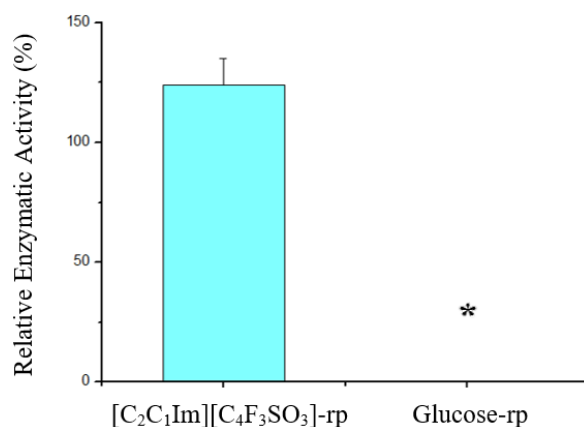


Figure 3. 15 Lysozyme relative enzymatic activity of 30%[C<sub>2</sub>C<sub>1</sub>Im][C<sub>4</sub>F<sub>9</sub>SO<sub>3</sub>]+25%Glucose. \* not possible to quantify enzymatic activity in this phase (below assay detection limit).

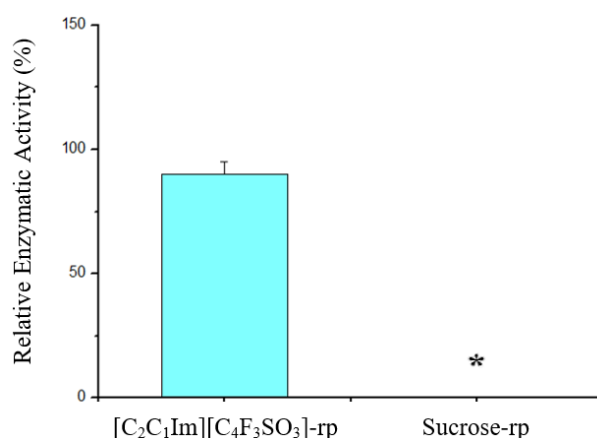


Figure 3. 16 Lysozyme relative enzymatic activity of 30%[C<sub>2</sub>C<sub>1</sub>Im][C<sub>4</sub>F<sub>9</sub>SO<sub>3</sub>]+25%Sucrose. \* not possible to quantify enzymatic activity in this phase (below assay detection limit).

First system being analyzed is represented in Figure 3.13 - 30% [C<sub>4</sub>C<sub>1</sub>Im][CF<sub>3</sub>SO<sub>3</sub>] + 20% [N<sub>11120H</sub>][H<sub>2</sub>PO<sub>4</sub>]. This system permitted major partition to salt-aqueous rich phase, as verified by both UV-Vis and BCA assays (extraction efficiency ranging 13.84% and 0.78%, respectively). It is evident the maintenance of Lys activity after the partition procedure for the target phase, in this case [N<sub>11120H</sub>][H<sub>2</sub>PO<sub>4</sub>]-rich phase; it was not possible, however, determine the enzymatic activity of Lys, possible due to insufficient concentration of the protein to apply the protocol.

Figures 3.14 to 3.16 represent Lys relative enzymatic activity of systems composed by [C<sub>2</sub>C<sub>1</sub>Im][C<sub>4</sub>F<sub>9</sub>SO<sub>3</sub>], which partition showed results of Extraction Efficiency above 96% to FIL aqueous rich phase. In this sense, this phase permitted the maintenance of Lys activity, as verified earlier in screening assays of this compound in water. It was not possible to detect Lys in the enzymatic activity assay for [N<sub>11120H</sub>][H<sub>2</sub>PO<sub>4</sub>] and carbohydrates-rich phase, due to low concentration of Lys in the phase and below the detection limit of the assay.

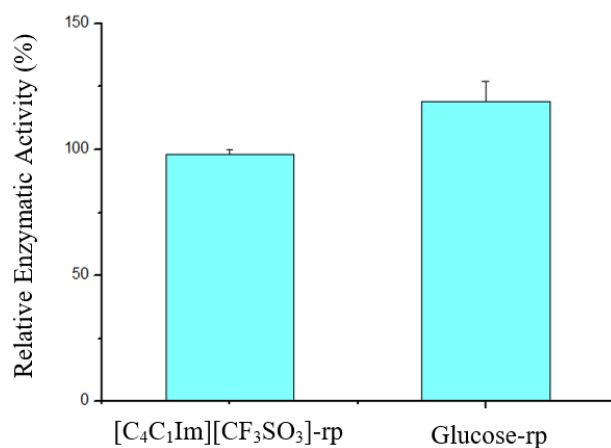


Figure 3. 17 Lysozyme relative enzymatic activity of 30% $[C_4C_1Im][CF_3SO_3]$ +25%Glucose.

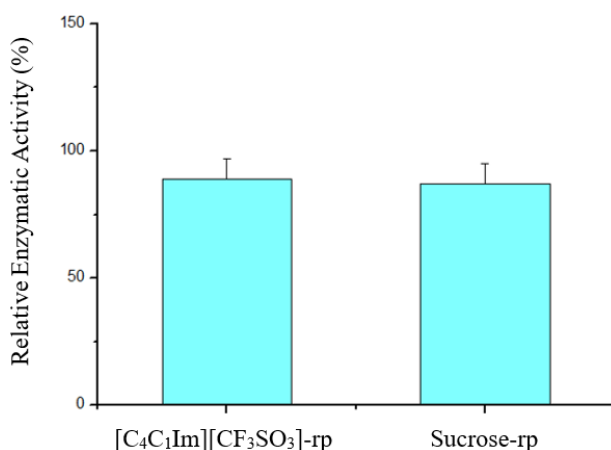


Figure 3. 18 Lysozyme relative enzymatic activity of 30% $[C_4C_1Im][CF_3SO_3]$ +25%Sucrose.

Figures 3.17 and 3.18 represent Lysozyme relative enzymatic activity for IL  $[C_4C_1Im][CF_3SO_3]$ -based systems composed by carbohydrates. Previously was determined extraction efficiency ranged the 15 and 30% for Glucose and Sucrose-based systems, using both UV-Vis spectroscopy and BCA assay. It was possible to determine Lys enzymatic activity for both phases in all the systems presented, and was verified the maintenance of Lys activity after partition in all phases tested, as predicted by screening enzymatic activity assays earlier. Therefore, it was confirmed the presence of Lys in both phases determined by detection methodology in previous section.

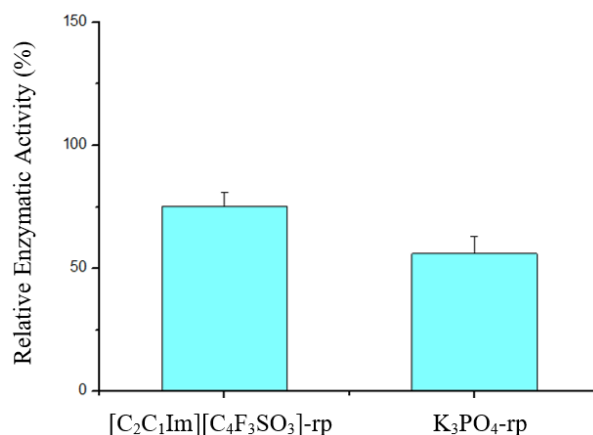


Figure 3. 19 Lysozyme relative enzymatic activity of 30%[C<sub>2</sub>C<sub>1</sub>Im][C<sub>4</sub>F<sub>9</sub>SO<sub>3</sub>]+2%K<sub>3</sub>PO<sub>4</sub>.

At last, it is represented in Figure 3.19 the system 30%[C<sub>2</sub>C<sub>1</sub>Im][C<sub>4</sub>F<sub>9</sub>SO<sub>3</sub>] + 2%K<sub>3</sub>PO<sub>4</sub>. In this case, for both UV-Vis spectroscopy and BCA assay, the extraction efficiency in above 91%. It is noticeable the maintenance of Lys activity after partition in FIL-rich phase (approximately 75% relatively to the respective Lys blank). However, it is perceptible a decrease of Lys enzymatic activity in IS-rich phase to 56%. This result was unexpected due to screening assays, which indicated the maintenance of Lys activity at this K<sub>3</sub>PO<sub>4</sub> concentration in aqueous solution. There is no indication of an interference in the assay reagents, due to the enzymatic kinetics detected at A<sub>450nm</sub> equivalent of the blank and remaining assays.

Besides these factors, it is important to consider the fact Lys was in contact with different compounds during extraction procedure, rather than an aqueous solution of one compound, as happened in screening assays. Therefore, it is important to consider the actual activity lost during extraction, rather than assume some protocol error, in particular due to maintenance of Lys enzymatic kinetics in this phase during the assay.

### 3.6. IL/FIL-Protein Interaction Studies

Several techniques were used in order to analyze the possibility of interactions between protein and the Ionic Liquid [C<sub>4</sub>C<sub>1</sub>Im][CF<sub>3</sub>SO<sub>3</sub>], the Fluorinated Ionic Liquid [C<sub>2</sub>C<sub>1</sub>Im][C<sub>4</sub>F<sub>9</sub>SO<sub>3</sub>] and salt [N<sub>11120H</sub>][H<sub>2</sub>PO<sub>4</sub>]. Study of these interactions is very important in order to understand the nature of interactions, and which changes are occurring in the protein, either stabilizing or not the protein. These interactions are dependent on the properties of both protein and ILs.<sup>30</sup>

In this Section are presented Turbidimetry, Absorbance, Tryptophan Intrinsic Fluorescence and nano Differential Scanning Calorimetry (nano DSC) studies.

#### Turbidimetry

Fluorinated Ionic Liquids are considered Surface Active ILs (SAILs), and interaction between FIL and protein must be taken in consideration. Lysozyme interacts with Surface Active Ionic Liquids (SAILs) either by electrostatic interaction, where positively charged net Lysozyme at pH 7.4 interacts with Surface Active Ionic Liquids in order to form a neutral complex, leading to a turbid aqueous solution; and by non-electrostatic interactions, where different levels of hydrophobicity lead to different interactions with the protein, also providing different degrees of turbidity.<sup>30 46</sup> Therefore, following the changes of turbidity of protein-IL aqueous solution may provide information relatively to interactions occurring between the two components.

In this work, were tested different concentrations of the IL [C<sub>4</sub>C<sub>1</sub>Im][CF<sub>3</sub>SO<sub>3</sub>] and FIL [C<sub>2</sub>C<sub>1</sub>Im][C<sub>4</sub>F<sub>9</sub>SO<sub>3</sub>] – 0.1 to 120mM. As mentioned before, this FIL has several CACs, at which the solvent self-aggregate in different structures. The concentration range was chosen in order to study the possibility of these structures influence the interaction with Lysozyme. Table 3.2 represents CACs for [C<sub>2</sub>C<sub>1</sub>Im][C<sub>4</sub>F<sub>9</sub>SO<sub>3</sub>].

*Table 3. 1 Critical aggregation concentrations (CACs) of [C<sub>2</sub>C<sub>1</sub>Im][C<sub>4</sub>F<sub>9</sub>SO<sub>3</sub>] in aqueous solutions determined by Isothermal Calorimetry at 25°C.<sup>25</sup>*

	CACs for [C <sub>2</sub> C <sub>1</sub> Im][C <sub>4</sub> F <sub>9</sub> SO <sub>3</sub> ] (mM)
First CAC	14.40
Second CAC	34.48
Third CAC	76.54
Fourth CAC	106.09

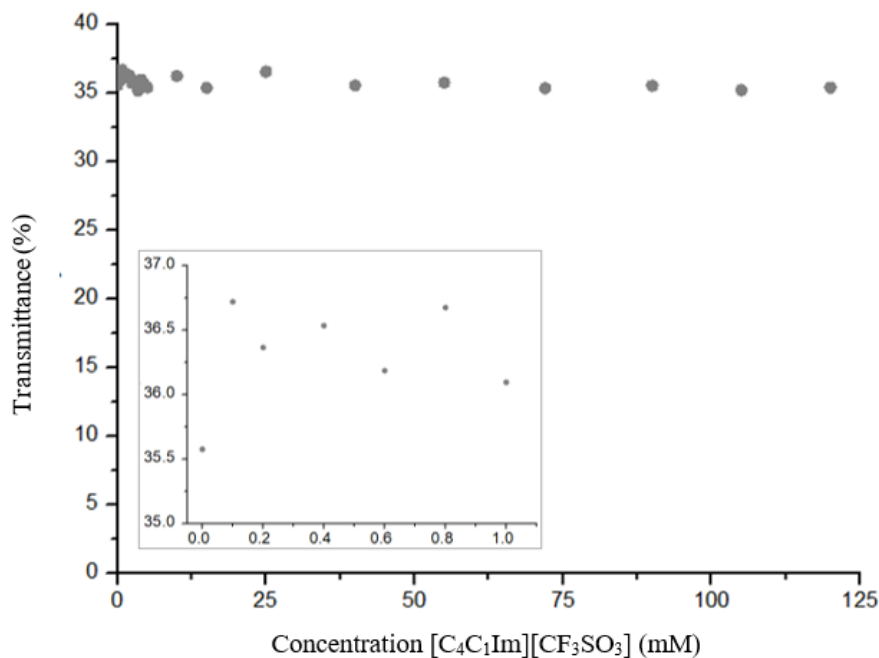


Figure 3. 20 Turbidity of Lysozyme (0.2mg/mL) as a function of IL [C<sub>4</sub>C<sub>1</sub>Im][CF<sub>3</sub>SO<sub>3</sub>] concentration at 25°C.

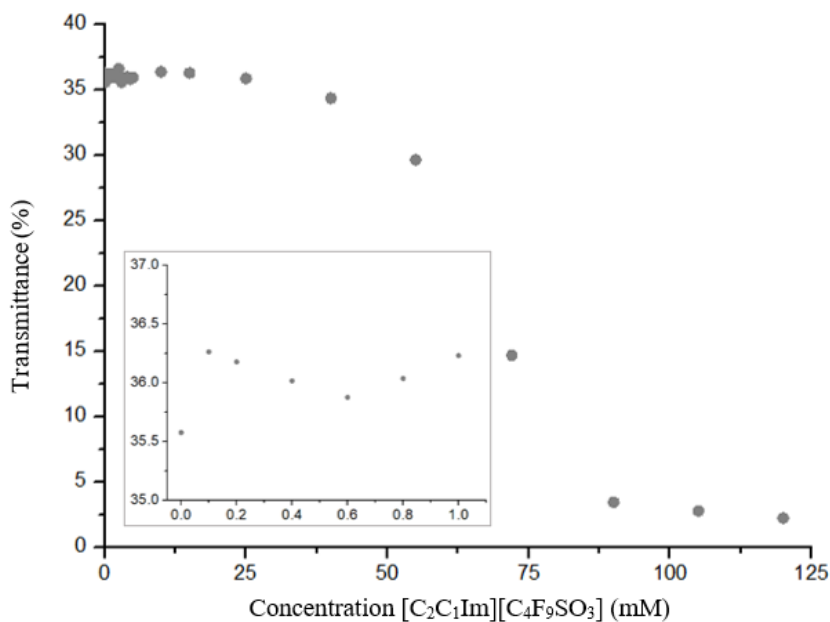


Figure 3. 21 Turbidity of Lysozyme (0.2mg/mL) as a function of IL [C<sub>2</sub>C<sub>1</sub>Im][C<sub>4</sub>F<sub>9</sub>SO<sub>3</sub>] concentration at 25°C.

Figures 3.20 and 3.21 represent the IL and FIL aqueous solutions turbidity in terms of its concentration, respectively, at which Lysozyme is at a constant concentration of 0.2mg/mL. It is possible to verify IL [C<sub>4</sub>C<sub>1</sub>Im][CF<sub>3</sub>SO<sub>3</sub>] shows constant turbidity with increasing IL concentrations, therefore, turbidity is independent of IL concentration, and no interaction is presumed by these results. On the other hand, FIL presents constant turbidity until concentration



of 15mM, slightly above the first CAC. After this concentration, it is showed an abrupt transmittance decay. Thus, it is assumed a strong interaction Lysozyme-FIL, possibly by a formation of protein-FIL aggregates, as occurred with this protein and another SAIL.<sup>46</sup>

The FIL [C<sub>2</sub>C<sub>1</sub>Im][C<sub>4</sub>F<sub>9</sub>SO<sub>3</sub>] presents a more hydrophobic character than the IL [C<sub>4</sub>C<sub>1</sub>Im][CF<sub>3</sub>SO<sub>3</sub>], due to an increased fluorinated alkyl chain of the anion. Once the FIL presented turbidity profiles that were not present in IL solution, it is possible to assume the increased hydrophobicity permitted non-electrostatic interaction between FIL and protein. Also, in this case, an increase of FIL concentration also led to a more pronounced interaction. At higher concentrations than the first CAC, several aggregate structures are formed and hydrophobicity is increased, possibly increasing the interaction between FIL and the protein.

However, for both IL and FIL it is verified an abrupt increase of turbidity from Lys in water and at lowest concentration of IL/FIL. This increased turbidity may be attributed to some electrostatic interaction starting to occur between the positively charged net of the protein and the negative counterpart of the IL/FIL, which results in turbid aqueous solutions.

Up to 1.0mM, [C<sub>4</sub>C<sub>1</sub>Im][CF<sub>3</sub>SO<sub>3</sub>] and [C<sub>2</sub>C<sub>1</sub>Im][C<sub>4</sub>F<sub>9</sub>SO<sub>3</sub>] present different behavior in terms of turbidity. IL present random turbidity variation; on the other hand, FIL exhibits “U” shape tendency, with minimum transmittance at 0.6mM. It is possible this tendency verified be also indicative of some interaction between protein and FIL monomers, but further studies are needed to confirm and understand the nature and extent of these interactions.

### Absorbance

Lysozyme contains aromatic amino acids, namely six residues of Tryptophan, that can be used as probes for protein conformational changes. Particularly, some of these residues are located in the active site and others in the hydrophobic region of the protein. This amino acid presents a characteristic band between 260 and 300 nm, with a maximum peak at 280 nm. Any deviations in this peak to 301 nm may be informative of conformational changes occurring in the local Tryptophan environment. Therefore, absorption measurements in the UV-Vis range are an informative of possible interactions occurring between IL/FIL and protein.<sup>47</sup>

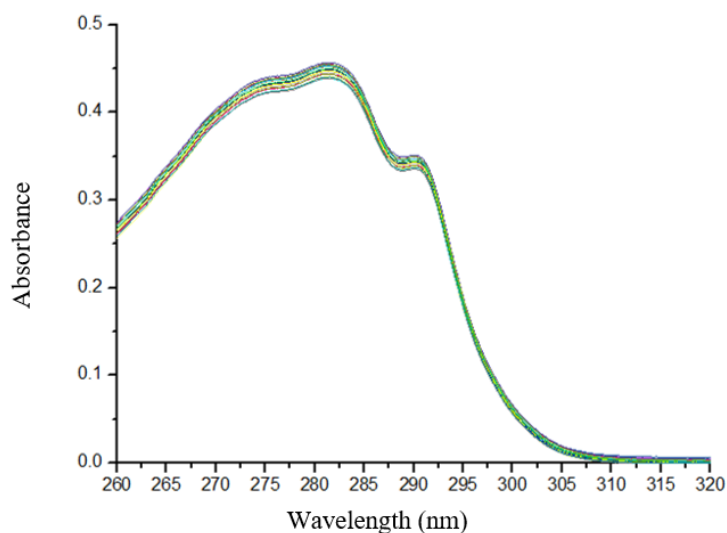


Figure 3. 22 UV-Vis absorption spectra of Lysozyme in the different concentrations of  $[C_4C_1Im][CF_3SO_3]$  studied in this work (0-120mM).

Figure 3.22 represents UV-Vis absorption spectra of Lysozyme at different concentrations of IL  $[C_4C_1Im][CF_3SO_3]$  (0-120mM). It is noticeable for all concentrations Lys characteristic spectra was kept, i.e. an absorbance band between 260 and 300 nm, with the maximum at 280 nm. On the other hand, spectra baseline was also preserved, thus the absence of turbidity in solution was confirmed. It is proposed the maintenance of Lysozyme conformation in these solutions due to lack of spectral deviations, and it was verified earlier the conservation of enzymatic activity in this IL, and therefore, not likely protein unfolding to occur.

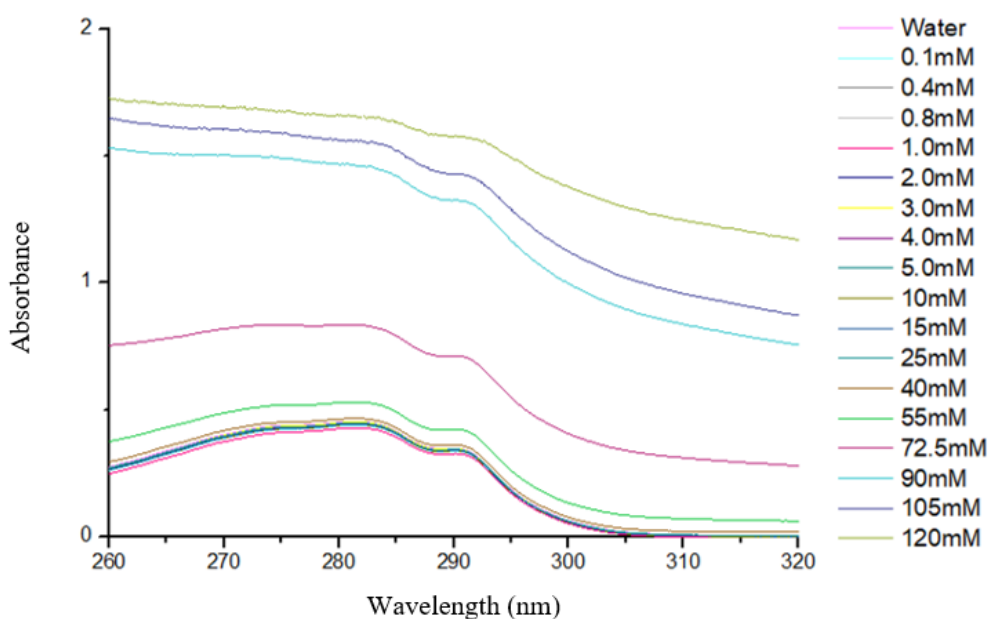


Figure 3. 23 UV-Vis absorption spectra of Lysozyme in the different concentrations of  $[C_2C_1Im][C_4F_9SO_3]$  studied in this work (0-120mM).

Figure 3.23 represents UV-Vis absorption spectra of Lysozyme at different concentrations of IL [C<sub>2</sub>C<sub>1</sub>Im][C<sub>4</sub>F<sub>9</sub>SO<sub>3</sub>] (0-120mM). Spectra for all concentration do not present any maximum peak deviation and have the same profile as Lysozyme in water, therefore, it is unlikely the unfolding of the protein.<sup>47</sup>

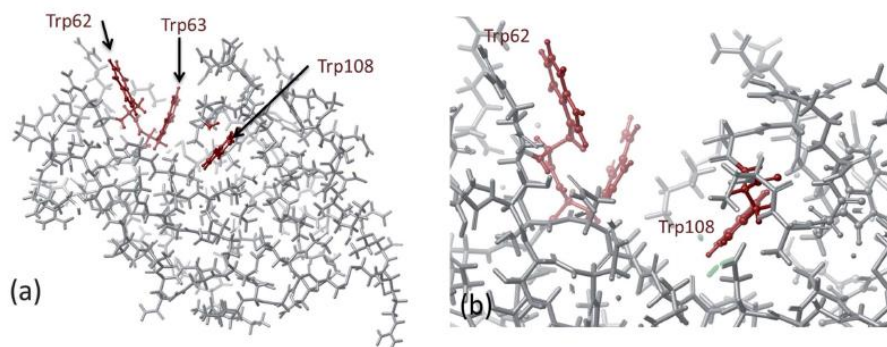
Up to 40mM, spectra are overposed to Lysozyme spectra in water, thus no interaction is projected. On the other hand, FIL solution above 55mM (between second and third CAC) presented turbidity and it is reflected on absorbance spectra, where the spectra lost its baseline, increased intensity and appears to become more flatted (more proeminent at concentrations above 90mM), and this behavior was previously proposed as possible encapsulation of lysozyme by the FIL.<sup>47</sup>

Due to the presence of turbidity of these solutions and these results together may be indicative of some interactions occuring and possibly encapsulation of Lysozyme in the structures formed by FIL. However, there is no deviation of the maximum peak, thus no unfolding is predicted.

## Fluorescence

Proteins' fluorescence studies are highly sensitive to biomolecule's conformational variations. Protein may contain intrinsic fluorescence, i.e. in its amino acid sequence it is present fluorescent emitting amino acid, such as phenylalanine, tyrosine or tryptophan. These amino acids emission is sensitive to its environment (usually polarity), therefore, changes on these residues' ambience may provide information on the conformational change process.<sup>48</sup>

Lysozyme contains six residues of Tryptophan in its primary structure (Trp 28, 62, 63, 108, 111 and 123). Residues Trp 62, 63 and 108 are localized in the substrate binding pocket; Trp 28 and 111 in hydrophobic region and Trp 123 apart from the other residues. It was verified in previous studies the majority of contribution of fluorescence emission are provoked by Trp 62 and 108, as represented in Figure 3.24, as the rest of the residue's fluorescence emission is quenched by vicinity residues disulphide linkages. Spectra were acquired exciting residues at 295nm. The excitation at this wavelength avoids the excitation of tyrosine and selectively excites tryptophan residues.<sup>49,50</sup>



In this section was carried Intrinsic Fluorescence studies, in order to determine possible conformational changes on Lysozyme due to the presence of  $[C_4C_1Im][CF_3SO_3]$ ,  $[C_2C_1Im][C_4F_9SO_3]$  and  $[N_{1112OH}][H_2PO_4]$ . Emission spectra were recorded in the wavelength range of 300-500nm for Lysozyme concentration of 0.2 mg/mL in the presence of several IL/FIL/salt concentrations, after excitation of Tryptophan residues at 295nm.

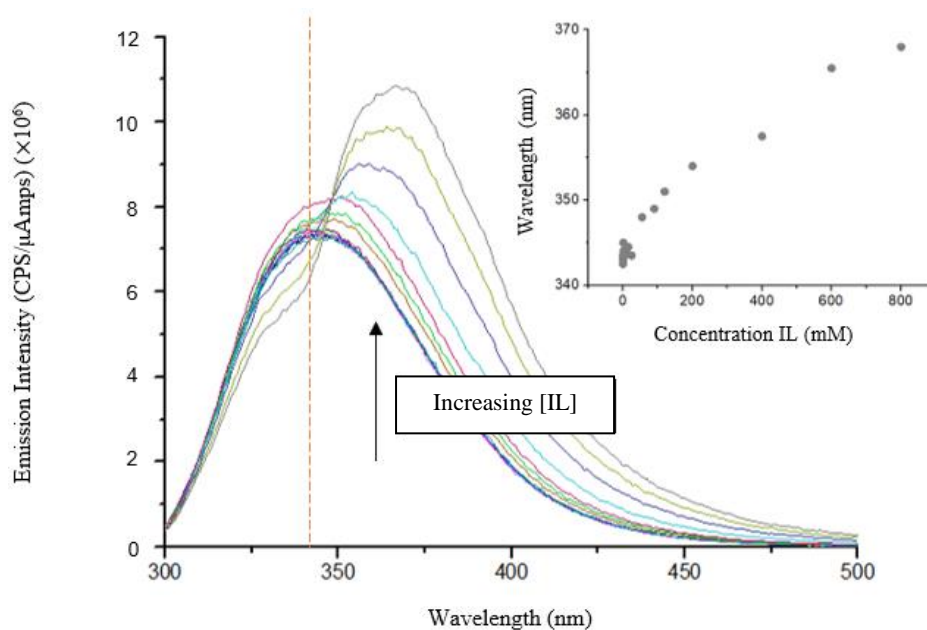


Figure 3. 25 Fluorescence spectra of Lysozyme acquired at 25°C for  $[C_4C_1Im][CF_3SO_3]$  concentrations (0-800mM).

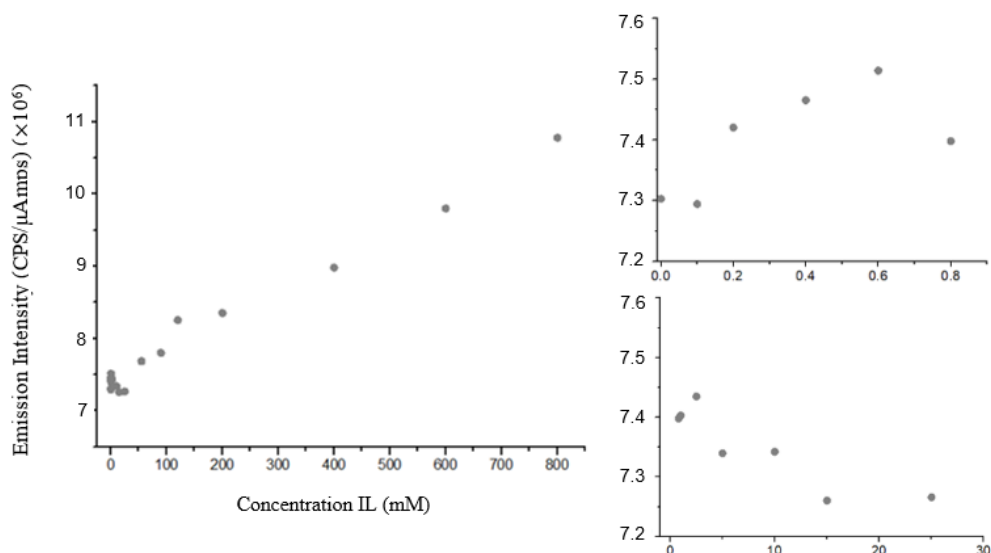


Figure 3. 26 Emission intensity of Lysozyme at 0.2mg/mL recorded at each maxima wavelength for  $[C_4C_1Im][CF_3SO_3]$ .

Figure 3.25 represents fluorescence spectra of Lysozyme in the presence of several concentrations of  $[C_4C_1Im][CF_3SO_3]$ . Until the concentration of 25mM, no peak shift is observed. However, above this concentration it is verified a red shift, from 334nm to 368nm. Red shift of  $\lambda_{max}$  is usually associated to globular protein unfolding, due to the presence of hydrophilic solvent.<sup>51</sup>

Figure 3.26 characterizes the fluorescence emission intensity at each wavelength is observed the maximum intensity. Overall, it is verified an increase in intensity with the increase of IL concentration, and more evident above 25mM. Some variations are observed at lower concentrations. Up to 0.6mM (Figure 3.26, up right) emission intensity increases, however, up to 25mM it is observed quenching of fluorescence (Figure 3.26, down right). After 25mM it is noticeable an more abrupt increase of fluorescence. This increment on fluorescence emission behavior was previous attributed to possibly a reduced Tryptophan quenching from surrounding residues, caused by the unfolding of the protein, leading to an increase of intensity.<sup>52</sup> This effect reinforces the unfolding suggested before by the red shift of  $\lambda_{max}$  above 25mM.

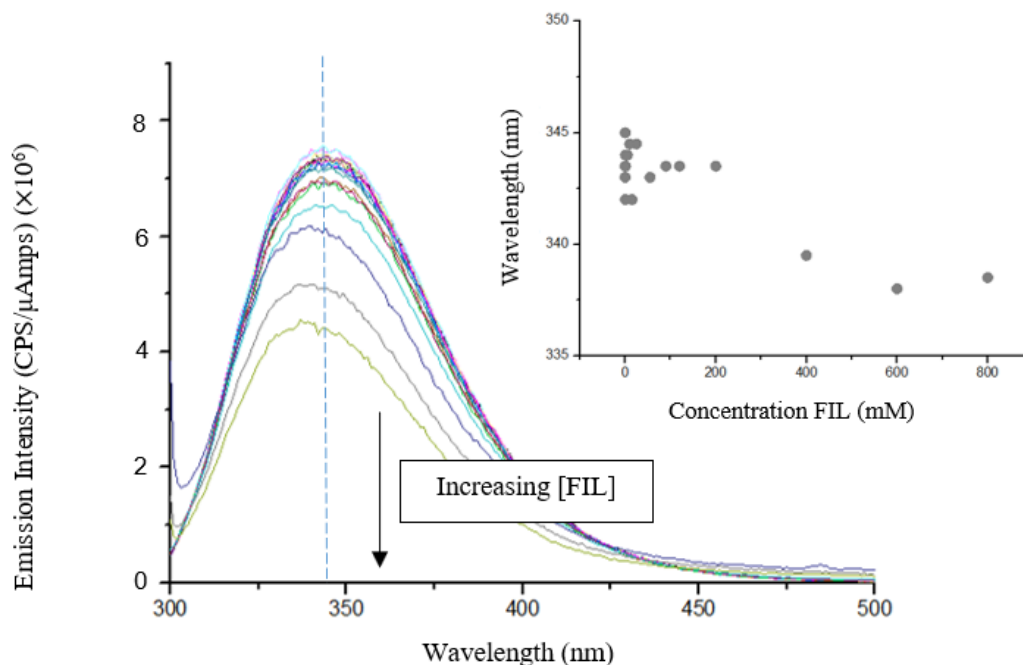


Figure 3. 27 Fluorescence spectra of Lysozyme acquired at 25°C for  $[C_2C_1Im][C_4F_9SO_3]$ .

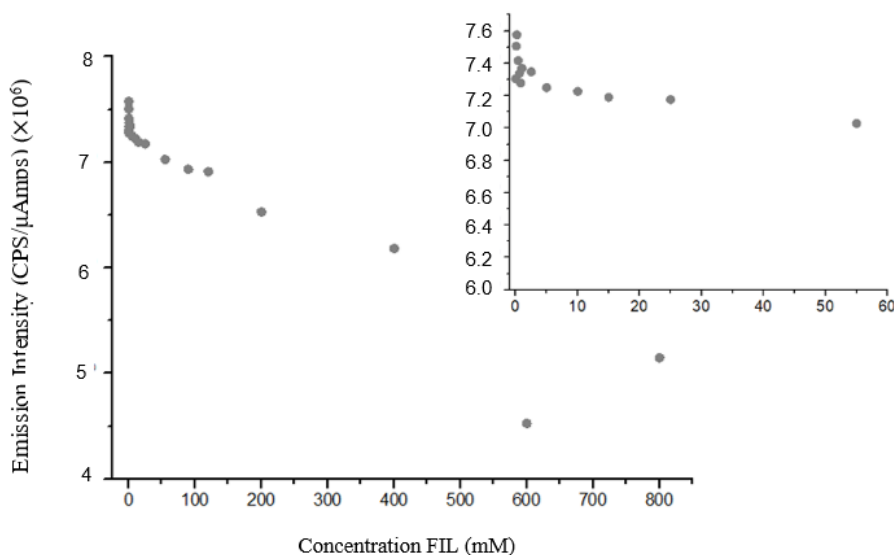


Figure 3. 28 Emission intensity of Lysozyme at 0.2mg/mL recorded at each maxima wavelength for  $[C_2C_1Im][C_4F_9SO_3]$ .

Figure 3.27 represents fluorescence spectra of Lysozyme in the presence of several concentrations of  $[C_2C_1Im][C_4F_9SO_3]$ . It is verified a blue shift above 400mM, from 343nm to 339nm. A blue shift is usually indicator of an increased hydrophobic environment in fluorophore, either by hydrophobic interaction with a nonpolar region of the FIL, or by the internalization of the fluorophore inner the protein core, leading to a more folded conformation.<sup>51 53</sup> Due to the fact  $[C_2C_1Im][C_4F_9SO_3]$  is more hydrophobic than previous  $[C_4C_1Im][CF_3SO_3]$ , it may be explained the more hydrophobic environment in this case. Besides, previous studies have demonstrated the formation of self-aggregation structures by  $[C_2C_1Im][C_4F_9SO_3]$ , which  $[C_4C_1Im][CF_3SO_3]$  is not

capable of forming, and consequently Lysozyme encapsulation in FILs micelles.<sup>25,42</sup> So, it is proposed the interaction of  $[C_4F_9SO_3]^-$  counterpart of FIL during Lysozyme encapsulation, which leads to a more hydrophobic environment of the Tryptophan residues.

Figure 3.28 represents the fluorescence emission intensity at each concentration maximum peak: until 200mM the maximum is at 343nm, meanwhile up to 400mM this peak is shifted to 339nm. At 5mM it is verified a slight decrease on intensity and intensity is maintained approximately constant until 25mM, as presented in Figure 3.28 (right). After this concentration, it is observed a more abrupt decrease of intensity with the increase of IL concentration – quenching of Tryptophan’s fluorescence emission.

Previous studies on Surface Active Ionic Liquids, as is the case of  $[C_2C_1Im][C_4F_9SO_3]$ , it was presented positively charged lysozyme at pH 7.4 can interact with these type of IL by electrostatic and hydrophobic interactions. Also, was proposed the increasing intensity of fluorescence emission is related to a competition between electrostatic and hydrophobic interaction between the IL and the protein, and on the other hand a decreasing in this intensity of emission is related to a dominance of hydrophobic interaction between the two components in solution. Also, this paper presents the formation of IL’s self-aggregation structures as a reason on the decrease of intensity of fluorescence emission.<sup>46</sup> Was also demonstrated in literature Lysozyme is encapsulated in  $[C_2C_1Im][C_4F_9SO_3]$  self-aggregation structures.<sup>29-42</sup> Therefore, the results presented in this section are close related to the literature. It is proposed not only the increased hydrophobic interactions, but also the encapsulation plays a role in diminishing intensity.

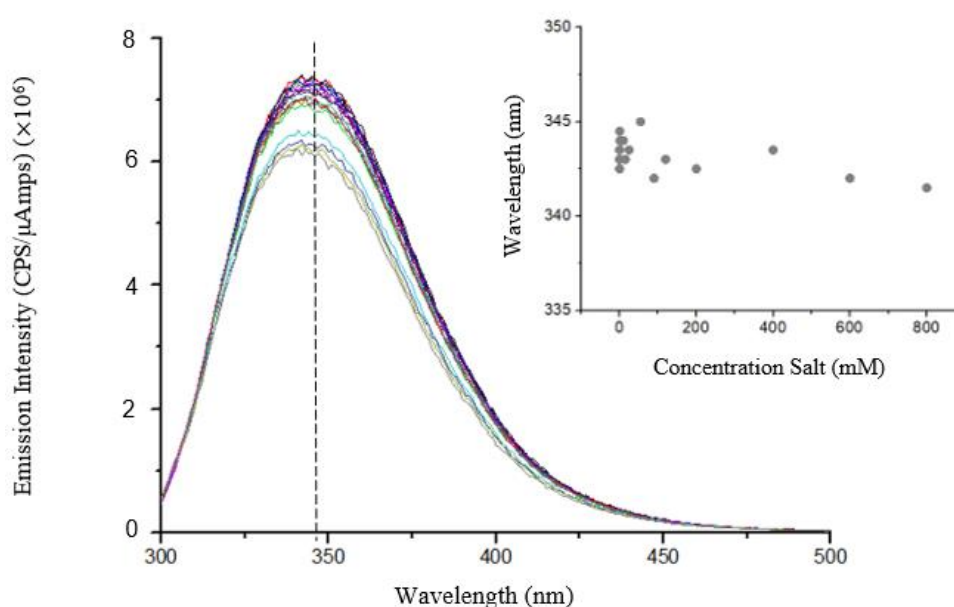


Figure 3. 29 Fluorescence spectra of Lysozyme acquired at 25°C for  $[N_{11120H}][H_2PO_4]$ .

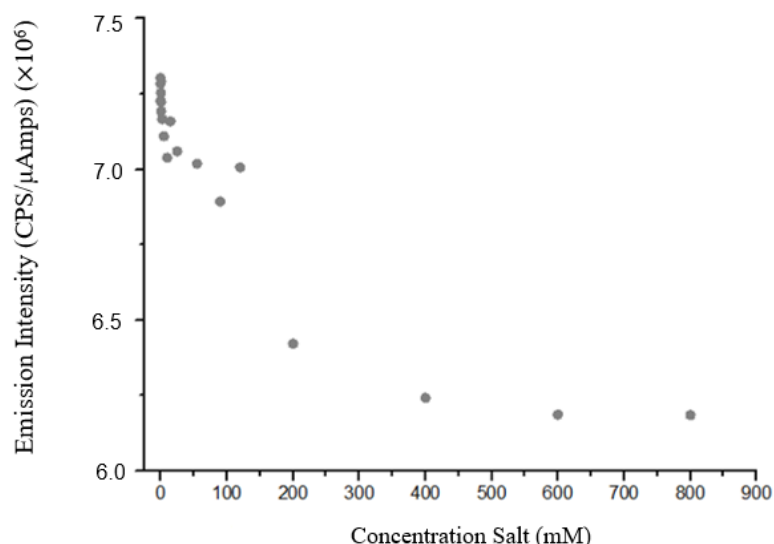


Figure 3.30 Emission intensity of Lysozyme at 0.2mg/mL recorded at 343nm for  $[N_{1112OH}][H_2PO_4]$ .

Figure 3.29 represents fluorescence spectra of Lysozyme in the presence of several concentrations of  $[N_{1112OH}][H_2PO_4]$ . In this case, no shift is observed for any concentration tested, thus it is not proposed any significant variations in polarity occurring in fluorophore environment, therefore no significant conformational changes are associated nearby the fluorophore. Figure 3.30 represents emission intensity of Lysozyme at 343nm. It is verified from 2.5 to 120mM approximately the same emission intensity between concentrations, and a more accentuated decrease in fluorescence emission intensity with increasing  $[N_{1112OH}][H_2PO_4]$  concentrations above 200mM.

This salt is described as a protein stabilizer, and it is proposed to stabilize the folded form of Lysozyme by the same method as other stabilizing salts: salt shields repulsive interactions, stabilizing protein surface electrostatics and reducing the tendency for unfolding.<sup>54</sup> Thus, also considering the results presented earlier for this salt,  $[N_{1112OH}][H_2PO_4]$  seems to contribute to a more folded conformation, indicated by a decrease of fluorescence emission intensity, however fluorophore environment polarity is kept unchanged.

Fluorescence quenching mechanism may be static, where occurs the formation of a ground-state complex between fluorophore and quencher; or on the other hand dynamic, which leads to collisions between fluorophore and the quencher. Both  $[C_2C_1Im][C_4F_9SO_3]$  and  $[N_{1112OH}][H_2PO_4]$  led to quenching of Trp residues of Lys, and collisional quenching mechanism may be represented by Stern-Volmer equation, as presented earlier in Section 2.8:

$$\frac{F_0}{F} = 1 + K_{SV}[Q] = 1 + k_q\tau_0[Q]$$



Where  $F_0$  and  $F$  represent the fluorescence intensities of the fluorophore in the absence and in the presence of quencher,  $[Q]$  is the concentration of the quencher, in this case either  $[C_2C_1Im][C_4F_9SO_3]$  or  $[N_{1112OH}][H_2PO_4]$  and  $K_{SV} = k_q\tau_0$  is the Stern-Volmer constant (considering dynamic quenching),  $k_q$  is the bimolecular quenching constant and  $\tau_0$  is the lifetime of the fluorophore in the absence of the quencher.

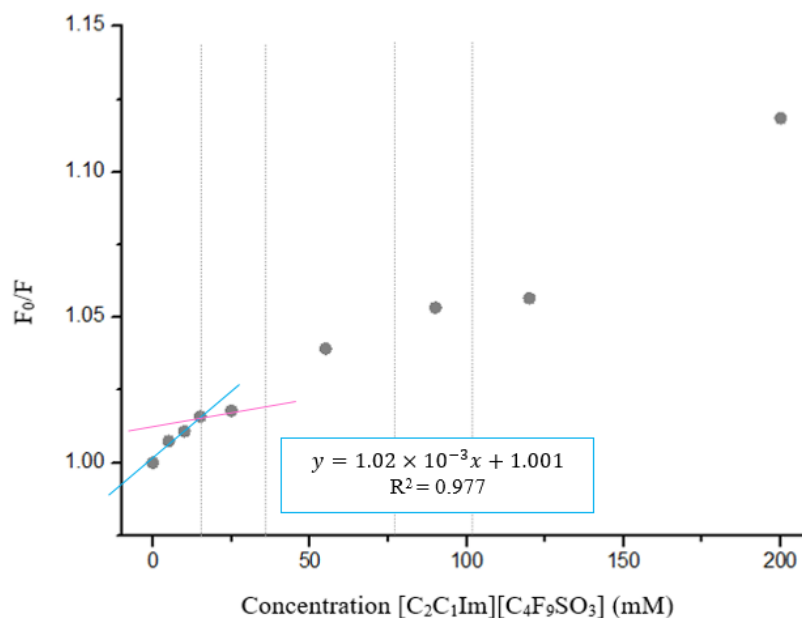


Figure 3.31 Stern-Volmer curves for fluorescence quenching of Lys in presence of  $[C_2C_1Im][C_4F_9SO_3]$ .

Figure 3.31 represents the Stern-Volmer fitting for concentrations 5 to 200mM of  $[C_2C_1Im][C_4F_9SO_3]$ , due to lack of quenching below 5mM and  $\lambda_{max}$  shift above 400mM. In vertical dotted lines are represented the CACs for this FIL, and it is possible to observe a change in the slope as concentrations reach by the first CAC (14.40mM), as occurred for the rest of CAC. It would be interesting to determine  $K_{SV}$  to each region between CAC, however there is not enough experimental data to this end. Therefore,  $K_{SV}$  were only calculated for concentrations up to 15mM (cutoff) and is  $1.02 \times 10^{-3} \text{mM}^{-1}$ . At these concentrations, FIL is in the form of monomer. For this region it is verified an efficient fitting to Stern-Volmer equation, therefore it is suggested a dynamic quenching mechanism provoked by the presence of FIL in monomer form.

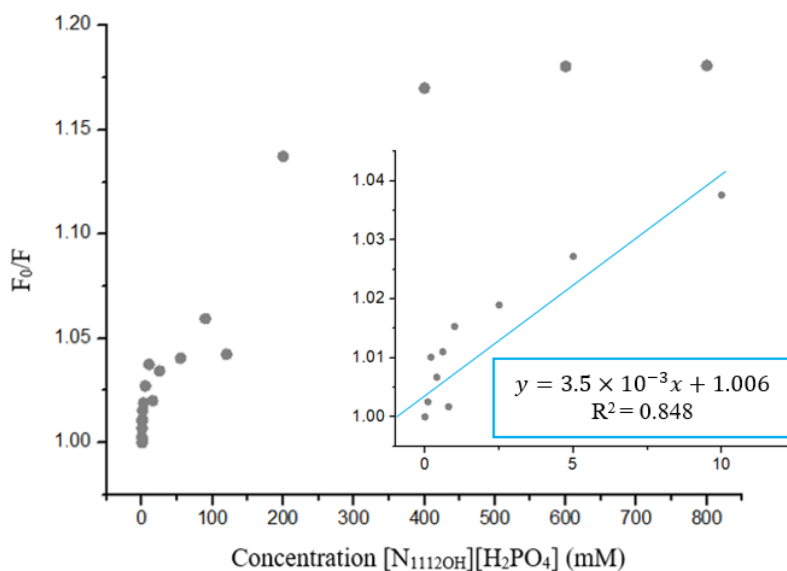


Figure 3.32 Stern-Volmer curves for fluorescence quenching of Lys in presence of [N<sub>1112</sub>OH][H<sub>2</sub>PO<sub>4</sub>].

Figure 3.32 represents the Stern-Volmer equation for concentrations 0 to 800mM of [N<sub>1112</sub>OH][H<sub>2</sub>PO<sub>4</sub>]. In this case, a relatively constant quenching is occurring, but fitting of this equation was only applied to the linear region, which is below 10mM.  $K_{SV}$  was determined by the slope of this region was  $3.5 \times 10^{-3} \text{mM}^{-1}$ . Comparing both  $K_{SV}$ , it is verified the higher value for [N<sub>1112</sub>OH][H<sub>2</sub>PO<sub>4</sub>] than [C<sub>2</sub>C<sub>1</sub>Im][C<sub>4</sub>F<sub>9</sub>SO<sub>3</sub>], so [N<sub>1112</sub>OH][H<sub>2</sub>PO<sub>4</sub>] is more efficient quencher than the monomer FIL at these conditions, for a similar concentration range.

For both cases was determined  $k_q$ , considering  $K_{SV} = k_q \tau_0$  and  $\tau_0 = 10^{-8} \text{ s}$  (fluorescence lifetime of a biopolymer)<sup>55</sup>, and are  $1.02 \times 10^5$  and  $3.5 \times 10^5 \text{mM}^{-1} \text{s}^{-1}$  for [C<sub>2</sub>C<sub>1</sub>Im][C<sub>4</sub>F<sub>9</sub>SO<sub>3</sub>] and [N<sub>1112</sub>OH][H<sub>2</sub>PO<sub>4</sub>] respectively. Comparing these values with the largest possible biomolecular quenching constant for dynamic collision,  $2.0 \times 10^7 \text{mM}^{-1} \text{s}^{-1}$ ,<sup>55</sup> it is verified that experimental constants are below this reference, and so it is possible to proposed for both cases it is dynamic quenching, and no ground-state complex is formed during quenching process.

### Nano-DSC

In this section, Lysozyme melting temperature ( $T_m$ ) was measured in the presence of an Ionic Liquid and Fluorinated Ionic Liquid aqueous solutions, and also in the presence of IL- and FIL-rich phases from four ABS analyzed earlier in Extraction Efficiency study Section.  $T_m$  represents the temperature at which an equilibrium between folded and unfolded states of a protein coexists. Any shift on this parameter is suggestive of changes in protein stability in the presence of Ionic Liquids, and afford important information relatively to interaction protein-IL.<sup>47</sup>

Firstly, the study on thermal stability of Lys in aqueous solutions of IL and FILs was carried. As observed at Fluorescence studies in previous section, some evidences on typology of

interactions were obtained at higher concentrations of IL and FIL, represented by the red and blue shift on the wavelengths, respectively. Therefore, some insights on the interaction at lower concentrations are needed. Besides, Ferreira et al.<sup>47</sup> carried thermal stability studies of Lys on  $[C_2C_1Im][C_4F_9SO_3]$  at concentrations above its first CAC (with formation of aggregates), and it was not possible to acquire  $T_m$  directly from the protein in solution due to aggregation of Lys in structures, and additional procedures were required to have some thermal stability information on the interactions. In this paper, it was needed to precipitate the aggregates of encapsulated Lys and resuspend afterwards in order to get a signal in the thermogram.

It was selected a Lys concentration of 1mg/mL and Lysozyme  $T_m$  were measured in  $[C_4C_1Im][CF_3SO_3]$  and  $[C_2C_1Im][C_4F_9SO_3]$  solutions at concentrations ranging 0.1 and 10mM. Results are presented in Figure 3.34.

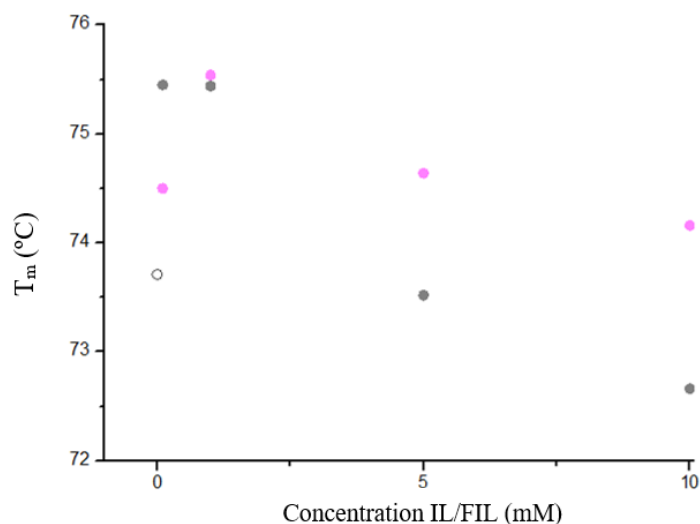


Figure 3. 33 Melting Temperature of ○ Lysozyme in water and in presence of different concentration of ●  $[C_4C_1Im][CF_3SO_3]$  and ●  $[C_2C_1Im][C_4F_9SO_3]$  (0.1-10mM)

At concentration range of 0-10mM, both IL and FIL described similar profiles, as presented at Figure 3.33. At minimal concentration of IL and FIL (0.1mM) it is verified an increase in  $T_m$  relative to Lys  $T_m$  in water. However, above 0.1mM, as concentration increases,  $T_m$  decreases for both compounds, and it is verified a more abrupt decrease for  $[C_2C_1Im][C_4F_9SO_3]$  than for  $[C_4C_1Im][CF_3SO_3]$ . As  $[C_2C_1Im][C_4F_9SO_3]$  has a more hydrophobic character than  $[C_4C_1Im][CF_3SO_3]$ , it is possible the hydrophobic interactions between FIL monomer and Lysozyme lead to a more accentuated decrease on protein stability.

Nevertheless, it is verified a Lys  $T_m$  maximum variation of almost 2°C in IL/FIL aqueous solution relatively to Lys  $T_m$  in water, which is considered not a very significative change, and by conjugating results from the Fluorescence section, it is not likely this decrease on  $T_m$  leads to a

severe change on native conformation of the protein at these concentrations IL and FIL aqueous solutions.

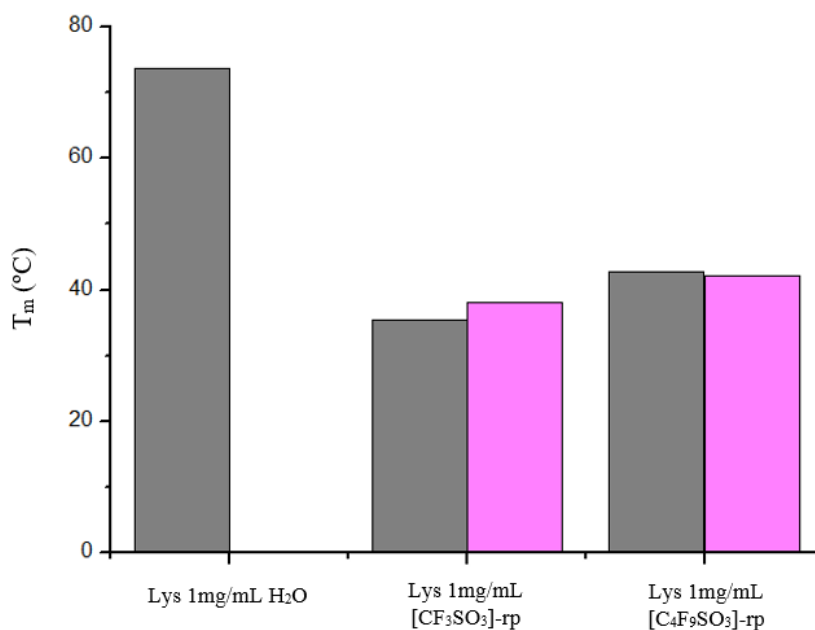


Figure 3. 34 Melting Temperature of Lysozyme in water and in presence of [C<sub>4</sub>C<sub>1</sub>Im][CF<sub>3</sub>SO<sub>3</sub>]-rich phase (30%IL+25%Glucose) and [C<sub>2</sub>C<sub>1</sub>Im][C<sub>4</sub>F<sub>9</sub>SO<sub>3</sub>]-rich phase (30%FIL+25%Glucose) • with stirring and • without stirring.

Next step, real phases from systems were measured. Firstly, was determined the influence of stirring during the nano-DSC protocol of  $T_m$  acquisition. Stirring during measurement of phases lead to the formation of foam on top of the solution. Therefore, was prepared a solution of 1mg/mL in [C<sub>4</sub>C<sub>1</sub>Im][CF<sub>3</sub>SO<sub>3</sub>]-rich phase and [C<sub>2</sub>C<sub>1</sub>Im][C<sub>4</sub>F<sub>9</sub>SO<sub>3</sub>]-rich phase obtained from systems 30%IL/FIL+25% Glucose. Thermograms with and without stirring were acquired and compared, and are presented in Appendix Figures 6.29-6.32.

Systems' determined  $T_m$  are presented in Figure 3.34. For [C<sub>2</sub>C<sub>1</sub>Im][C<sub>4</sub>F<sub>9</sub>SO<sub>3</sub>]-rich phase for the systems referred above,  $T_m$  obtained with and without stirring are  $42.73 \pm 0.027$  and  $42.1 \pm 0.017$ , respectively. Besides similar  $T_m$  were obtained, thermograms are also very alike in terms of Lys band shape. For [C<sub>4</sub>C<sub>1</sub>Im][CF<sub>3</sub>SO<sub>3</sub>] were obtained  $35.49 \pm 0.025$  and  $38.03 \pm 0.086$  for stirred and unstirred solution. In this case, Lysozyme band shape was more affected than using [C<sub>2</sub>C<sub>1</sub>Im][C<sub>4</sub>F<sub>9</sub>SO<sub>3</sub>], which stirred solution presented deformed peak, meanwhile unstirred solution showed some loss of baseline, but peak was left intact. Considering these effects in thermogram and relative similar  $T_m$  acquired, was defined to measure the  $T_m$  without the stirring while measuring solution composed by systems phase, in order to avoid the formation of the foam, and diminish error in acquisitions.

At last, thermal stability analysis of Lys in aqueous phases of IL- and FIL-based ABS after partition process was accessed. In this analysis, were considered systems 30%IL/FIL + 25% carbohydrate, sucrose and glucose. Results are presented in Figure 3.35.

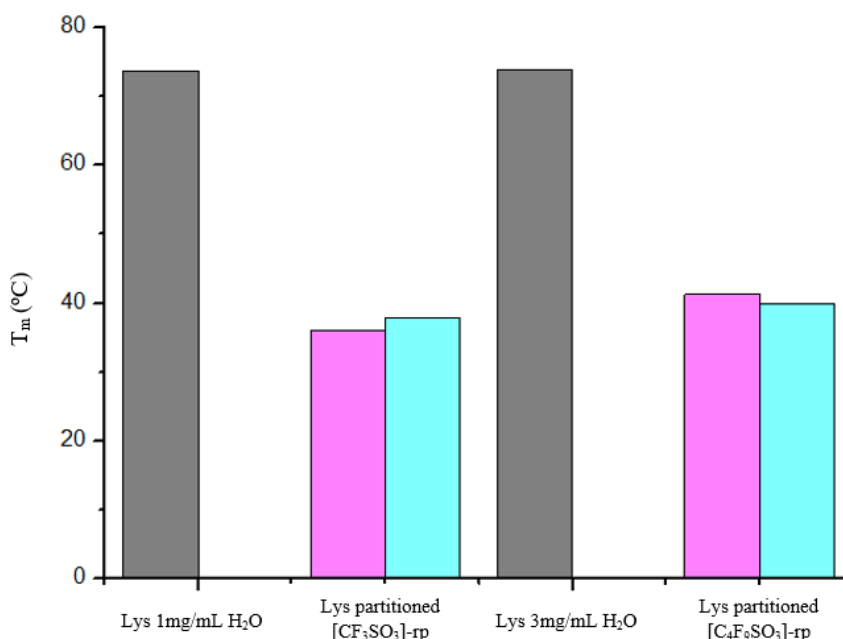


Figure 3. 35 Melting Temperature of Lysozyme in water (1 and 3 mg/mL) and partitioned for [C<sub>4</sub>C<sub>1</sub>Im][CF<sub>3</sub>SO<sub>3</sub>]-rich phase (30%IL+25%Glucose) and [C<sub>2</sub>C<sub>1</sub>Im][C<sub>4</sub>F<sub>9</sub>SO<sub>3</sub>]-rich phase (30%FIL+25%Glucose). • Glucose • Sucrose.

Considering partition results, as presented in Tables 6.26-6.29 from Appendix, was selected a Lys concentration to use as a reference in measurements, similar to Lys concentration after partition. Thus, for 30% [C<sub>2</sub>C<sub>1</sub>Im][C<sub>4</sub>F<sub>9</sub>SO<sub>3</sub>] + 25% carbohydrate was selected 3mg/mL and for 30% [C<sub>4</sub>C<sub>1</sub>Im][CF<sub>3</sub>SO<sub>3</sub>] + 25% carbohydrate was selected 1mg/mL, and T<sub>m</sub> for each system is compared to respective reference concentration of Lysozyme.

Bearing in mind systems composed by [C<sub>2</sub>C<sub>1</sub>Im][C<sub>4</sub>F<sub>9</sub>SO<sub>3</sub>], major quantity of solute after partition is detected in FIL-rich phase (approximately 3mg/mL), so for only this phase was measured the T<sub>m</sub> and compared to Lys 3mg/mL in water. Considering the partition results of systems composed by [C<sub>4</sub>C<sub>1</sub>Im][CF<sub>3</sub>SO<sub>3</sub>], as it was not verified total partition to one of the phases, both phases were measured. It was attempted to measure carbohydrate-rich phase, but background signal did not allow Lys signal acquisition in CH-rich phase. Thus, only [C<sub>4</sub>C<sub>1</sub>Im][CF<sub>3</sub>SO<sub>3</sub>]-rich phase are analyzed in this section, and used as reference a 1mg/mL Lys solution in water. Relatively to each reference in water, it is observable a decrease in T<sub>m</sub> in a certain extent for Lys in phase, so Lys in ABS phase does not maintain complete thermal stability. However, comparing Lysozyme T<sub>m</sub> in both [C<sub>4</sub>C<sub>1</sub>Im][CF<sub>3</sub>SO<sub>3</sub>]- and [C<sub>2</sub>C<sub>1</sub>Im][C<sub>4</sub>F<sub>9</sub>SO<sub>3</sub>]-rich phase, it is possible to conclude a larger thermal stabilization in FIL-rich phase.

Thus, the application of either IL or FIL at higher concentrations, leads to a decrease of the  $T_m$  comparatively to Lys in water. However, taking in mind the Lysozyme enzymatic activity assays presented earlier in this work, the implementation of either compounds up until 35% (w/w) did not lead to a significant decrease on enzymatic activity. So, although it is verified a decrease on thermal stability, the changes on conformation that de-stabilize the protein are not enough to provoke loss of enzymatic activity. Also, Absorbance studies did not show deviations on maxima peak, so no detectable changes on conformation in the Trp environment are occurring for either IL/FIL.

Previous Intrinsic Fluorescence studies pointed out the possible higher stabilization of Lys on  $[C_2C_1Im][C_4F_9SO_3]$ , even though were carried in aqueous solutions. It was observed  $[C_4C_1Im][CF_3SO_3]$  led to an unfolding, due to an increased fluorescence intensity and red shift at higher concentrations; on the other hand,  $[C_2C_1Im][C_4F_9SO_3]$  seems to lead to a more folded state, inferred by the fluorescence intensity quenching and blue shift occurring at higher concentrations, also relatively similar results compared with an stabilizing salt ( $[N_{1112OH}][H_2PO_4]$ ). A more folded state may lead to major conservation of the thermal stability allowed by FIL-rich phase.

For aqueous solutions until 10mM, both  $[C_4C_1Im][CF_3SO_3]$  and  $[C_2C_1Im][C_4F_9SO_3]$  permitted an increase of thermal stability, however, IL induced a bigger increment on stabilization than FIL at those concentrations. When comparing this effect on higher concentrations (after partition), the tendency is reversed, and  $[C_2C_1Im][C_4F_9SO_3]$  allows an higher thermal stabilization than the IL. This may be pointed out as one reason for the increased partition to FIL-rich phase in this carbohydrate systems, when compared to IL-based systems (minimum of 3-fold for carbohydrate systems), possibly due an augmented stability in protein-FIL aggregated-structure.

*Table 3. 2 Melting Temperature ( $T_m$ ) of Lysozyme in water and in phase, either simulated (left) and partitioned (right).*

	$T_m$ (°C)	Error		$T_m$ (°C)	Error
Lys 1.0 mg/ml H <sub>2</sub> O	73.71	0.004	Lys 3.0 mg/mL H <sub>2</sub> O	73.85	0.005
Lys 1.0 mg/ml CF <sub>3</sub> SO <sub>3</sub> -rp	35.49	0.025	Lys partitioned CF <sub>3</sub> SO <sub>3</sub> -rp	36.09	0.015
Lys 1.0 mg/ml C <sub>4</sub> F <sub>9</sub> SO <sub>3</sub> -rp	42.73	0.027	Lys partitioned C <sub>4</sub> F <sub>9</sub> SO <sub>3</sub> -rp	41.3	0.008

It is important to notice the resemblance between the simulated 1mg/mL Lysozyme in the respective phase and the  $T_m$  after partition (Table 3.2). By this comparison, it is possible to access the partition process and interaction with all systems' components during phase demixing effect on thermal stability of protein. Thus, it is possible to conclude the partition process does not seem to influence the thermal stability of the protein, and only the interaction with the phase components shows an impact.





## 4. Conclusions

In this work, several components, namely ILs and FIL, among numerous salting-out agents were tested to compose ABS for Lysozyme extraction, and several features were considered for this analysis. The ability of these components to form ABS was tested and was showed that FILs, not only permitted a bigger biphasic region than hydrogenated alkylic chain IL, but formed ABS with weak salting-out agents as carbohydrates, not achievable with IL. Besides, FIL-based systems showed enhanced partition to  $[\text{C}_2\text{C}_1\text{Im}][\text{C}_4\text{F}_9\text{SO}_3]$ -rich phase relatively to other systems, especially noticeable in systems composed by carbohydrates. In  $[\text{N}_{11120\text{H}}][\text{H}_2\text{PO}_4]$ -based systems, this extent of partition showed to be salt concentration-dependent, where at increased salt concentration partition presented to be major to salt-rich phase, however at salt lowest concentration EE% was near 100%. These components maintain Lysozyme activity either in aqueous solutions and after partition protocol was carried, except for 30%  $[\text{C}_2\text{C}_1\text{Im}][\text{C}_4\text{F}_9\text{SO}_3]$ +2%  $\text{K}_3\text{PO}_4$ , but was pointed out as a possible quantification default. Therefore, IL functionalization with fluorous tags equal to or longer than four carbons permit a more versatile and amenable ABS than alkylated ILs. Bigger biphasic regions allowed a more versatile extraction system, since a wider range of salting-out agent concentrations could be used, and permitted to design extraction to either FIL or salt-rich phase, depending on salt concentration used. Moreover, it was possible to develop ABS using fluorinated compounds, which would not be able to be applied in the first place due to limited solubility of fluorocarbon compounds. FILs are totally miscible in water, which allows its application in ABS.

In order to understand the reason for these differences in partition between IL and FIL, several techniques were used. Turbidity measures were carried and both  $[\text{C}_4\text{C}_1\text{Im}][\text{CF}_3\text{SO}_3]$  and  $[\text{C}_2\text{C}_1\text{Im}][\text{C}_4\text{F}_9\text{SO}_3]$  aqueous solutions caused an increase in solution turbidity, so both interact with protein at some extent. However, only FIL caused changes in a concentration-dependent way due to increase of hydrophobic interaction character among the electrostatic and non-electrostatic interaction occurring. This result was confirmed by the absorbance spectra, which becomes more flatted and baseline is lost. The presence of both IL and FIL did not cause maxima peak shifting to 301nm, indicative of maintenance of conformation given the sensibility of this technique, and so these compounds do not lead to an unfolded conformation. Also, Intrinsic Fluorescence studies indicate a change in environment polarity in fluorophore Trp vicinity provoked by the presence of both IL and FIL, confirming the interaction between IL/FIL and protein, previously verified in turbidity and absorbance studies. By this results,  $[\text{C}_4\text{C}_1\text{Im}][\text{CF}_3\text{SO}_3]$  led to Trp exposed to a hydrophilic solvent; meanwhile  $[\text{C}_2\text{C}_1\text{Im}][\text{C}_4\text{F}_9\text{SO}_3]$  led to exposure of a more hydrophobic solvent.

Intrinsic Fluorescence studies were also carried in the presence  $[N_{1112OH}][H_2PO_4]$  aqueous solutions. The presence of this salt led to a increasing quenching effect on Trp fluorescence emission, which may be indicative of a more compact conformation. The “competitive behavior” for Lys solubilization in systems of  $[C_2C_1Im][C_4F_9SO_3]$  with variable concentration of  $[N_{1112OH}][H_2PO_4]$  may be explained by the similar effects on conformation they provoke on protein.

Nano-DSC studies of partitioned Lys indicate that both IL and FIL led to a decrease on  $T_m$  relatively Lys in water. However, when Lys is solubilize in the extraction phase conditions,  $[C_2C_1Im][C_4F_9SO_3]$  permitted relatively higher  $T_m$  than  $[C_4C_1Im][CF_3SO_3]$ . Therefore, the preference of partition to FIL-rich phase compared to IL-based systems may also be due relatively higher thermal stability in  $[C_2C_1Im][C_4F_9SO_3]$ -rich phase, therefore more favourable to the protein.

Thus, although  $[C_2C_1Im][C_4F_9SO_3]$  is more hydrophobic than  $[C_4C_1Im][CF_3SO_3]$ , its unique properties permitted the formation of self-aggregation structures and Lys encapsulation. This structures may present a more stable environment to solubilize protein, and increase its extraction to FIL-rich phase during extraction. Besides protein-friendly, as mentioned before, FILs permit a application of a compound of a more hydrophobic character but with water solubility maintenance, which permits its application in ABS. Its usage allows a bigger biphasic region and have a wider range of concentrations to tailor the target phase and extraction efficiencies, increasing adaptability of these systems.

In future experiments, more studies in terms of secondary structure in the presence of these components-rich phases are needed, and so Circular Dichroism is proposed. There are limitations of this technique on Imidazolium-based components due to high intensity signals from Imidazolium cation. However, it can be carried in salt-rich phase of systems  $30\% [C_2C_1Im][C_4F_9SO_3] + 6-20\% [N_{1112OH}][H_2PO_4]$  and also  $30\% [N_{1112OH}][C_4F_9SO_3] + 30\% [N_{1112OH}][H_2PO_4]$ , in order to have more detailed comprehension on its influence on protein structure that would explain better the competition between these two phases for Lysozyme partition.

Isothermal Calorimetry (ITC) was considered initially for this work, however impossible to proceed with the analysis due to COVID-19 pandemic equipment restrictions. This technique gives useful information on the thermodynamic behavior of complexes, therefore may provide insights on the binding constants and thermodynamic parameters between these components and proteins, and supplement information acquire until this moment.

Molecular docking allows the study of the lowest energy conformation of proteins in the presence of components. Therefore, this study would give some understanding on how these components interact with the protein, and sum all the evidences obtained by previous techniques and develop a model of the most probable conformation in these conditions.

## 5. References

1. Mondal, K., Gupta, M. N. & Roy, I. Affinity-Based Strategies for Protein Purification. *Anal. Chem.* 3499–3504 (2006).
2. Lee, S. Y., Khoiroh, I., Ooi, C. W., Ling, T. C. & Show, P. L. Recent Advances in Protein Extraction Using Ionic Liquid-based Aqueous Two-phase Systems. *Sep. Purif. Rev.* **46**, 291–304 (2017).
3. Martínez-Aragón, M., Burghoff, S., Goetheer, E. L. V. & de Haan, A. B. Guidelines for solvent selection for carrier mediated extraction of proteins. *Sep. Purif. Technol.* **65**, 65–72 (2009).
4. Puetz, J. & Wurm, F. M. Recombinant Proteins for Industrial versus Pharmaceutical Purposes: A Review of Process and Pricing. *Processes* **7**, 476 (2019).
5. Santos, J. H. *et al.* Ionic liquid-based aqueous biphasic systems as a versatile tool for the recovery of antioxidant compounds. *Biotechnol. Prog.* **31**, 70–77 (2015).
6. Azevedo, E. G; Alves, A. M. *Engenharia de Processos de Separação*. (IST Press, 2009).
7. Albertsson, P. Å. A. Partition of proteins in liquid polymer-polymer two-phase systems. *Nature* **182**, 918 (1958).
8. Freire, M. G. *et al.* Aqueous biphasic systems: A boost brought about by using ionic liquids. *Chem. Soc. Rev.* **41**, 4966–4995 (2012).
9. Albertsson, P. *Partition of cell particles and macromolecules. Advances in Protein Chemistry* (Wiley, New York, 1986). doi:10.1016/S0065-3233(08)60244-2
10. Iqbal, M. *et al.* Aqueous two-phase system (ATPS): an overview and advances in its applications. *Biol. Proced. Online* **18**, 1–18 (2016).
11. Freire, M. G. Introduction to Ionic-Liquid-Based Aqueous Biphasic Systems (ABS). in *Ionic-Liquid-Based Aqueous Biphasic Systems* (ed. Green Chemistry and Sustainable Technology) 1–25 (Springer-Verlag Berlin Heidelberg, 2016). doi:10.1007/978-3-662-52875-4\_1
12. Hofmeister. On the understanding of the effects of salts. *Arch. Exp. Pathol. Pharmacol* **24**, 247–260 (1888).
13. Hyde, A. M. *et al.* General Principles and Strategies for Salting-Out Informed by the Hofmeister Series. *Org. Process Res. Dev.* **21**, 1355–1370 (2017).
14. Flieger, J., Grushka, E. B., Czajkowska, C.-Z. & Żelazko, A. Ionic Liquids as Solvents in Separation Processes. *Austin J Anal Pharm Chem. Austin J Anal Pharm Chem* **1**, 1009–2 (2014).
15. Hong Yang, A. M. G. Aqueous Two-Phase Extraction Advances for Bioseparation. *J. Bioprocess. Biotech.* **04**, 1–8 (2013).
16. Ferreira, A. M. *et al.* Enhanced tunability afforded by aqueous biphasic systems formed by fluorinated ionic liquids and carbohydrates. *Green Chem.* **18**, 1070–1079 (2016).
17. Cvjetko Bubalo, M., Radošević, K., Radojčić Redovniković, I., Halambek, J. & Gaurina Srček, V. A brief overview of the potential environmental hazards of ionic liquids. *Ecotoxicol. Environ. Saf.* **99**, 1–12 (2014).
18. Thuy Pham, T. P., Cho, C. W. & Yun, Y. S. Environmental fate and toxicity of ionic liquids: A review. *Water Res.* **44**, 352–372 (2010).
19. Keith E. Gutowski, Grant A. Broker, Heather D. Willauer, J. G. H. & Richard P. Swatloski, John D. Holbrey, and R. D. R. Controlling the Aqueous Miscibility of Ionic Liquids: Aqueous Biphasic Systems of Water-Miscible Ionic Liquids and Water-Structuring Salts for Recycle, Metathesis, and Separations. *J. Chem. Soc.* **125**, 6632–6633 (2003).
20. Freire, M. G. *et al.* High-performance extraction of alkaloids using aqueous two-phase systems with ionic liquids. *Green Chem.* **12**, 1715–1718 (2010).
21. Tomé, L. I. N. *et al.* Tryptophan extraction using hydrophobic ionic liquids. *Sep. Purif. Technol.* **72**, 167–173 (2010).
22. Ventura, S. P. M. *et al.* Production and purification of an extracellular lipolytic enzyme using ionic liquid-based aqueous two-phase systems. *Green Chem.* **14**, 734–740 (2012).

23. Vieira, N. S. M. *et al.* Fluorination effects on the thermodynamic, thermophysical and surface properties of ionic liquids. *J. Chem. Thermodyn.* **97**, 354–361 (2016).
24. Bastos, J. C. *et al.* Design of task-specific fluorinated ionic liquids: Nanosegregation: versus hydrogen-bonding ability in aqueous solutions. *Chem. Commun.* **54**, 3524–3527 (2018).
25. Pereira, A. B. *et al.* Aggregation behavior and total miscibility of fluorinated ionic liquids in water. *Langmuir* **31**, 1283–1295 (2015).
26. Pereira, A. B. *et al.* Fluorinated ionic liquids: Properties and applications. *ACS Sustain. Chem. Eng.* **1**, 427–439 (2013).
27. Vieira, N. S. M. *et al.* Acute Aquatic Toxicity and Biodegradability of Fluorinated Ionic Liquids. *ACS Sustain. Chem. Eng.* **7**, 3733–3741 (2019).
28. Vieira, N. S. M. *et al.* Human cytotoxicity and octanol/water partition coefficients of fluorinated ionic liquids. *Chemosphere* **216**, 576–586 (2019).
29. Alves, M. *et al.* Fluorinated ionic liquids for protein drug delivery systems: Investigating their impact on the structure and function of lysozyme. *Int. J. Pharm.* **526**, 309–320 (2017).
30. Alves, M. M. S., Araújo, J. M. M., Martins, I. C., Pereira, A. B. & Archer, M. Insights into the interaction of Bovine Serum Albumin with Surface-Active Ionic Liquids in aqueous solution. *J. Mol. Liq.* **322**, (2021).
31. Aminlari, L., Mohammadi Hashemi, M. & Aminlari, M. Modified Lysozymes as Novel Broad Spectrum Natural Antimicrobial Agents in Foods. *J. Food Sci.* **79**, 1–14 (2014).
32. Chia, S. R. *et al.* Recent Developments of Reverse Micellar Techniques for Lysozyme, Bovine Serum Albumin, and Bromelain Extraction. *Mol. Biotechnol.* **61**, 715–724 (2019).
33. Imoto, T., Forster, L. S., Rupley, J. A. & Tanaka, F. Fluorescence of lysozyme: emissions from tryptophan residues 62 and 108 and energy migration. *Proc. Natl. Acad. Sci. U. S. A.* **69**, 1151–1155 (1972).
34. Merchuk, J. C., Andrews, B. A. & Asenjo, J. A. Aqueous two-phase systems for protein separation Studies on phase inversion. **711**, 285–293 (1998).
35. Lima, S. & Freire, M. G. Ionic Liquid Based Aqueous Biphasic Systems with Controlled pH: The Ionic Liquid Cation Effect. *J. Chem. Eng. Data* **56**, 4253–4260 (2011).
36. Freire, M. G., Neves, C. M. S. S. & Marrucho, I. M. Impact of Self-Aggregation on the Formation of Ionic-Liquid-Based Aqueous Biphasic Systems. (2012).
37. Shahriari, S. *et al.* Aqueous biphasic systems: A benign route using cholinium-based ionic liquids. *RSC Adv.* **3**, 1835–1843 (2013).
38. Neves, C. M. S. S., Ventura, S. P. M., Freire, M. G., Marrucho, I. M. & Coutinho, J. A. P. Evaluation of Cation Influence on the Formation and Extraction Capability of Ionic-Liquid-Based Aqueous Biphasic Systems. *J. Phys. Chem. B* **113**, 5194–5199 (2009).
39. Freire, M. G., Louros, C. L. S., Rebelo, L. P. N. & Coutinho, J. A. P. Aqueous biphasic systems composed of a water-stable ionic liquid + carbohydrates and their applications. *Green Chem.* **13**, 1536–1545 (2011).
40. Zhang, C., Wang, H., Malhotra, S. V., Dodge, C. J. & Francis, A. J. Biodegradation of pyridinium-based ionic liquids by an axenic culture of soil Corynebacteria. *Green Chem.* **12**, 851–85 (2010).
41. Canongia Lopes, J. N. ABS Composed of Ionic Liquids and Inorganic Salts. 27–35 (2016). doi:10.1007/978-3-662-52875-4\_2
42. Vieira, N. S. M., Castro, P. J., Marques, D. F., Araújo, J. M. M. & Pereira, A. B. Tailor-made fluorinated ionic liquids for protein delivery. *Nanomaterials* **10**, 1–16 (2020).
43. Reslan, M. & Kayser, V. Ionic liquids as biocompatible stabilizers of proteins. *Biophys. Rev.* **10**, 781–793 (2018).
44. Lukanov, B. & Firoozabadi, A. Specific ion effects on the self-assembly of ionic surfactants: A molecular thermodynamic theory of micellization with dispersion forces. *Langmuir* **30**, 6373–6383 (2014).
45. Santos, F. K. G., Neto, E. L. B., Moura, M. C. P. A., Dantas, T. N. C. & Neto, A. A. D. Molecular behavior of ionic and nonionic surfactants in saline medium. *Colloids Surfaces A Physicochem. Eng. Asp.* **333**, 156–162 (2009).

46. Rather, M. A., Dar, T. A., Singh, L. R., Rather, G. M. & Bhat, M. A. Structural-functional integrity of lysozyme in imidazolium based surface active ionic liquids. *Int. J. Biol. Macromol.* **156**, 271–279 (2020).
47. Ferreira, M. L., Vieira, N. S. M., Araújo, J. M. M. & Pereira, A. B. Unveiling the Influence of Non-Toxic Fluorinated Ionic Liquids Aqueous Solutions in the Encapsulation and Stability of Lysozyme. *Sustain. Chem.* **2**, 149–166 (2021).
48. Togashi, D. M., Ryder, A. G. & O’Shaughnessy, D. Monitoring local unfolding of bovine serum albumin during denaturation using steady-state and time-resolved fluorescence spectroscopy. *J. Fluoresc.* **20**, 441–452 (2010).
49. Balme, S. *et al.* Structure, orientation and stability of lysozyme confined in layered materials. *Soft Matter* **9**, 3188–3196 (2013).
50. Kumari, M., Dohare, N., Maurya, N., Dohare, R. & Patel, R. Effect of 1-methyl-3-octyleimidazolium chloride on the stability and activity of lysozyme: a spectroscopic and molecular dynamics studies. *J. Biomol. Struct. Dyn.* **35**, 2016–2030 (2017).
51. Kumar, S., Kukutla, P., Devunuri, N. & Venkatesu, P. How does cholinium cation surpass tetraethylammonium cation in amino acid-based ionic liquids for thermal and structural stability of serum albumins? *Int. J. Biol. Macromol.* **148**, 615–626 (2020).
52. Alkudaisi, N., Russell, B. A., Jachimska, B., Birch, D. J. S. & Chen, Y. Detecting lysozyme unfolding: Via the fluorescence of lysozyme encapsulated gold nanoclusters. *J. Mater. Chem. B* **7**, 1167–1175 (2019).
53. Singh, T., Bharmoria, P., Morikawa, M. A., Kimizuka, N. & Kumar, A. Ionic liquids induced structural changes of bovine serum albumin in aqueous media: A detailed physicochemical and spectroscopic study. *J. Phys. Chem. B* **116**, 11924–11935 (2012).
54. Weaver, K. D. *et al.* Structure and function of proteins in hydrated choline dihydrogen phosphate ionic liquid. *Phys. Chem. Chem. Phys.* **14**, 790–801 (2012).
55. Ding, F., Zhao, G., Huang, J., Sun, Y. & Zhang, L. Fluorescence spectroscopic investigation of the interaction between chloramphenicol and lysozyme. *Eur. J. Med. Chem.* **44**, 4083–4089 (2009).



## 6. Appendix

### 6.1. Aqueous Biphasic Systems

Table 6. 1 Experimental weight fraction data for  $[N_{1112OH}]Cl + K_3PO_4$  and  $[C_2C_1Py]Br + K_3PO_4$  at 25°C.

$[N_{1112OH}]Cl$ (1) + $K_3PO_4$ (2) + $H_2O$ (3) at 25°C				$[C_2C_1Py]Br$ (1) + $K_3PO_4$ (2) + $H_2O$ (3) at 25°C			
100 w1	100 w2	100 w1	100 w2	100 w1	100 w2	100 w1	100 w2
7.126	36.475	28.586	19.067	45.130	3.337	21.673	13.279
8.352	35.048	29.293	18.581	42.951	3.539	21.018	13.704
9.450	34.088	29.944	18.127	41.328	3.937	20.449	14.039
10.250	33.260	30.607	17.677	40.483	4.199	20.004	14.304
11.320	32.297	31.020	17.332	39.715	4.384	19.574	14.571
13.054	31.020	31.883	16.715	38.080	5.390	18.950	14.975
13.943	29.989	32.830	16.092	36.831	5.485	18.303	15.398
15.141	29.040	33.806	15.545	35.544	6.045	17.698	15.788
16.001	28.271	34.265	15.146	34.503	6.401	17.132	16.165
16.559	27.832	35.975	14.038	33.372	6.905	16.514	16.549
17.880	26.873	37.005	13.466	32.502	7.387	15.898	16.951
18.886	26.057	37.656	13.117	31.598	7.905	15.321	17.331
20.087	25.184	38.266	12.728	30.794	8.173	14.968	17.580
21.124	24.421	39.383	12.168	29.865	8.605	14.360	17.994
21.960	23.764	39.832	11.856	28.805	9.187	13.929	18.310
23.005	23.033	40.425	11.504	27.801	9.751	13.450	18.651
23.968	22.348	40.953	11.167	26.830	10.330	13.036	18.951
24.710	21.783	42.235	10.551	25.967	10.808	12.581	19.315
25.527	21.190	43.049	10.108	25.163	11.252	12.066	19.707
26.282	20.664	43.862	9.700	24.416	11.659	11.577	20.098
27.097	20.104	44.583	9.321	23.702	12.059	11.121	20.469
27.859	19.576	45.669	8.854	23.030	12.453	10.678	20.843
28.586	19.067	46.328	8.551	22.285	12.927		

Table 6. 2 Experimental weight fraction data for  $[C_2C_1Im]Cl + K_3PO_4$  and  $[C_2C_1Im][C_1CO_2] + K_3PO_4$  at 25°C.

<b><math>[C_2C_1Im]Cl</math> (1) + <math>K_3PO_4</math> (2) + <math>H_2O</math> (3) at 298.15 K</b>				<b><math>[C_2C_1Im][C_1CO_2]</math> (1) + <math>K_3PO_4</math> (2) + <math>H_2O</math> (3) at 298.15 K</b>			
<b>100 w1</b>	<b>100 w2</b>	<b>100 w1</b>	<b>100 w2</b>	<b>100 w1</b>	<b>100 w2</b>	<b>100 w1</b>	<b>100 w2</b>
43.874	2.794	15.475	19.953	33.715	5.959	12.997	21.988
43.241	2.967	14.926	20.441	32.615	6.379	12.642	22.336
41.956	3.509	14.385	20.928	31.864	6.787	12.323	22.650
40.757	3.830	13.953	21.314	30.969	7.368	11.999	22.972
39.312	4.332	13.525	21.688	30.126	7.922	11.682	23.308
38.198	4.827	13.043	22.136	29.291	8.475	11.409	23.578
37.287	5.114	12.591	22.554	28.475	9.031	11.148	23.833
35.761	5.825	12.146	22.977	27.740	9.529	10.898	24.075
34.159	6.615	10.888	24.209	27.026	10.012	10.631	24.345
32.725	7.322	10.542	24.545	26.230	10.606	10.403	24.578
31.118	8.249	10.072	25.030	25.457	11.183	10.126	24.865
29.993	8.916	9.749	25.367	24.870	11.570	9.890	25.110
28.882	9.619	9.272	25.894	24.298	11.963	9.550	25.470
27.848	10.289	8.775	26.436	23.266	12.756	9.200	25.847
26.974	10.842	8.256	27.032	22.239	13.591	8.882	26.190
25.949	11.557	7.274	28.212	21.190	14.482	8.559	26.554
24.912	12.311	6.452	29.279	20.356	15.147	8.227	26.934
23.909	13.046			19.774	15.627	7.927	27.285
22.880	13.840			19.233	16.107	7.662	27.584
21.919	14.614			18.584	16.701	7.404	27.882
21.076	15.227			18.027	17.204	7.145	28.195
20.462	15.721			17.450	17.740	6.895	28.489
19.956	16.113			16.904	18.257	6.632	28.820
19.359	16.619			16.411	18.715	6.372	29.161
18.896	16.997			15.903	19.201	6.125	29.470
18.358	17.470			15.443	19.628	5.782	29.939
17.353	18.308			14.990	20.061	5.476	30.356
16.679	18.897			14.537	20.490	5.115	30.885
16.062	19.436			14.113	20.903	4.640	31.639
				13.718	21.285		
				13.352	21.640		



Table 6. 3 Experimental weight fraction data for  $[C_2C_1Im][CF_3SO_3] + K_3PO_4$  at 25°C.

<b><math>[C_2C_1Im][CF_3SO_3]</math> (1) + <math>K_3PO_4</math> (2) + <math>H_2O</math> (3) at 298.15 K</b>							
<b>100 w1</b>	<b>100 w2</b>	<b>100 w1</b>	<b>100 w2</b>	<b>100 w1</b>	<b>100 w2</b>	<b>100 w1</b>	<b>100 w2</b>
50.889	2.608	33.500	6.484	19.246	10.892	8.098	17.257
49.875	2.781	32.755	6.658	18.726	11.108	7.740	17.586
48.819	2.953	32.005	6.866	18.259	11.270	7.350	18.118
47.784	3.133	31.290	7.067	17.830	11.471	7.117	18.306
47.041	3.297	30.518	7.365	17.427	11.663	6.820	18.614
46.343	3.458	29.859	7.523	16.896	11.934	6.544	18.893
45.470	3.588	29.263	7.627	16.392	12.144	6.281	19.085
44.789	3.734	28.561	7.904	15.874	12.329	5.957	19.671
44.264	3.788	27.942	8.034	15.350	12.563	5.647	20.035
43.700	3.923	27.021	8.386	14.821	12.858		
43.129	4.062	26.492	8.499	14.303	13.156		
42.261	4.253	25.899	8.660	13.798	13.347		
41.711	4.406	25.271	8.864	13.127	13.744		
41.119	4.556	24.805	9.027	12.413	14.147		
40.595	4.671	24.272	9.160	11.782	14.553		
40.006	4.815	23.581	9.398	11.169	14.911		
39.480	4.922	22.923	9.607	10.915	14.896		
38.446	5.178	22.326	9.809	10.557	15.357		
37.406	5.481	21.821	9.927	10.063	15.690		
36.477	5.725	21.207	10.219	9.671	15.946		
35.988	5.851	20.662	10.349	9.228	16.348		
35.115	6.074	20.177	10.520	8.852	16.693		
34.283	6.285	19.699	10.723	8.510	16.918		

Table 6. 4 Experimental weight fraction data for  $[C_4C_1Im][CF_3SO_3] + K_3PO_4$  and  $[C_2C_1im][C_4F_9SO_3] + K_3PO_4$  at 25°C.

<b><math>[C_4C_1Im][CF_3SO_3]</math> (1) + <math>K_3PO_4</math> (2) + <math>H_2O</math> (3) at 298.15 K</b>				<b><math>[C_2C_1im][C_4F_9SO_3]</math> (1) + <math>K_3PO_4</math> (2) + <math>H_2O</math> (3) at 298.15 K</b>			
<b>100 w1</b>	<b>100 w2</b>	<b>100 w1</b>	<b>100 w2</b>	<b>100 w1</b>	<b>100 w2</b>	<b>100 w1</b>	<b>100 w2</b>
51.639	1.233	24.543	3.931	67.073	0.180	32.108	1.092
50.352	1.326	23.909	4.024	63.998	0.206	31.333	1.146
49.175	1.403	23.309	4.114	61.090	0.229	30.694	1.183
47.777	1.574	22.750	4.202	58.822	0.252	29.975	1.233
45.960	1.700	22.205	4.288	57.026	0.282	29.003	1.301
44.903	1.767	21.544	4.473	54.961	0.315	28.250	1.361
43.899	1.831	21.006	4.583	53.023	0.340	27.504	1.422
42.941	1.895	20.529	4.693	51.658	0.364	26.796	1.473
41.812	2.045	20.032	4.807	49.643	0.409	25.786	1.558
40.847	2.107	19.460	4.949	48.365	0.432	24.764	1.652
39.810	2.212	18.936	5.077	46.901	0.482	24.034	1.720
38.981	2.260	18.368	5.237	45.257	0.526	23.099	1.807
37.943	2.390	17.837	5.388	44.383	0.539	22.036	1.915
37.107	2.442	17.314	5.556	43.692	0.560	20.888	2.040
36.079	2.574	16.629	5.771	42.823	0.596	19.743	2.168
35.137	2.671	15.999	5.974	42.130	0.616	18.258	2.346
34.278	2.762	15.338	6.232	41.519	0.633		
33.404	2.854	14.779	6.434	40.669	0.671		
32.458	2.934	14.169	6.690	39.618	0.704		
31.653	3.023	13.569	6.968	38.467	0.756		
30.755	3.102	12.990	7.252	37.728	0.792		
29.801	3.231	12.404	7.555	37.005	0.825		
28.800	3.352	11.873	7.835	36.291	0.859		
28.167	3.422	11.217	8.239	35.643	0.889		
27.440	3.487	10.806	8.440	34.990	0.920		
26.656	3.606	10.289	8.853	34.199	0.968		
25.913	3.719	9.599	9.355	33.188	1.024		
25.280	3.789						

Table 6. 5 Experimental weight fraction data for  $[C_2C_1Py][C_4F_9SO_3] + K_3PO_4$  at 25°C.

<b><math>[C_2C_1Py][C_4F_9SO_3]</math> (1) + <math>K_3PO_4</math> (2) + <math>H_2O</math> (3) at 298.15 K</b>					
<b>100 w1</b>	<b>100 w2</b>	<b>100 w1</b>	<b>100 w2</b>	<b>100 w1</b>	<b>100 w2</b>
60.408	0.108	31.787	0.541	18.092	1.290
57.341	0.122	31.205	0.564	17.685	1.325
55.790	0.139	30.626	0.584	17.233	1.368
52.816	0.163	30.242	0.594	16.719	1.412
50.631	0.181	29.773	0.614	16.328	1.448
48.728	0.197	29.222	0.634	15.925	1.491
46.635	0.213	28.613	0.665	15.572	1.522
45.117	0.228	28.072	0.683	15.281	1.552
44.009	0.242	27.536	0.706	14.963	1.586
43.231	0.260	27.212	0.725	14.638	1.624
42.476	0.278	26.769	0.741	14.334	1.660
41.619	0.295	26.324	0.766	13.942	1.710
40.626	0.309	25.822	0.788	13.562	1.753
39.935	0.320	25.192	0.828	13.210	1.798
39.199	0.333	24.746	0.848	12.829	1.850
38.388	0.357	24.244	0.875	12.410	1.906
37.685	0.370	23.835	0.900	12.058	1.958
37.004	0.382	23.475	0.921	11.612	2.027
36.256	0.408	22.902	0.956	11.085	2.109
35.540	0.420	22.314	0.989	10.634	2.188
34.877	0.446	21.776	1.018	10.055	2.293
34.216	0.456	21.181	1.058	9.660	2.370
33.900	0.471	20.567	1.101		
33.586	0.483	19.983	1.138		
33.075	0.499	19.368	1.181		
32.601	0.509	19.030	1.212		
32.321	0.520	18.690	1.241		
32.072	0.531	18.466	1.256		

Table 6. 6 Experimental weight fraction data for  $[N_{11120H}][C_4F_9SO_3] + [N_{11120H}][H_2PO_4]$  and  $[C_4C_1Im][CF_3SO_3] + [N_{11120H}][H_2PO_4]$  at 25°C.

<b><math>[N_{11120H}][C_4F_9SO_3]</math> (1) + <math>[N_{11120H}][H_2PO_4]</math> (2) + <math>H_2O</math> (3) at 298.15 K</b>			<b><math>[C_4C_1Im][CF_3SO_3]</math> (1) + <math>[N_{11120H}][H_2PO_4]</math> (2) + <math>H_2O</math> (3) at 298.15 K</b>		
<b>100 w1</b>	<b>100 w2</b>	<b>100 w3</b>	<b>100 w1</b>	<b>100 w2</b>	<b>100 w3</b>
54.887	14.579	30.534	62.226	6.401	31.372
49.753	17.008	33.239	59.394	7.237	33.370
42.944	20.335	36.720	56.149	7.908	35.943
37.705	23.109	39.186	52.537	8.975	38.488
32.122	26.123	41.755	49.256	10.014	40.731
27.091	28.846	44.063	46.390	10.940	42.670
25.418	29.778	44.804	43.729	11.811	44.460
24.043	30.540	45.417	41.273	12.759	45.968
21.905	31.772	46.323	39.080	13.488	47.432
20.236	32.717	47.047	36.880	14.428	48.692
19.106	33.411	47.483	34.902	15.271	49.827
18.038	34.087	47.875	33.083	15.988	50.929
16.571	35.025	48.404	31.170	16.923	51.908
15.241	35.903	48.856	29.781	17.549	52.670
13.888	36.868	49.244	28.025	18.528	53.447
12.493	37.931	49.576	26.015	19.692	54.293
10.650	39.443	49.907	23.907	21.120	54.973
			22.298	22.360	55.342
			20.473	23.944	55.583
			19.182	25.187	55.632

Table 6. 7 Experimental weight fraction data for  $[C_2C_1Im][C_4F_9SO_3] + [N_{11120H}][H_2PO_4]$  + and  $[C_2C_1Py][C_4F_9SO_3] + [N_{11120H}][H_2PO_4]$  at 25°C.

<b><math>[C_2C_1Im][C_4F_9SO_3]</math> (1) + <math>[N_{11120H}][H_2PO_4]</math> (2) + <math>H_2O</math> (3) at 298.15 K</b>			<b><math>[C_2C_1Py][C_4F_9SO_3]</math> (1) + <math>[N_{11120H}][H_2PO_4]</math> (2) + <math>H_2O</math> (3) at 298.15 K</b>		
<b>100 w1</b>	<b>100 w2</b>	<b>100 w3</b>	<b>100 w1</b>	<b>100 w2</b>	<b>100 w3</b>
71.203	1.077	27.719	48.220	0.766	51.014
64.497	1.240	34.263	47.294	0.801	51.905
57.079	1.378	41.543	46.269	0.829	52.902
53.227	1.560	45.213	45.356	0.870	53.774
50.424	1.724	47.852	44.573	0.898	54.529
46.821	1.954	51.225	43.800	0.927	55.273
42.981	2.270	54.749	43.015	0.958	56.027
41.274	2.414	56.312	41.869	0.999	57.132
36.650	2.972	60.377	40.857	1.047	58.096
			39.619	1.108	59.274
			38.377	1.170	60.452
			37.242	1.230	61.528
			36.432	1.277	62.291
			35.216	1.353	63.431
			33.536	1.464	65.000
			32.152	1.565	66.282
			30.695	1.683	67.622
			28.977	1.838	69.185
			27.628	1.972	70.400
			25.620	2.193	72.186

Table 6. 8 Experimental weight fraction data for  $[C_2C_1Im]Cl + K_2HPO_4 +$  and  $[C_4C_1Im][CF_3SO_3] +$  Sucrose at 25°C.

<b><math>[C_2C_1Im]Cl</math> (1) + <math>K_2HPO_4</math> (2) + <math>H_2O</math> (3) at 298.15 K</b>			<b><math>[C_4C_1Im][CF_3SO_3]</math> (1) + Sucrose (2) + <math>H_2O</math> (3) at 298.15 K</b>		
<b>100 w1</b>	<b>100 w2</b>	<b>100 w3</b>	<b>100 w1</b>	<b>100 w2</b>	<b>100 w3</b>
52.57826	0.85667	46.56507	44.04848	14.68016	41.27136
50.37784	1.40582	48.21634	41.76079	15.62309	42.61613
46.56972	2.26095	51.16932	39.37049	16.86762	43.76189
43.11551	3.13707	53.74742	37.61540	17.66968	44.71491
40.38769	4.14487	55.46745	36.10785	18.41020	45.48195
38.28419	4.85229	56.86352	34.32036	19.35611	46.32353
36.82287	5.35485	57.82227	32.66295	20.22283	47.11422
35.48546	6.01732	58.49722	31.24453	20.94867	47.80680
34.25359	6.63802	59.10839	29.25857	22.08441	48.65702
32.59596	7.56414	59.83990	27.37116	23.16171	49.46713
30.97286	8.56077	60.46637	25.66438	24.18385	50.15176
29.58702	9.47045	60.94253	24.65479	24.91077	50.43443
28.04169	10.57265	61.38565	23.52638	25.72430	50.74932
26.45547	11.80000	61.74453	21.98711	27.12097	50.89191
24.78999	13.16877	62.04124	20.40454	28.50905	51.08640
22.97868	14.74255	62.27877	18.35457	30.52716	51.11827
20.98419	16.61166	62.40415			
18.37634	19.22683	62.39683			
16.17899	21.55865	62.26236			
14.74945	23.11031	62.14024			
12.92094	25.15637	61.92269			

Table 6. 9 Experimental weight fraction data for [C<sub>2</sub>C<sub>1</sub>im][C<sub>4</sub>F<sub>9</sub>SO<sub>3</sub>] + Sucrose at 25°C.

<b>[C<sub>2</sub>C<sub>1</sub>im][C<sub>4</sub>F<sub>9</sub>SO<sub>3</sub>] (1) + Sucrose (2) + H<sub>2</sub>O (3) at 298.15 K</b>					
<b>100 w1</b>	<b>100 w2</b>	<b>100 w3</b>	<b>100 w1</b>	<b>100 w2</b>	<b>100 w3</b>
73.618	4.223	22.159	16.468	30.478	53.054
69.129	5.373	25.497	15.981	30.799	53.220
64.446	6.822	28.733	15.583	31.043	53.374
60.247	8.677	31.076	15.087	31.357	53.556
57.217	9.960	32.823	14.633	31.705	53.662
51.994	12.488	35.518	14.135	32.032	53.832
49.110	13.808	37.082	13.760	32.302	53.937
46.546	14.997	38.457	13.419	32.519	54.062
44.199	16.104	39.698	13.040	32.801	54.159
41.149	17.634	41.217	12.567	33.134	54.298
39.267	18.483	42.250	12.227	33.384	54.389
36.542	19.883	43.575	11.848	33.678	54.475
34.366	20.918	44.716	11.349	34.129	54.522
32.372	21.803	45.825	10.948	34.431	54.621
30.632	22.665	46.703	10.503	34.827	54.670
28.853	23.658	47.489	10.124	35.121	54.755
27.449	24.332	48.220	9.789	35.385	54.827
26.040	25.090	48.871	9.308	35.778	54.914
24.794	25.748	49.458	8.945	36.092	54.962
23.688	26.305	50.007	8.656	36.362	54.982
22.893	26.767	50.340	8.304	36.725	54.971
21.988	27.174	50.838	7.916	37.173	54.911
21.340	27.548	51.111	7.526	37.647	54.826
20.517	28.023	51.460	7.222	37.846	54.932
19.625	28.552	51.823	6.837	38.280	54.883
19.090	28.893	52.018	6.423	38.779	54.798
18.426	29.256	52.318	6.010	39.213	54.777
17.786	29.644	52.569	5.344	40.283	54.372
17.078	30.098	52.824	5.043	40.656	54.302

Table 6. 10 Experimental weight fraction data for  $[C_2C_1Py][C_4F_9SO_3] + \text{Sucrose}$  at  $25^\circ C$ .

<b><math>[C_2C_1Py][C_4F_9SO_3]</math> (1) + Sucrose (2) + <math>H_2O</math> (3) at 298.15 K</b>								
<b>100 w1</b>	<b>100 w2</b>	<b>100 w3</b>	<b>100 w1</b>	<b>100 w2</b>	<b>100 w3</b>	<b>100 w1</b>	<b>100 w2</b>	<b>100 w3</b>
59.584	7.529	32.887	25.672	19.426	54.902	12.735	25.749	61.516
58.004	7.974	34.023	25.166	19.599	55.235	12.296	26.054	61.650
56.590	8.395	35.015	24.343	19.921	55.737	11.923	26.294	61.783
54.869	9.036	36.095	23.745	20.158	56.097	11.765	26.434	61.802
52.926	9.743	37.330	23.211	20.382	56.407	11.211	26.928	61.861
51.244	10.142	38.613	22.907	20.533	56.560	10.620	27.558	61.821
48.997	10.923	40.080	22.408	20.736	56.856	10.097	27.937	61.966
48.030	11.335	40.635	21.905	20.953	57.142	9.239	28.434	62.326
46.841	11.767	41.392	21.569	21.075	57.355	8.664	28.788	62.548
45.787	12.063	42.149	21.102	21.277	57.621	8.142	29.498	62.360
44.503	12.564	42.933	20.688	21.439	57.873	7.729	29.742	62.529
42.835	13.209	43.955	20.266	21.659	58.075	7.388	30.207	62.404
41.352	13.648	45.000	19.869	21.846	58.285	6.945	30.821	62.234
39.926	14.190	45.885	19.594	21.968	58.438	6.496	31.510	61.994
39.002	14.475	46.523	19.153	22.169	58.677			
37.540	14.994	47.466	18.735	22.450	58.816			
36.459	15.306	48.235	18.150	22.708	59.142			
35.232	15.860	48.908	17.625	22.936	59.439			
34.738	16.045	49.216	17.102	23.209	59.689			
33.912	16.331	49.757	16.638	23.456	59.906			
32.814	16.765	50.421	16.170	23.706	60.124			
31.737	17.183	51.080	15.759	23.903	60.339			
30.952	17.370	51.679	15.308	24.234	60.458			
30.017	17.710	52.272	14.737	24.631	60.632			
29.187	18.046	52.767	14.364	24.787	60.849			
28.132	18.468	53.399	13.930	25.014	61.055			
27.656	18.611	53.733	13.511	25.226	61.263			
27.053	18.882	54.065	13.107	25.565	61.328			
26.395	19.110	54.495						



Table 6. 11 Experimental weight fraction data for  $[C_4C_1im][CF_3SO_3]$  + Glucose and  $[C_2C_1im][C_4F_9SO_3]$  + Glucose at 25°C.

<b><math>[C_4C_1Im][CF_3SO_3]</math> (1) + Glucose (2) + H<sub>2</sub>O (3) at 298.15 K</b>			<b><math>[C_2C_1Im][C_4F_9SO_3]</math> (1) + Glucose (2) + H<sub>2</sub>O (3) at 298.15 K</b>		
<b>100 w1</b>	<b>100 w2</b>	<b>100 w3</b>	<b>100 w1</b>	<b>100 w2</b>	<b>100 w3</b>
68.054	5.766	26.180	66.344	6.814	26.842
63.794	6.436	29.770	57.761	9.990	32.249
61.760	6.892	31.348	52.637	11.960	35.403
59.052	7.530	33.419	46.380	14.397	39.223
56.807	8.183	35.010	41.029	16.587	42.384
54.784	8.749	36.467	37.995	17.836	44.169
52.906	9.265	37.829	35.571	18.827	45.602
50.827	9.963	39.210	33.092	19.873	47.035
48.919	10.615	40.466	31.010	20.749	48.241
47.248	11.196	41.556	28.799	21.747	49.455
45.617	11.800	42.583	27.129	22.466	50.405
44.025	12.344	43.631	25.690	23.091	51.219
42.245	13.044	44.711	24.139	23.821	52.040
40.856	13.516	45.628	22.431	24.697	52.872
39.331	14.109	46.560	20.346	25.739	53.915
37.380	14.845	47.775	17.854	26.980	55.166
36.016	15.337	48.647	15.798	28.180	56.022
34.646	15.930	49.424	13.794	29.318	56.887
33.165	16.415	50.420	12.628	29.965	57.407
31.658	17.031	51.311	9.776	32.187	58.037
30.138	17.696	52.166			
29.200	18.108	52.692			
28.332	18.482	53.185			
27.430	18.906	53.664			
26.567	19.312	54.120			
25.769	19.722	54.510			
24.820	20.236	54.944			
23.539	20.938	55.523			
22.431	21.626	55.944			

Table 6. 12 Experimental weight fraction data for  $[C_2C_1Py][C_4F_9SO_3] + Glucose$  at 25°C.

<b><math>[C_2C_1Py][C_4F_9SO_3]</math> (1) + Glucose (2) + H<sub>2</sub>O (3) at 298.15 K</b>					
<b>100 w1</b>	<b>100 w2</b>	<b>100 w3</b>	<b>100 w1</b>	<b>100 w2</b>	<b>100 w3</b>
72.336	4.162	23.502	25.835	15.896	58.269
69.568	4.619	25.813	25.106	16.155	58.739
67.272	4.888	27.841	24.485	16.345	59.170
65.313	5.252	29.435	23.796	16.599	59.604
63.432	5.624	30.944	23.168	16.801	60.031
61.154	6.201	32.645	22.577	16.989	60.434
59.415	6.521	34.065	22.037	17.154	60.809
57.315	7.016	35.669	21.466	17.383	61.152
55.699	7.506	36.795	20.749	17.634	61.617
54.389	7.813	37.799	20.151	17.881	61.968
52.589	8.243	39.168	19.488	18.112	62.400
51.190	8.695	40.115	18.748	18.467	62.784
49.599	9.074	41.327	18.139	18.714	63.147
47.838	9.598	42.564	17.517	19.001	63.483
46.423	9.922	43.655	17.023	19.166	63.811
44.909	10.360	44.730	16.459	19.450	64.091
43.466	10.809	45.724	15.843	19.732	64.425
41.706	11.334	46.960	15.341	19.944	64.714
40.223	11.669	48.107	14.857	20.199	64.944
38.473	12.196	49.331	14.392	20.420	65.187
37.102	12.578	50.320	13.890	20.652	65.458
35.780	12.949	51.271	13.376	20.930	65.694
34.502	13.321	52.177	12.696	21.255	66.049
33.340	13.620	53.040	11.991	21.711	66.298
32.543	13.837	53.621	11.232	22.167	66.601
31.801	14.066	54.132	10.506	22.621	66.874
31.034	14.284	54.682	9.860	23.074	67.066
30.295	14.490	55.215	9.422	23.357	67.221
29.576	14.741	55.683	8.881	23.784	67.335
28.738	14.980	56.282	8.213	24.302	67.485
27.929	15.222	56.849	7.833	24.671	67.496
27.267	15.461	57.271	7.391	25.138	67.471
26.572	15.645	57.784			

Table 6. 13 Fitted parameters for experimental binodal data for the systems by Equation 1.

System	A	B	$10^{-5}$ C	R	$\frac{\sum(w_{IL}^{calc} - w_{IL}^{exp})^2}{n}$ <sup>a</sup>
[N <sub>11120H</sub> ]+K <sub>3</sub> PO <sub>4</sub>	92.1295	-0.2321	2.2899	0.9999	0.0208
[N <sub>11120H</sub> ][CF <sub>3</sub> SO <sub>3</sub> ] +K <sub>3</sub> PO <sub>4</sub>	119.6701	-0.3222	5.2558	0.9996	0.1408
[N <sub>11120H</sub> ][C <sub>4</sub> F <sub>9</sub> SO <sub>3</sub> ] +[N <sub>11120H</sub> ][H <sub>2</sub> PO <sub>4</sub> ]	118.0273	-0.1850	2.0142	1.0000	0.0158
[C <sub>2</sub> C <sub>1</sub> Im]Cl+K <sub>3</sub> PO <sub>4</sub>	69.6341	-0.2734	3.5902	1.0000	0.0049
[C <sub>2</sub> C <sub>1</sub> Im]Cl +K <sub>2</sub> HPO <sub>4</sub>	68.5192	-0.2654	2.14704	0.9996	0.1010
[C <sub>2</sub> C <sub>1</sub> Py]Br+K <sub>3</sub> PO <sub>4</sub>	77.4844	-0.3099	6.2839	0.9996	0.0696
[C <sub>2</sub> C <sub>1</sub> Im][C <sub>1</sub> CO <sub>2</sub> ] +K <sub>3</sub> PO <sub>4</sub>	63.3316	-0.2580	3.5894	0.9999	0.0071
[C <sub>2</sub> C <sub>1</sub> Im][CF <sub>3</sub> SO <sub>3</sub> ] +K <sub>3</sub> PO <sub>4</sub>	109.0697	-0.4563	14.8097	0.9987	0.3823
[C <sub>4</sub> C <sub>1</sub> Im][CF <sub>3</sub> SO <sub>3</sub> ]					
K <sub>3</sub> PO <sub>4</sub>	141.4550	-0.8693	14.6423	0.9981	0.5319
[N <sub>11120H</sub> ][H <sub>2</sub> PO <sub>4</sub> ]	168.7574	-0.3872	1.7182	0.9994	0.1993
Glucose	147.5752	-0.3249	3.8750	0.9998	0.0847
Sucrose	211.0421	-0.3999	0.89404	0.9995	0.0590
[C <sub>2</sub> C <sub>1</sub> Im][C <sub>4</sub> F <sub>9</sub> SO <sub>3</sub> ]					
K <sub>3</sub> PO <sub>4</sub>	104.2573	-1.1356	0	0.9985	0.4769
[N <sub>11120H</sub> ][H <sub>2</sub> PO <sub>4</sub> ]	194.4365	-1.0066	0	0.9858	3.1908
Glucose	119.5509	-0.2194	3.8754	1.0000	0.0207
Sucrose	111.0099	-0.2011	2.7949	1.0000	0.0295
[C <sub>2</sub> C <sub>1</sub> Py][C <sub>4</sub> F <sub>9</sub> SO <sub>3</sub> ]					
K <sub>3</sub> PO <sub>4</sub>	93.3170	-1.4606	0	0.9978	0.4938
[N <sub>11120H</sub> ][H <sub>2</sub> PO <sub>4</sub> ]	121.5894	-1.0615	0	0.9996	0.0332
Glucose	137.7044	-0.3157	10.0161	0.9998	0.1090
Sucrose	125.7863	-0.2619	5.8611	0.9998	0.0541

<sup>a</sup>  $w_{IL}^{calc}$  is the Ionic Liquid weight fraction calculated by Equation 1 and  $w_{IL}^{exp}$  is the Ionic Liquid experimental weight fraction and n represents the number of binodal points.

## 6.2. NMR $^1\text{H}$ and $^{17}\text{F}$ Spectra

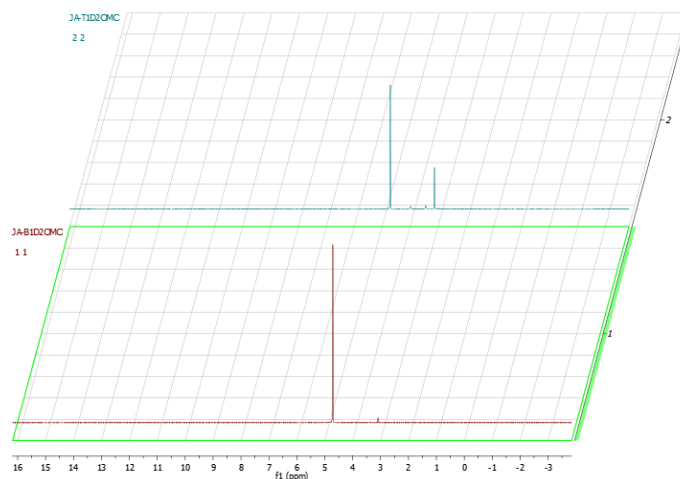


Figure 6. 1  $^1\text{H}$  NMR spectra of Top (up) and Bottom (down) phase of system  $30\%[\text{N}_{11120\text{H}}]\text{Cl} + 20\%\text{K}_3\text{PO}_4$  in  $\text{D}_2\text{O}$ .

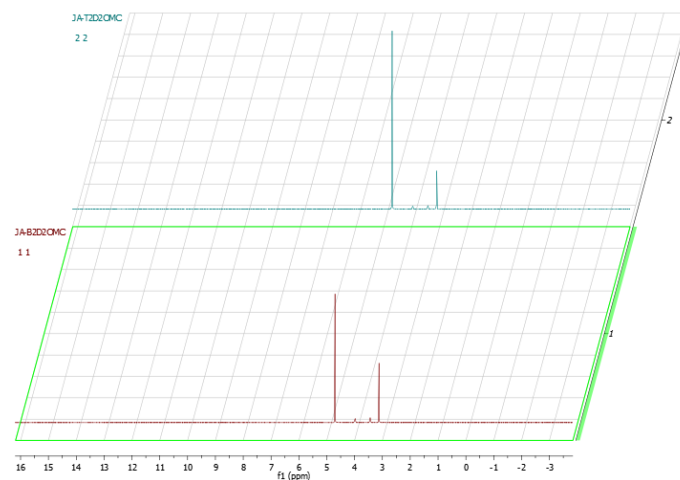


Figure 6. 2  $^1\text{H}$  NMR spectra of Top (up) and Bottom (down) phase of system  $30\%[\text{N}_{11120\text{H}}][\text{C}_4\text{F}_9\text{SO}_3] + 30\%[\text{N}_{11120\text{H}}][\text{H}_2\text{PO}_4]$  in  $\text{D}_2\text{O}$ .

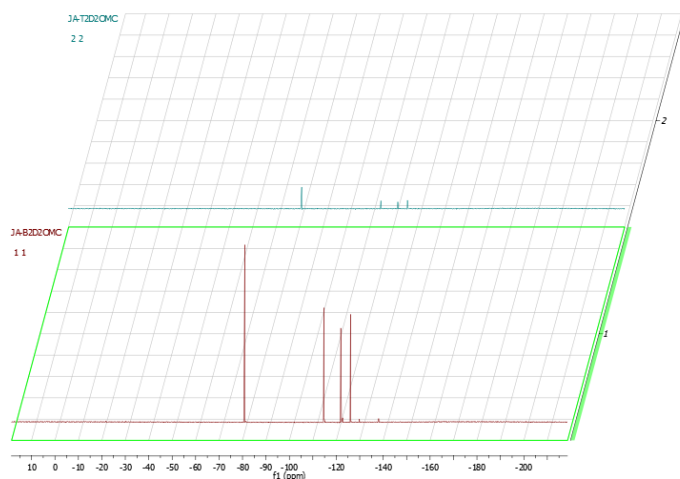


Figure 6. 3  $^{19}\text{F}$  NMR spectra of Top (up) and Bottom (down) phase of system  $30\%[\text{N}_{11120\text{H}}][\text{C}_4\text{F}_9\text{SO}_3] + 30\%[\text{N}_{11120\text{H}}][\text{H}_2\text{PO}_4]$  in  $\text{D}_2\text{O}$ .

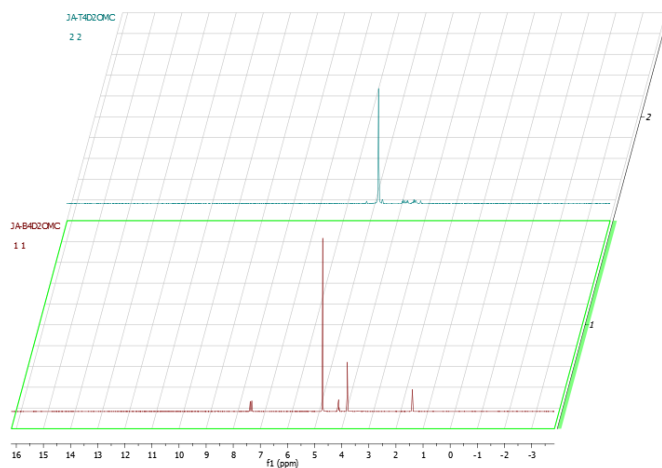


Figure 6.  $^1\text{H}$  NMR spectra of Top (up) and Bottom (down) phase of system  $30\%[\text{C}_2\text{C}_1\text{Im}][\text{C}_4\text{F}_9\text{SO}_3] + 25\%\text{Glucose}$  in  $\text{D}_2\text{O}$ .

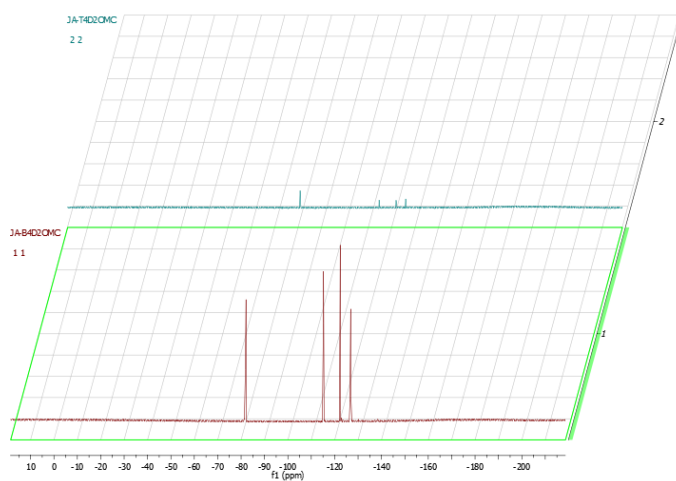


Figure 6.  $^{19}\text{F}$  NMR spectra of Top (up) and Bottom (down) phase of system  $30\%[\text{C}_2\text{C}_1\text{Im}][\text{C}_4\text{F}_9\text{SO}_3] + 25\%\text{Glucose}$  in  $\text{D}_2\text{O}$ .

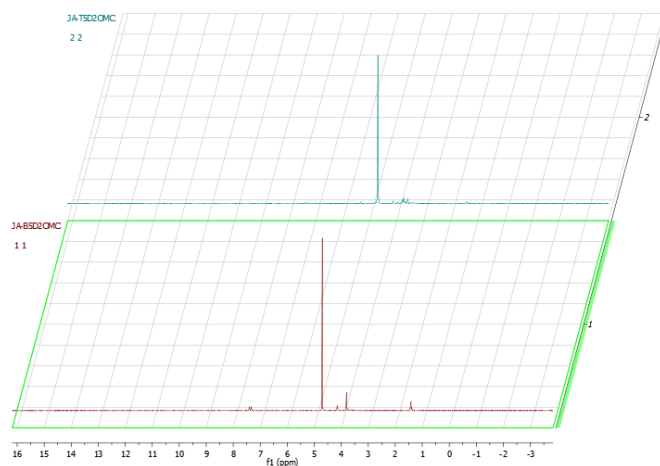


Figure 6.  $^1\text{H}$  NMR spectra of Top (up) and Bottom (down) phase of system  $30\%[\text{C}_2\text{C}_1\text{Im}][\text{C}_4\text{F}_9\text{SO}_3] + 25\%\text{Sucrose}$  in  $\text{D}_2\text{O}$ .

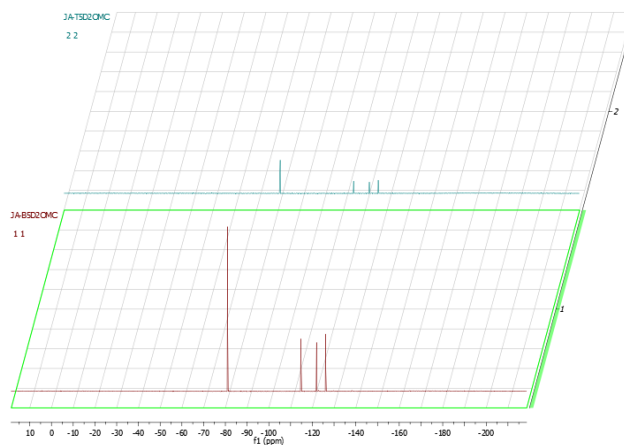


Figure 6.  ${}^7\text{F}$  NMR spectra of Top (up) and Bottom (down) phase of system  $30\%[\text{C}_2\text{C}_1\text{Im}][\text{C}_4\text{F}_9\text{SO}_3] + 25\%\text{Sucrose}$  in  $\text{D}_2\text{O}$ .

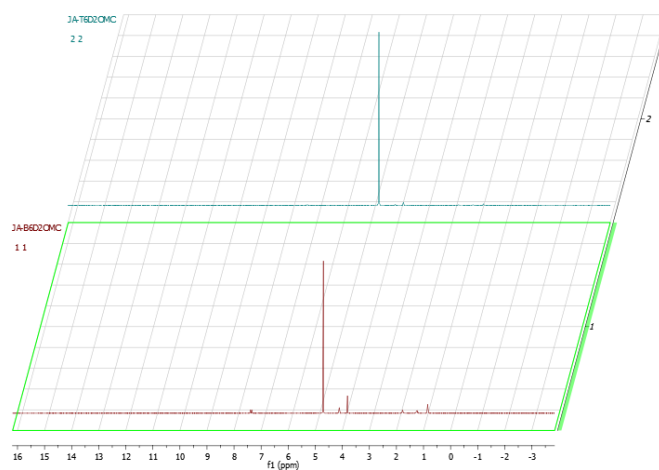


Figure 6.  ${}^1\text{H}$  NMR spectra of Top (up) and Bottom (down) phase of system  $30\%[\text{C}_4\text{C}_1\text{Im}][\text{CF}_3\text{SO}_3] + 5\%\text{K}_3\text{PO}_4$  in  $\text{D}_2\text{O}$ .

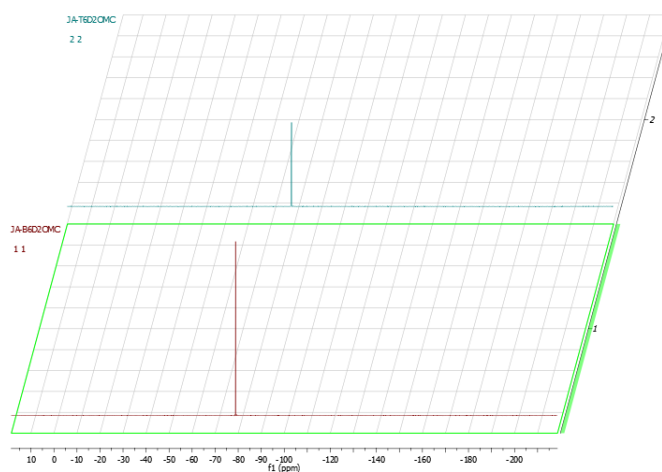


Figure 6.  ${}^{19}\text{F}$  NMR spectra of Top (up) and Bottom (down) phase of system  $30\%[\text{C}_4\text{C}_1\text{Im}][\text{CF}_3\text{SO}_3] + 5\%\text{K}_3\text{PO}_4$  in  $\text{D}_2\text{O}$ .

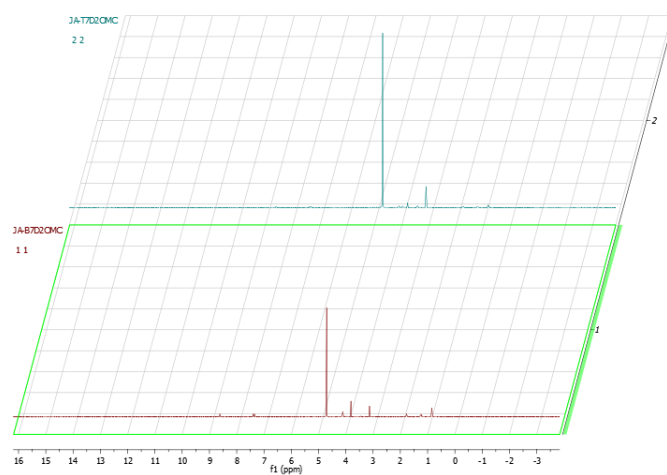


Figure 6. 10  $^1\text{H}$  NMR spectra of Top (up) and Bottom (down) phase of system  $30\%[\text{C}_4\text{C}_1\text{Im}][\text{CF}_3\text{SO}_3] + 20\%[\text{N}_{1112}\text{OH}][\text{H}_2\text{PO}_4]$  in  $\text{D}_2\text{O}$ .

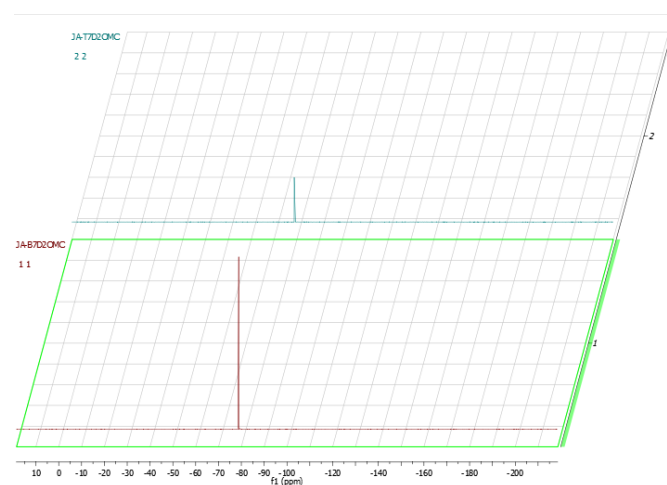


Figure 6. 11  $^{19}\text{F}$  NMR spectra of Top (up) and Bottom (down) phase of system  $30\%[\text{C}_4\text{C}_1\text{Im}][\text{CF}_3\text{SO}_3] + 20\%[\text{N}_{1112}\text{OH}][\text{H}_2\text{PO}_4]$  in  $\text{D}_2\text{O}$ .

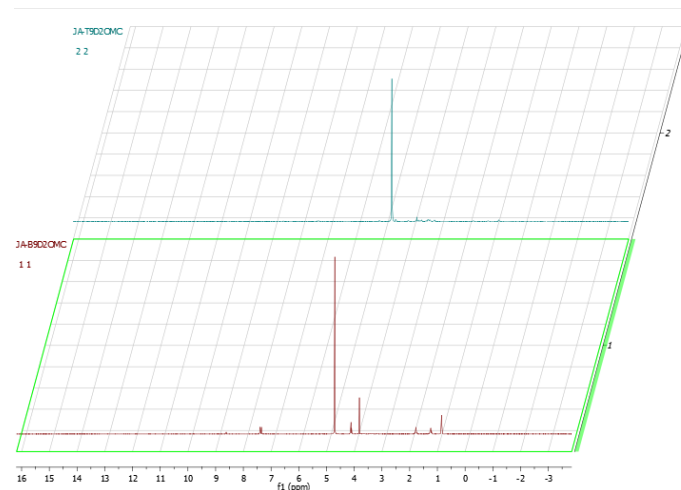


Figure 6. 12  $^1\text{H}$  NMR spectra of Top (up) and Bottom (down) phase of system  $30\%[\text{C}_4\text{C}_1\text{Im}][\text{CF}_3\text{SO}_3] + 25\%\text{Glucose}$  in  $\text{D}_2\text{O}$ .

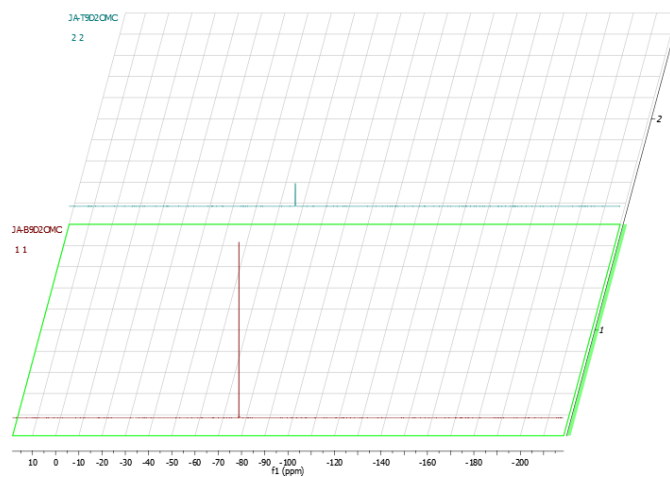


Figure 6. 13  $^{19}\text{F}$  NMR spectra of Top (up) and Bottom (down) phase of system 30% $[\text{C}_4\text{C}_1\text{Im}][\text{CF}_3\text{SO}_3]$  + 25%Glucose in  $\text{D}_2\text{O}$ .

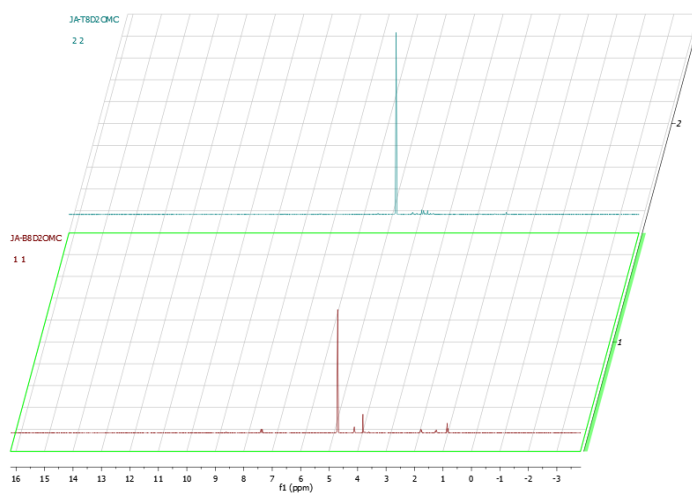


Figure 6. 14  $^1\text{H}$  NMR spectra of Top (up) and Bottom (down) phase of system 30% $[\text{C}_4\text{C}_1\text{Im}][\text{CF}_3\text{SO}_3]$  + 25%Sucrose in  $\text{D}_2\text{O}$ .

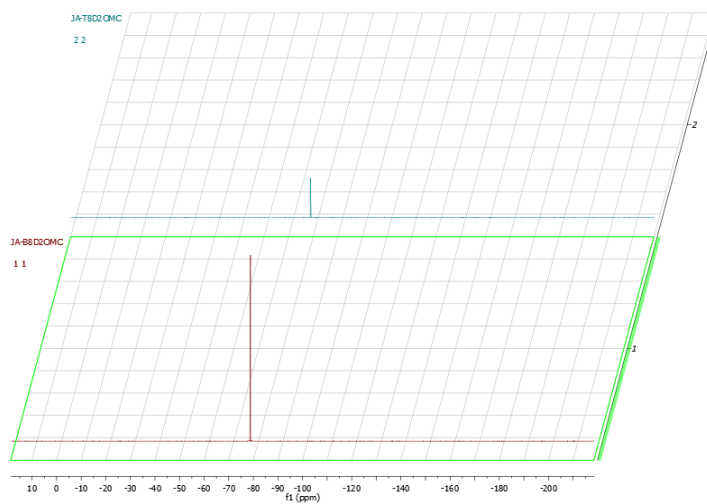


Figure 6. 15  $^{15}\text{F}$  NMR spectra of Top (up) and Bottom (down) phase of system 30% $[\text{C}_4\text{C}_1\text{Im}][\text{CF}_3\text{SO}_3]$  + 25%Sucrose in  $\text{D}_2\text{O}$



### 6.3. Phase Identification and pH

Table 6. 14 Characterization of Top and Bottom phases in terms of volume and pH.

System	Total Volume (mL)	Top Phase		Bottom Phase	
		Volume (mL)	pH	Volume (mL)	pH
30% wt [N <sub>11120H</sub> ]Cl + 20% wt K <sub>3</sub> PO <sub>4</sub>	1.6	1.15	14	0.45	14
30% wt [N <sub>11120H</sub> ][C <sub>4</sub> F <sub>9</sub> SO <sub>3</sub> ] + 30% wt [N <sub>11120H</sub> ][H <sub>2</sub> PO <sub>4</sub> ]	1.6	1	5	0.6	4-5
30% wt [C <sub>2</sub> C <sub>1</sub> Im]Cl + 15% wt K <sub>3</sub> PO <sub>4</sub>	1.7	1.2	14	0.5	14
30% wt [C <sub>2</sub> C <sub>1</sub> Py]Br + 15% wt K <sub>3</sub> PO <sub>4</sub>	1.7	1.15	14	0.55	14
30% wt [C <sub>2</sub> C <sub>1</sub> Im][C <sub>1</sub> CO <sub>2</sub> ] + 15% wt K <sub>3</sub> PO <sub>4</sub>	1.7	1.3	14	0.4	14
30% wt [C <sub>2</sub> C <sub>1</sub> Im][CF <sub>3</sub> SO <sub>3</sub> ] + 10% wt K <sub>3</sub> PO <sub>4</sub>	1.6	1	14	0.6	14
30% wt [C <sub>4</sub> C <sub>1</sub> Im][CF <sub>3</sub> SO <sub>3</sub> ] + 5% wt K <sub>3</sub> PO <sub>4</sub>	1.75	1.25	14	0.5	12
30% wt [C <sub>4</sub> C <sub>1</sub> Im][CF <sub>3</sub> SO <sub>3</sub> ] + 20% wt [N <sub>11120H</sub> ][H <sub>2</sub> PO <sub>4</sub> ]	1.75	1.4	5	0.35	5
30% wt [C <sub>4</sub> C <sub>1</sub> Im][CF <sub>3</sub> SO <sub>3</sub> ] + 25% wt Glucose	1.7	1.2	8	0.5	8
30% wt [C <sub>4</sub> C <sub>1</sub> Im][CF <sub>3</sub> SO <sub>3</sub> ] + 25% wt Sucrose	1.6	1.15	7-8	0.45	8
30% wt [C <sub>2</sub> C <sub>1</sub> Im][C <sub>4</sub> F <sub>9</sub> SO <sub>3</sub> ] + 2% wt K <sub>3</sub> PO <sub>4</sub>	1.75	0.9	13-14	0.85	12-13
30% wt [C <sub>2</sub> C <sub>1</sub> Im][C <sub>4</sub> F <sub>9</sub> SO <sub>3</sub> ] + 6% wt [N <sub>11120H</sub> ][H <sub>2</sub> PO <sub>4</sub> ]	1.7	0.9	4	0.8	4
30% wt [C <sub>2</sub> C <sub>1</sub> Im][C <sub>4</sub> F <sub>9</sub> SO <sub>3</sub> ] + 10% wt [N <sub>11120H</sub> ][H <sub>2</sub> PO <sub>4</sub> ]	1.75	1.1	4	0.65	4
30% wt [C <sub>2</sub> C <sub>1</sub> Im][C <sub>4</sub> F <sub>9</sub> SO <sub>3</sub> ] + 20% wt [N <sub>11120H</sub> ][H <sub>2</sub> PO <sub>4</sub> ]	1.7	1.2	4-5	0.5	4-5
30% wt [C <sub>2</sub> C <sub>1</sub> Im][C <sub>4</sub> F <sub>9</sub> SO <sub>3</sub> ] + 25% wt Glucose	1.65	1.15	8	0.5	8
30% wt [C <sub>2</sub> C <sub>1</sub> Im][C <sub>4</sub> F <sub>9</sub> SO <sub>3</sub> ] + 25% wt Sucrose	1.6	1.2	8	0.4	8
30% wt [C <sub>2</sub> C <sub>1</sub> Py][C <sub>4</sub> F <sub>9</sub> SO <sub>3</sub> ] + 2% wt K <sub>3</sub> PO <sub>4</sub>	1.75	1.05	13	0.7	12
30% wt [C <sub>2</sub> C <sub>1</sub> Py][C <sub>4</sub> F <sub>9</sub> SO <sub>3</sub> ] + 6% wt [N <sub>11120H</sub> ][H <sub>2</sub> PO <sub>4</sub> ]	1.75	1.15	4	0.6	4
30% wt [C <sub>2</sub> C <sub>1</sub> Py][C <sub>4</sub> F <sub>9</sub> SO <sub>3</sub> ] + 25% wt Glucose	1.6	1.1	7-8	0.5	7-8
30% wt [C <sub>2</sub> C <sub>1</sub> Py][C <sub>4</sub> F <sub>9</sub> SO <sub>3</sub> ] + 25% wt Sucrose	1.6	1.1	7-8	0.5	7-8

Table 6. 15 Phase identification for each system in terms of FIL/IL-rp and respective Salting-Out Agent (IS, Salt or CH) and respective identification methods.

System	Top Phase	Bottom Phase	Identification Method
30% wt [N <sub>11120H</sub> ]Cl + 20% wt K <sub>3</sub> PO <sub>4</sub>	IL-rp	IS-rp	NMR
30% wt [N <sub>11120H</sub> ][C <sub>4</sub> F <sub>9</sub> SO <sub>3</sub> ] + 30% wt [N <sub>11120H</sub> ][H <sub>2</sub> PO <sub>4</sub> ]	Salt-rp	FIL-rp	NMR
30% wt [C <sub>2</sub> C <sub>1</sub> Im]Cl + 15% wt K <sub>3</sub> PO <sub>4</sub>	IL-rp	IS-rp	pH and Color
30% wt [C <sub>2</sub> C <sub>1</sub> Py]Br + 15% wt K <sub>3</sub> PO <sub>4</sub>	IL-rp	IS-rp	Color
30% wt [C <sub>2</sub> C <sub>1</sub> Im][C <sub>1</sub> CO <sub>2</sub> ] + 15% wt K <sub>3</sub> PO <sub>4</sub>	IL-rp	IS-rp	pH
30% wt [C <sub>2</sub> C <sub>1</sub> Im][CF <sub>3</sub> SO <sub>3</sub> ] + 10% wt K <sub>3</sub> PO <sub>4</sub>	IS-rp	IL-rp	NMR
30% wt [C <sub>4</sub> C <sub>1</sub> Im][CF <sub>3</sub> SO <sub>3</sub> ] + 5% wt K <sub>3</sub> PO <sub>4</sub>	IS-rp	FIL-rp	pH and NMR
30% wt [C <sub>4</sub> C <sub>1</sub> Im][CF <sub>3</sub> SO <sub>3</sub> ] + 20% wt [N <sub>11120H</sub> ][H <sub>2</sub> PO <sub>4</sub> ]	Salt-rp	FIL-rp	NMR
30% wt [C <sub>4</sub> C <sub>1</sub> Im][CF <sub>3</sub> SO <sub>3</sub> ] + 25% wt Glucose	CH-rp	FIL-rp	NMR
30% wt [C <sub>4</sub> C <sub>1</sub> Im][CF <sub>3</sub> SO <sub>3</sub> ] + 25% wt Sucrose	CH-rp	FIL-rp	NMR
30% wt [C <sub>2</sub> C <sub>1</sub> Im][C <sub>4</sub> F <sub>9</sub> SO <sub>3</sub> ] + 2% wt K <sub>3</sub> PO <sub>4</sub>	IS-rp	FIL-rp	pH
30% wt [C <sub>2</sub> C <sub>1</sub> Im][C <sub>4</sub> F <sub>9</sub> SO <sub>3</sub> ] + 6% wt [N <sub>11120H</sub> ][H <sub>2</sub> PO <sub>4</sub> ]	Salt-rp	FIL-rp	NMR
30% wt [C <sub>2</sub> C <sub>1</sub> Im][C <sub>4</sub> F <sub>9</sub> SO <sub>3</sub> ] + 10% wt [N <sub>11120H</sub> ][H <sub>2</sub> PO <sub>4</sub> ]	Salt-rp	FIL-rp	NMR
30% wt [C <sub>2</sub> C <sub>1</sub> Im][C <sub>4</sub> F <sub>9</sub> SO <sub>3</sub> ] + 20% wt [N <sub>11120H</sub> ][H <sub>2</sub> PO <sub>4</sub> ]	Salt-rp	FIL-rp	NMR
30% wt [C <sub>2</sub> C <sub>1</sub> Im][C <sub>4</sub> F <sub>9</sub> SO <sub>3</sub> ] + 25% wt Glucose	CH-rp	FIL-rp	NMR
30% wt [C <sub>2</sub> C <sub>1</sub> Im][C <sub>4</sub> F <sub>9</sub> SO <sub>3</sub> ] + 25% wt Sucrose	CH-rp	FIL-rp	NMR
30% wt [C <sub>2</sub> C <sub>1</sub> Py][C <sub>4</sub> F <sub>9</sub> SO <sub>3</sub> ] + 2% wt K <sub>3</sub> PO <sub>4</sub>	IS-rp	FIL-rp	pH and Color
30% wt [C <sub>2</sub> C <sub>1</sub> Py][C <sub>4</sub> F <sub>9</sub> SO <sub>3</sub> ] + 6% wt [N <sub>11120H</sub> ][H <sub>2</sub> PO <sub>4</sub> ]	Salt-rp	FIL-rp	pH and Color
30% wt [C <sub>2</sub> C <sub>1</sub> Py][C <sub>4</sub> F <sub>9</sub> SO <sub>3</sub> ] + 25% wt Glucose	CH-rp	FIL-rp	pH and Color
30% wt [C <sub>2</sub> C <sub>1</sub> Py][C <sub>4</sub> F <sub>9</sub> SO <sub>3</sub> ] + 25% wt Sucrose	CH-rp	FIL-rp	pH and Color

#### 6.4. Lys Enzymatic Activity Screening

Table 6. 16 Relative Enzymatic Activity of Lysozyme in 0.2, 0.5 and 1.0 mg/mL at 5%-35% (w/w) of  $K_3PO_4$  in water.

Compound	Concentration Lys (mg/mL)	Compound Concentration (wt%)	EA relative %	Error (%)
$K_3PO_4$	0.2	5	94.4	8.0
		10	107.7	6.9
		15	142.9	9.1
		25	130.4	7.2
		35	103.7	13.9
	0.5	5	123.2	1.4
		10	133.6	6.2
		15	138.4	6.0
		25	107.5	11.0
		35	91.2	18.5
	1	5	113.8	1.8
		10	128.5	10.1
		15	132.7	2.1
		25	119.4	6.9
		35	149.6	5.4

Table 6. 17 Relative Enzymatic Activity of Lysozyme in 0.2, 0.5 and 1.0 mg/mL at 5%-35% (w/w) of  $K_2HPO_4$  in water.

Compound	Concentration Lys (mg/mL)	Compound Concentration (wt%)	EA relative %	Error (%)
$K_2HPO_4$	0.2	5	79.1	3.4
		10	91.3	3.7
		15	134.9	6.3
		25	137.2	3.2
		35	132.2	6.1
	0.5	5	113.3	3.9
		10	120.2	4.4
		15	124.7	2.4
		25	108.2	8.5
		35	121.9	5.7
	1	5	113.5	1.1
		10	118.4	0.8
		15	118.4	5.7
		25	119.5	5.0
		35	123.2	0.0

Table 6. 18 Relative Enzymatic Activity of Lysozyme in 0.2, 0.5 and 1.0 mg/mL at 5%-35% (w/w) of K<sub>3</sub>Citrate in water.

Compound	Concentration Lys (mg/mL)	Compound Concentration (wt%)	EA relative %	Error (%)
K <sub>3</sub> Citrate	0.2	5	119.1	1.9
		10	121.9	1.2
		15	124.9	7.8
		25	119.1	1.8
		35	90.9	4.9
	0.5	5	111.7	5.7
		10	122.2	1.4
		15	120.1	6.7
		25	110.1	3.9
		35	114.2	8.2
	1	5	119.7	4.9
		10	120.1	2.9
		15	124.2	5.4
		25	121.0	5.3
		35	124.7	8.1

Table 6. 19 Relative Enzymatic Activity of Lysozyme in 0.2, 0.5 and 1.0 mg/mL at 5%-35% (w/w) of Sucrose in water.

Compound	Concentration Lys (mg/mL)	Compound Concentration (wt%)	EA relative %	Error (%)
Sucrose	0.2	5%	109.8	1.9
		10%	110.5	0.9
		15%	106.8	3.0
		25%	106.0	1.2
		35%	105.7	1.8
	0.5	5%	97.3	3.4
		10%	95.1	1.2
		15%	85.6	1.7
		25%	119.0	4.4
		35%	119.2	5.5
	1	5%	104.2	3.7
		10%	97.3	0.0
		15%	90.2	5.3
		25%	98.6	0.0
		35%	94.9	9.3

Table 6. 20 Relative Enzymatic Activity of Lysozyme in 0.2, 0.5 and 1.0 mg/mL at 5%-35% (w/w) of [C<sub>2</sub>C<sub>1</sub>Im]Cl in water.

Compound	Concentration Lys (mg/mL)	Compound Concentration (wt%)	EA relative %	Error (%)
[C <sub>2</sub> C <sub>1</sub> Im] Cl	0.2	5%	107.0	2.5
		10%	112.0	6.2
		15%	104.6	3.7
		25%	108.4	3.6
		35%	113.2	3.6
	0.5	5%	110.8	2.1
		10%	91.9	9.4
		15%	108.9	3.2
		25%	101.3	8.2
		35%	113.4	4.6
	1	5%	130.7	4.2
		10%	152.6	7.3
		15%	144.3	7.3
		25%	138.5	8.3
		35%	144.2	5.7

Table 6. 21 Relative Enzymatic Activity of Lysozyme in 0.2, 0.5 and 1.0 mg/mL at 5%-35% (w/w) of [C<sub>2</sub>C<sub>1</sub>Im][C<sub>1</sub>CO<sub>2</sub>] in water.

Compound	Concentration Lys (mg/mL)	Compound Concentration (wt%)	EA relative %	Error (%)
[C <sub>2</sub> C <sub>1</sub> Im] [C <sub>1</sub> CO <sub>2</sub> ]	0.2	5%	103.8	3.3
		10%	108.4	5.7
		15%	113.2	2.6
		25%	107.6	3.6
		35%	107.8	2.5
	0.5	5%	105.4	3.2
		10%	108.4	5.0
		15%	110.6	10.2
		25%	107.6	9.6
		35%	114.7	5.1
	1	5%	108.2	2.8
		10%	108.9	6.9
		15%	110.0	2.9
		25%	111.8	4.3
		35%	112.5	4.5

Table 6. 22 Relative Enzymatic Activity of Lysozyme in 0.2, 0.5 and 1.0 mg/mL at 5%-35% (w/w) of [C<sub>2</sub>C<sub>1</sub>Im][CF<sub>3</sub>SO<sub>3</sub>] in water.

Compound	Concentration Lys (mg/mL)	Compound Concentration (wt%)	EA relative %	Error (%)
[C <sub>2</sub> C <sub>1</sub> Im] [CF <sub>3</sub> SO <sub>3</sub> ]	0.2	5%	108.5	5.4
		10%	120.4	3.0
		15%	106.1	4.0
		25%	122.8	1.5
		35%	111.7	2.3
	0.5	5%	113.0	3.7
		10%	106.6	1.1
		15%	108.3	4.5
		25%	108.3	5.9
		35%	109.0	2.1
	1	5%	105.5	5.2
		10%	106.3	4.3
		15%	105.5	4.3
		25%	107.0	2.3
		35%	105.5	1.2

Table 6. 23 Relative Enzymatic Activity of Lysozyme in 0.2, 0.5 and 1.0 mg/mL at 5%-35% (w/w) of [C<sub>2</sub>C<sub>1</sub>Im][C<sub>4</sub>F<sub>9</sub>SO<sub>3</sub>] in water.

Compound	Concentration Lys (mg/mL)	Compound Concentration (wt%)	EA relative %	Error (%)
[C <sub>2</sub> C <sub>1</sub> Im] [C <sub>4</sub> F <sub>9</sub> SO <sub>3</sub> ]	0.2	5%	113.9	2.2
		10%	117.4	2.7
		15%	120.9	2.0
		25%	117.7	0.6
		35%	124.0	2.3
	0.5	5%	110.6	3.6
		10%	104.3	1.1
		15%	106.0	4.4
		25%	106.0	5.8
		35%	106.7	2.1
	1	5%	100.2	0.6
		10%	106.0	4.6
		15%	116.4	2.1
		25%	116.5	1.0
		35%	125.7	0.0

Table 6. 24 Relative Enzymatic Activity of Lysozyme in 0.2, 0.5 and 1.0 mg/mL at 5%-35% (w/w) of [C<sub>4</sub>C<sub>1</sub>Im]Cl in water.

Compound	Concentration Lys (mg/mL)	Compound Concentration (wt%)	EA relative %	Error (%)
[C <sub>4</sub> C <sub>1</sub> Im]Cl	0.2	5%	112.4	2.8
		10%	110.2	2.2
		15%	106.8	5.8
		25%	85.7	3.7
		35%	119.9	1.2
	0.5	5%	107.9	1.0
		10%	105.8	6.1
		15%	103.8	2.9
		25%	101.7	7.1
		35%	112.7	4.5
	1	5%	124.9	10.8
		10%	137.6	3.4
		15%	143.0	0.0
		25%	138.0	3.0
		35%	148.0	6.4

Table 6. 25 Relative Enzymatic Activity of Lysozyme in 0.2, 0.5 and 1.0 mg/mL at 5%-35% (w/w) of [C<sub>2</sub>C<sub>1</sub>Py]Br in water.

Compound	Concentration Lys (mg/mL)	Compound Concentration (wt%)	EA relative %	Error (%)
[C <sub>2</sub> C <sub>1</sub> Py]Br	0.2	5%	112.5	3.0
		10%	114.5	6.2
		15%	96.8	6.2
		25%	103.0	1.2
		35%	116.1	3.2
	0.5	5%	104.6	1.1
		10%	108.7	3.2
		15%	109.8	1.3
		25%	90.0	4.7
		35%	116.3	2.6
	1	5%	136.5	3.0
		10%	135.4	7.1
		15%	147.7	11.9
		25%	154.9	3.7
		35%	140.5	5.1

Table 6. 26 Relative Enzymatic Activity of Lysozyme in 0.2, 0.5 and 1.0 mg/mL at 5%-35% (w/w) of  $[N_{11120H}][H_2PO_4]$  in water.

Compound	Concentration Lys (mg/mL)	Compound Concentration (wt%)	EA relative %	Error (%)
$[N_{11120H}][Cl]$	0.2	5%	101.6	1.7
		10%	110.3	3.7
		15%	114.0	0.9
		25%	115.2	3.3
		35%	110.1	1.0
	0.5	5%	102.1	1.4
		10%	106.0	1.1
		15%	108.3	1.4
		25%	109.1	3.8
		35%	106.6	2.4
	1	5%	110.1	3.0
		10%	121.7	12.2
		15%	103.8	5.0
		25%	107.4	3.3
		35%	106.0	9.9



## 6.5. UV-VIS Calibration

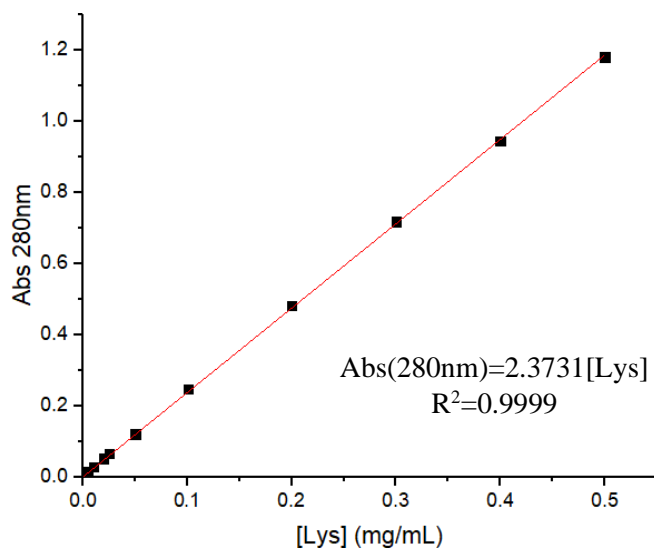


Figure 6. 16 Calibration curve for Lysozyme in water at 280 nm for 0.4mL Quartz cuvette.

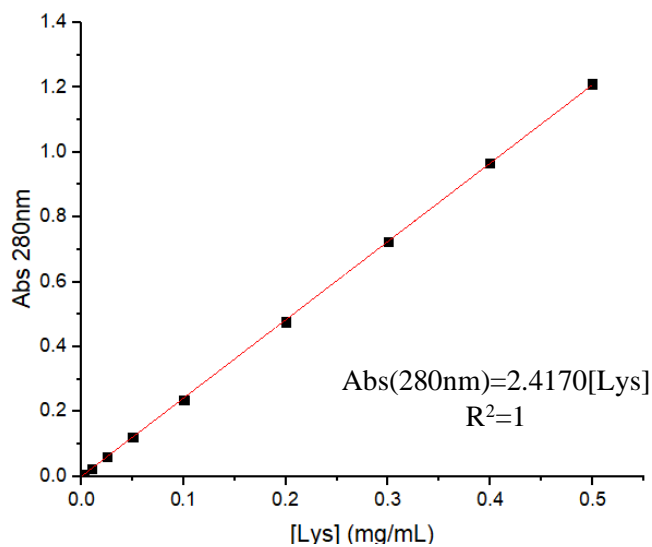


Figure 6. 17 Calibration curve for Lysozyme in water at 280 nm for 4mL Quartz cuvette.

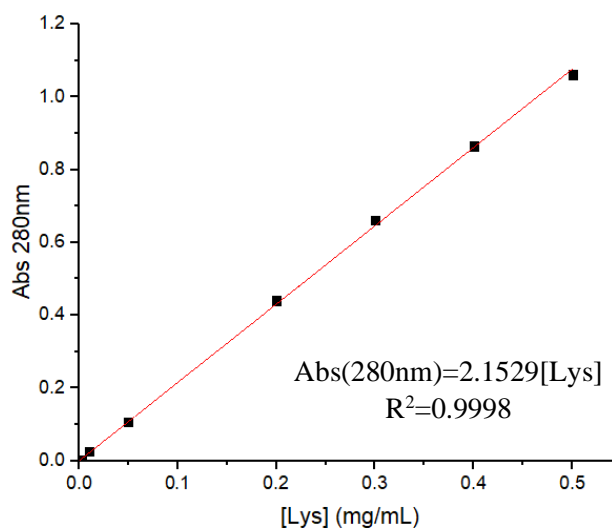


Figure 6. 18 Calibration curve for Lysozyme in 0.1%  $K_3PO_4$  at 280 nm for 0.4 mL Quartz cuvette.

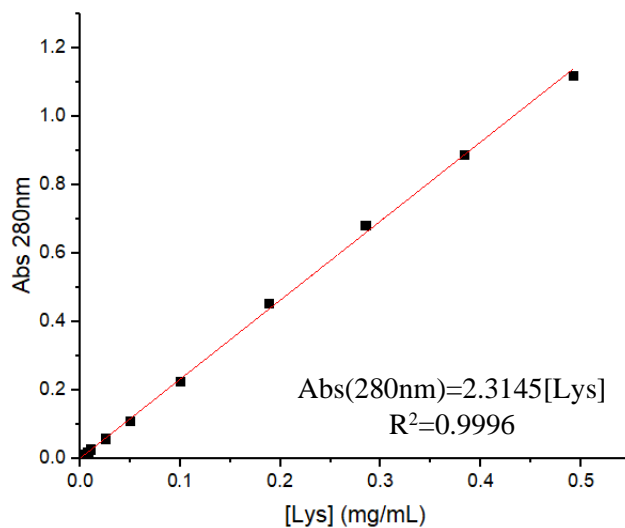


Figure 6. 19 Calibration curve for Lysozyme in 0.1%  $K_3PO_4$  at 280nm for 4.0 mL Quartz cuvette.

## 6.6. Extraction Efficiency

Table 6. 27 Extraction efficiency by UV-Vis spectroscopy detection methodology for all systems available.

System	UV-Vis			
	[Lys] <sub>IL/FIL-rp</sub> (mg/mL)	[Lys] <sub>Salt/CH-rp</sub> (mg/mL)	EE (%)	Error (%)
30% wt [N <sub>11120H</sub> ]Cl + 20% wt K <sub>3</sub> PO <sub>4</sub>	-	0.0625 <sup>a</sup>	98.25	-
30% wt [N <sub>11120H</sub> ][C <sub>4</sub> F <sub>9</sub> SO <sub>3</sub> ] + 30% wt [N <sub>11120H</sub> ][H <sub>2</sub> PO <sub>4</sub> ]	-	1.1978	25.23	-
30% wt [C <sub>2</sub> C <sub>1</sub> Im]Cl + 15% wt K <sub>3</sub> PO <sub>4</sub>	0.7770	-	56.51	-
30% wt [C <sub>2</sub> C <sub>1</sub> Py]Br + 15% wt K <sub>3</sub> PO <sub>4</sub>	*	*	-	-
30% wt [C <sub>2</sub> C <sub>1</sub> Im][C <sub>1</sub> CO <sub>2</sub> ] + 15% wt K <sub>3</sub> PO <sub>4</sub>	1.1547	-	78.05	-
30% wt [C <sub>2</sub> C <sub>1</sub> Im][CF <sub>3</sub> SO <sub>3</sub> ] + 10% wt K <sub>3</sub> PO <sub>4</sub>	-	0.0625 <sup>a</sup>	97.11	-
30% wt [C <sub>4</sub> C <sub>1</sub> Im][CF <sub>3</sub> SO <sub>3</sub> ] + 5% wt K <sub>3</sub> PO <sub>4</sub>	-	-	-	-
30% wt [C <sub>4</sub> C <sub>1</sub> Im][CF <sub>3</sub> SO <sub>3</sub> ] + 20% wt [N <sub>11120H</sub> ][H <sub>2</sub> PO <sub>4</sub> ]	-	1.0767	13.84	-
30% wt [C <sub>4</sub> C <sub>1</sub> Im][CF <sub>3</sub> SO <sub>3</sub> ] + 25% wt Glucose	-	1.1460	19.21	17.5
30% wt [C <sub>4</sub> C <sub>1</sub> Im][CF <sub>3</sub> SO <sub>3</sub> ] + 25% wt Sucrose	-	0.9749	29.99	-
30% wt [C <sub>2</sub> C <sub>1</sub> Im][C <sub>4</sub> F <sub>9</sub> SO <sub>3</sub> ] + 2% wt K <sub>3</sub> PO <sub>4</sub>	-	0.0625 <sup>a</sup>	96.25	-
30% wt [C <sub>2</sub> C <sub>1</sub> Im][C <sub>4</sub> F <sub>9</sub> SO <sub>3</sub> ] + 6% wt [N <sub>11120H</sub> ][H <sub>2</sub> PO <sub>4</sub> ]	-	0.0625 <sup>a</sup>	96.69	-
30% wt [C <sub>2</sub> C <sub>1</sub> Im][C <sub>4</sub> F <sub>9</sub> SO <sub>3</sub> ] + 10% wt [N <sub>11120H</sub> ][H <sub>2</sub> PO <sub>4</sub> ]	-	0.0313	98.04	0
30% wt [C <sub>2</sub> C <sub>1</sub> Im][C <sub>4</sub> F <sub>9</sub> SO <sub>3</sub> ] + 20% wt [N <sub>11120H</sub> ][H <sub>2</sub> PO <sub>4</sub> ]	-	1.1238	20.82	3.2
30% wt [C <sub>2</sub> C <sub>1</sub> Im][C <sub>4</sub> F <sub>9</sub> SO <sub>3</sub> ] + 25% wt Glucose	(2.7847) <sup>b</sup>	0.0189	98.68	-
30% wt [C <sub>2</sub> C <sub>1</sub> Im][C <sub>4</sub> F <sub>9</sub> SO <sub>3</sub> ] + 25% wt Sucrose	(1.8397) <sup>b</sup>	0.0156	98.83	-
30% wt [C <sub>2</sub> C <sub>1</sub> py][C <sub>4</sub> F <sub>9</sub> SO <sub>3</sub> ] + 2% wt K <sub>3</sub> PO <sub>4</sub>	*	*	-	-
30% wt [C <sub>2</sub> C <sub>1</sub> py][C <sub>4</sub> F <sub>9</sub> SO <sub>3</sub> ] + 6% wt [N <sub>11120H</sub> ][H <sub>2</sub> PO <sub>4</sub> ]	*	*	-	-
30% wt [C <sub>2</sub> C <sub>1</sub> py][C <sub>4</sub> F <sub>9</sub> SO <sub>3</sub> ] + 25% wt Glucose	*	*	-	-
30% wt [C <sub>2</sub> C <sub>1</sub> py][C <sub>4</sub> F <sub>9</sub> SO <sub>3</sub> ] + 25% wt Sucrose	*	*	-	-

\* Pyridinium-based IL/FIL peak at 280nm. Impossible to quantify Lys in both phases by UV-Vis methodology.

<sup>a</sup> concentration calculated from detection limit

<sup>b</sup> concentration with qualitative character.

Table 6. 28 Extraction efficiency by BCA assay detection methodology for all systems available.

System	BCA			
	[Lys] <sub>IL/FIL-rp</sub> (mg/mL)	[Lys] <sub>Salt/CH-rp</sub> (mg/mL)	EE (%)	Error (%)
30% wt [N <sub>11120H</sub> ]Cl + 20% wt K <sub>3</sub> PO <sub>4</sub>	-	-	-	-
30% wt [N <sub>11120H</sub> ][C <sub>4</sub> F <sub>9</sub> SO <sub>3</sub> ] + 30% wt [N <sub>11120H</sub> ][H <sub>2</sub> PO <sub>4</sub> ]	1.1795	0.9008	44.00	1.20
30% wt [C <sub>2</sub> C <sub>1</sub> Im]Cl + 15% wt K <sub>3</sub> PO <sub>4</sub>	2.0280 <sup>b</sup>	-	>100	-
30% wt [C <sub>2</sub> C <sub>1</sub> Py]Br + 15% wt K <sub>3</sub> PO <sub>4</sub>	1.3172	-	88.95	-
30% wt [C <sub>2</sub> C <sub>1</sub> Im][C <sub>1</sub> CO <sub>2</sub> ] + 15% wt K <sub>3</sub> PO <sub>4</sub>	1.2937	-	87.44	7.76
30% wt [C <sub>2</sub> C <sub>1</sub> Im][CF <sub>3</sub> SO <sub>3</sub> ] + 10% wt K <sub>3</sub> PO <sub>4</sub>	2.0654	-	77.43	-
30% wt [C <sub>4</sub> C <sub>1</sub> Im][CF <sub>3</sub> SO <sub>3</sub> ] + 5% wt K <sub>3</sub> PO <sub>4</sub>	1.9787	-	56.52	-
30% wt [C <sub>4</sub> C <sub>1</sub> Im][CF <sub>3</sub> SO <sub>3</sub> ] + 20% wt [N <sub>11120H</sub> ][H <sub>2</sub> PO <sub>4</sub> ]	-	1.2410	0.78	-
30% wt [C <sub>4</sub> C <sub>1</sub> Im][CF <sub>3</sub> SO <sub>3</sub> ] + 25% wt Glucose	1.1071	a	32.51	-
30% wt [C <sub>4</sub> C <sub>1</sub> Im][CF <sub>3</sub> SO <sub>3</sub> ] + 25% wt Sucrose	0.5349	1.2282	15.01	0.00
30% wt [C <sub>2</sub> C <sub>1</sub> Im][C <sub>4</sub> F <sub>9</sub> SO <sub>3</sub> ] + 2% wt K <sub>3</sub> PO <sub>4</sub>	1.8833	-	91.55	-
30% wt [C <sub>2</sub> C <sub>1</sub> Im][C <sub>4</sub> F <sub>9</sub> SO <sub>3</sub> ] + 6% wt [N <sub>11120H</sub> ][H <sub>2</sub> PO <sub>4</sub> ]	3.0529 <sup>b</sup>	< Detection Limit	>100	-
30% wt [C <sub>2</sub> C <sub>1</sub> Im][C <sub>4</sub> F <sub>9</sub> SO <sub>3</sub> ] + 10% wt [N <sub>11120H</sub> ][H <sub>2</sub> PO <sub>4</sub> ]	2.3744	< Detection Limit	88.21	-
30% wt [C <sub>2</sub> C <sub>1</sub> Im][C <sub>4</sub> F <sub>9</sub> SO <sub>3</sub> ] + 20% wt [N <sub>11120H</sub> ][H <sub>2</sub> PO <sub>4</sub> ]	0.1182	1.5651	3.47	28.80
30% wt [C <sub>2</sub> C <sub>1</sub> Im][C <sub>4</sub> F <sub>9</sub> SO <sub>3</sub> ] + 25% wt Glucose	a	a	-	-
30% wt [C <sub>2</sub> C <sub>1</sub> Im][C <sub>4</sub> F <sub>9</sub> SO <sub>3</sub> ] + 25% wt Sucrose	2.7265	a	68.08	-
30% wt [C <sub>2</sub> C <sub>1</sub> py][C <sub>4</sub> F <sub>9</sub> SO <sub>3</sub> ] + 2% wt K <sub>3</sub> PO <sub>4</sub>	2.3520	-	94.05	-
30% wt [C <sub>2</sub> C <sub>1</sub> py][C <sub>4</sub> F <sub>9</sub> SO <sub>3</sub> ] + 6% wt [N <sub>11120H</sub> ][H <sub>2</sub> PO <sub>4</sub> ]	2.4813	-	85.06	-
30% wt [C <sub>2</sub> C <sub>1</sub> py][C <sub>4</sub> F <sub>9</sub> SO <sub>3</sub> ] + 25% wt Glucose	a	a	-	-
30% wt [C <sub>2</sub> C <sub>1</sub> py][C <sub>4</sub> F <sub>9</sub> SO <sub>3</sub> ] + 25% wt Sucrose	1.6848	a	52.69	-

<sup>a</sup> interference of carbohydrates on assay – not possible to quantify Lys in the respective phase.

<sup>b</sup> concentration with qualitative character.

Table 6. 29 Extraction efficiency by  $\mu$ BCA assay detection methodology for all systems available.

System	$\mu$ BCA			
	[Lys] <sub>IL/FIL-rp</sub> (mg/mL)	[Lys] <sub>Salt/CH-rp</sub> (mg/mL)	EE (%)	Error (%)
30% wt [C <sub>2</sub> C <sub>1</sub> Im]Cl + 15% wt K <sub>3</sub> PO <sub>4</sub>	1.6298 <sup>b</sup>	-	>100	-
30% wt [C <sub>2</sub> C <sub>1</sub> Im][C <sub>1</sub> CO <sub>2</sub> ] + 15% wt K <sub>3</sub> PO <sub>4</sub>	2.4623 <sup>b</sup>	-	>100	-
30% wt [C <sub>4</sub> C <sub>1</sub> Im][CF <sub>3</sub> SO <sub>3</sub> ] + 25% wt Glucose	1.1754	a	34.51	-
30% wt [C <sub>2</sub> C <sub>1</sub> Im][C <sub>4</sub> F <sub>9</sub> SO <sub>3</sub> ] + 20% wt [N <sub>1112</sub> OH][H <sub>2</sub> PO <sub>4</sub> ]	0.0792	1.3021	2.33	-

<sup>a</sup> Interference of Carbohydrates on assay – not possible to quantify Lys.

<sup>b</sup> concentration with qualitative character.

Table 6. 30 Extraction efficiency by Coomassie assay detection methodology for all systems available.

System	Coomassie			
	[Lys] <sub>IL/FIL-rp</sub> (mg/mL)	[Lys] <sub>Salt/CH-rp</sub> (mg/mL)	EE (%)	Error (%)
30% wt [N <sub>1112</sub> OH][C <sub>4</sub> F <sub>9</sub> SO <sub>3</sub> ] + 30% wt [N <sub>1112</sub> OH][H <sub>2</sub> PO <sub>4</sub> ]	0.3051	0.7486	11.34	-
30% wt [C <sub>4</sub> C <sub>1</sub> Im][CF <sub>3</sub> SO <sub>3</sub> ] + 25% wt Glucose	a	a	-	-
30% wt [C <sub>4</sub> C <sub>1</sub> Im][CF <sub>3</sub> SO <sub>3</sub> ] + 25% wt Sucrose	0.3600	1.9230	10.12	48.21
30% wt [C <sub>2</sub> C <sub>1</sub> Im][C <sub>4</sub> F <sub>9</sub> SO <sub>3</sub> ] + 25% wt Glucose	a	a	-	-
30% wt [C <sub>2</sub> C <sub>1</sub> Im][C <sub>4</sub> F <sub>9</sub> SO <sub>3</sub> ] + 25% wt Sucrose	3.1148	a	77.79	5.79

<sup>a</sup> Interference of Carbohydrates on assay – not possible to quantify Lys.

## 6.7. Nano-DSC

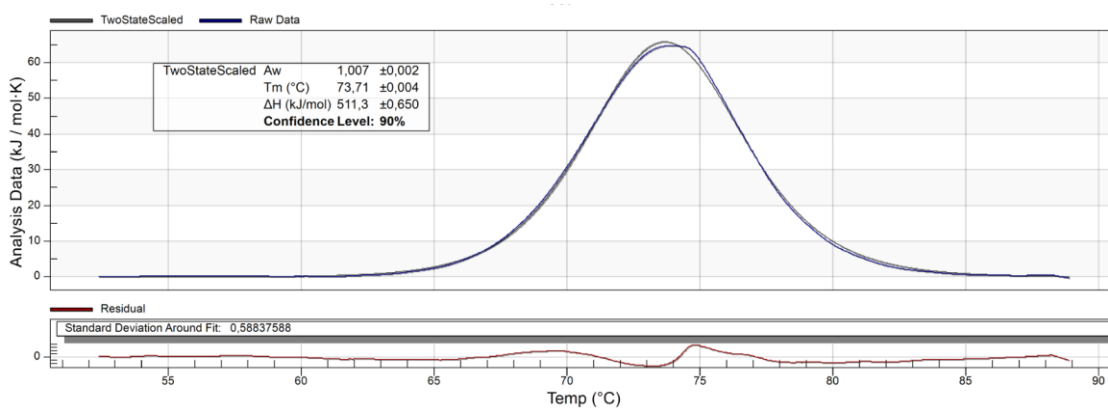


Figure 6. 20 Thermogram of Lys 1mg/mL in water.

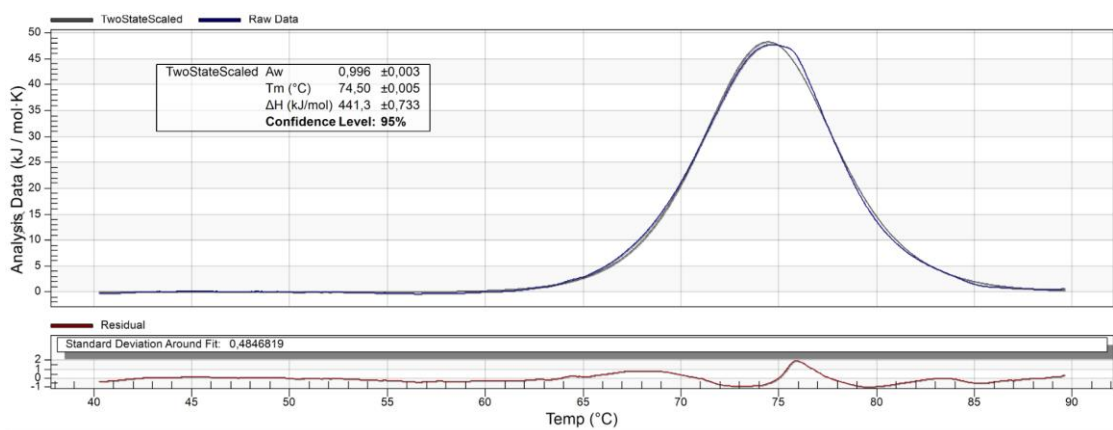


Figure 6. 21 Thermogram of Lys 1mg/mL in 0.1mM [C<sub>4</sub>C<sub>1</sub>Im][CF<sub>3</sub>SO<sub>3</sub>].

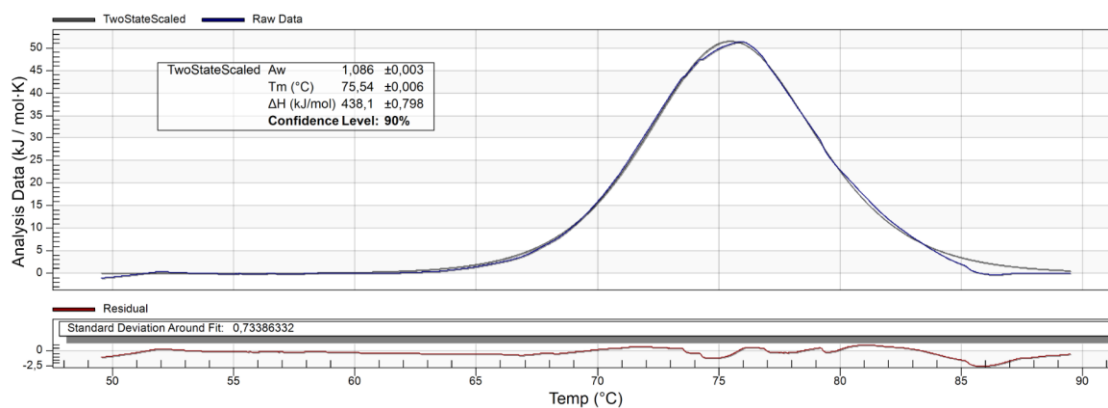


Figure 6. 22 Thermogram of Lys 1mg/mL in 1.0 mM [C<sub>4</sub>C<sub>1</sub>Im][CF<sub>3</sub>SO<sub>3</sub>].

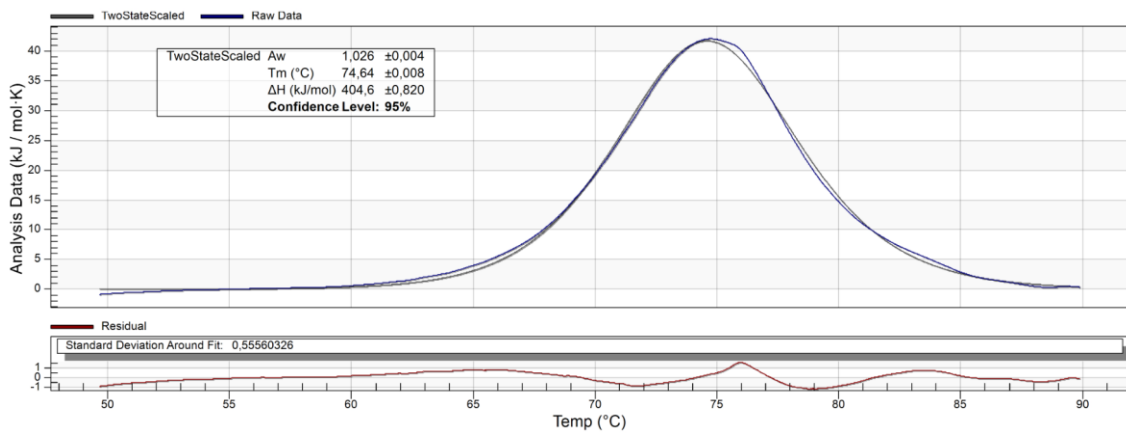


Figure 6. 23 Thermogram of Lys 1mg/mL in 5.0 mM  $[C_4C_1Im][CF_3SO_3]$ .

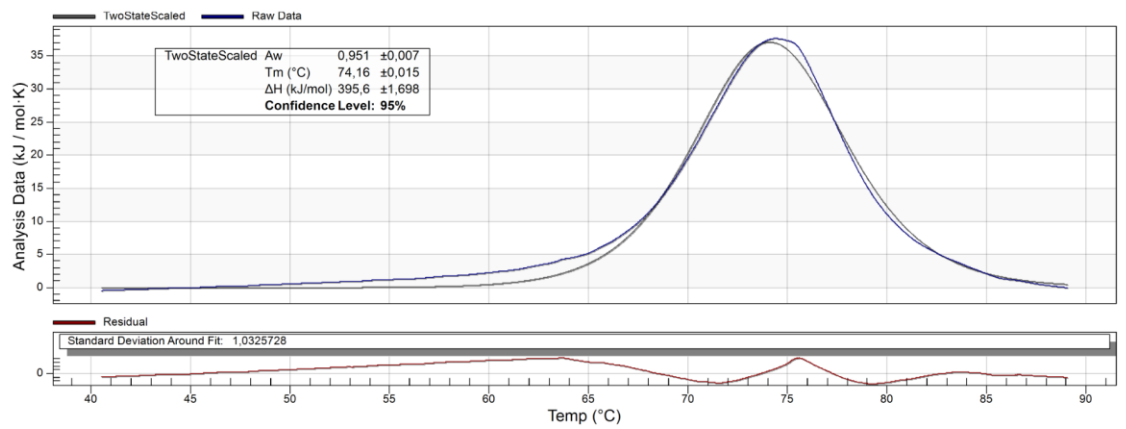


Figure 6. 24 Thermogram of Lys 1mg/mL in 10.0 mM  $[C_4C_1Im][CF_3SO_3]$ .

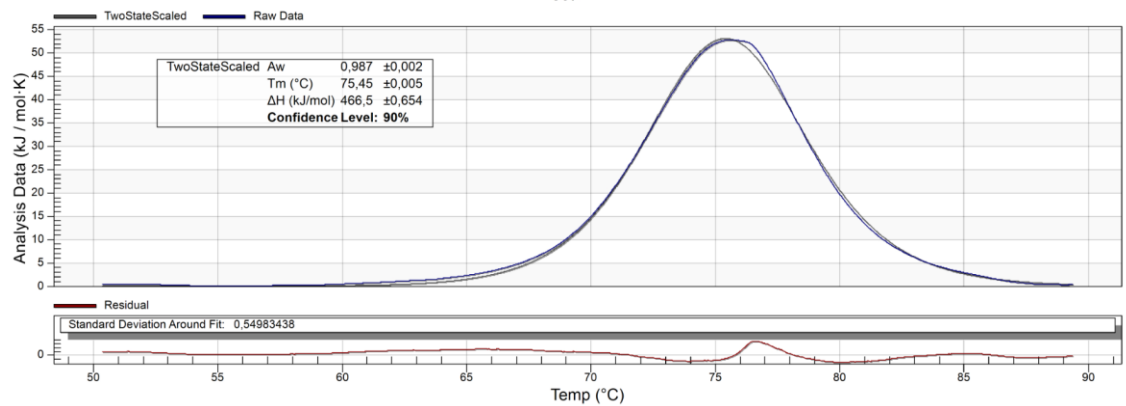


Figure 6. 25 Thermogram of Lys 1mg/mL in 0.1 mM  $[C_2C_1Im][C_4F_9SO_3]$ .

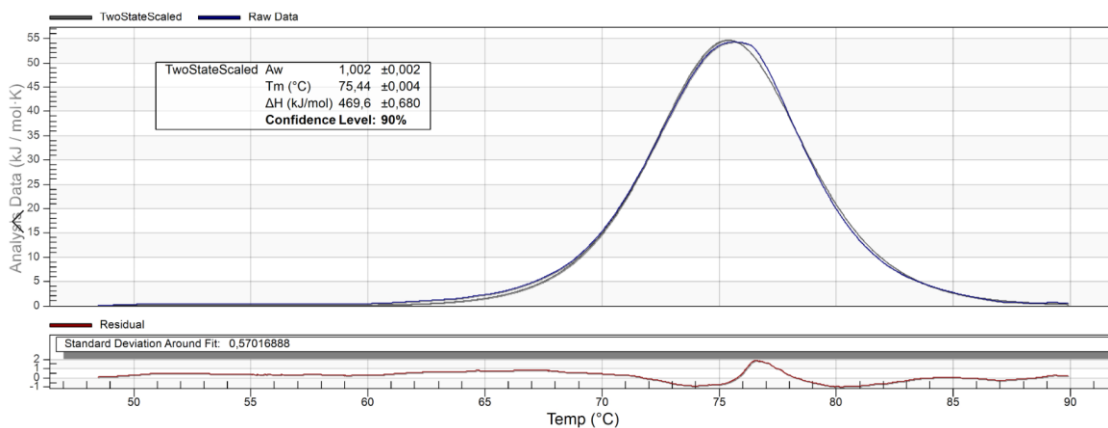


Figure 6. 26 Thermogram of Lys 1mg/mL in 1.0 mM [C<sub>2</sub>C<sub>1</sub>Im][C<sub>4</sub>F<sub>9</sub>SO<sub>3</sub>].

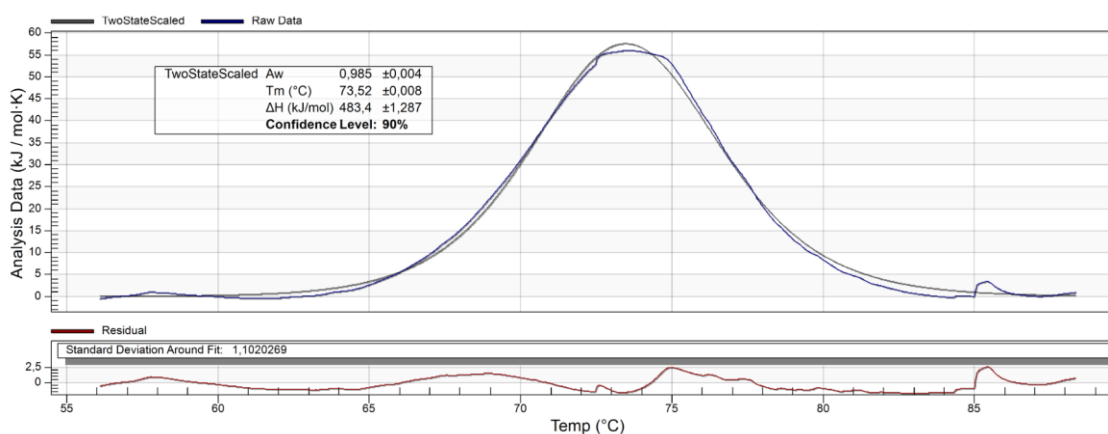


Figure 6. 27 Thermogram of Lys 1mg/mL in 5.0 mM [C<sub>2</sub>C<sub>1</sub>Im][C<sub>4</sub>F<sub>9</sub>SO<sub>3</sub>].

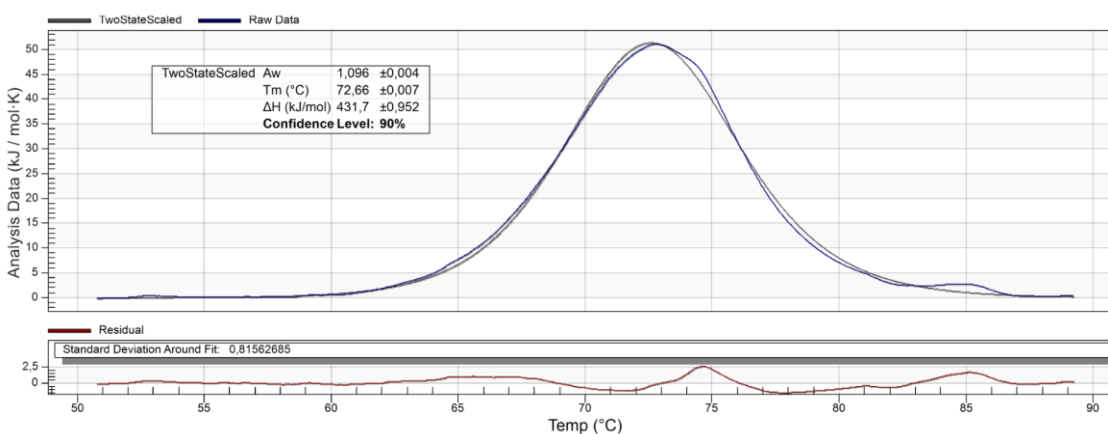


Figure 6. 28 Thermogram of Lys 1mg/mL in 10.0 mM [C<sub>2</sub>C<sub>1</sub>Im][C<sub>4</sub>F<sub>9</sub>SO<sub>3</sub>].



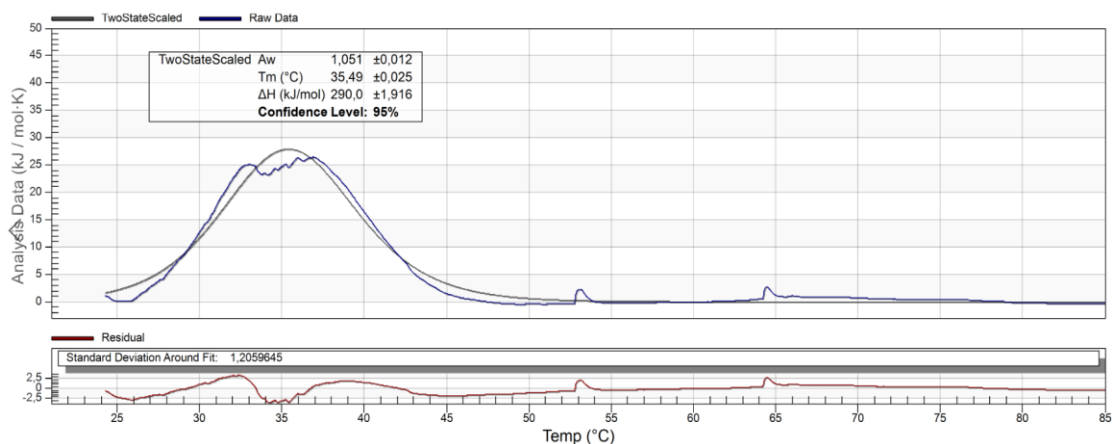


Figure 6. 29 Thermogram of Lys 1mg/mL in  $[C_4C_1Im][CF_3SO_3]$ -rich phase (30% $[C_4C_1Im][CF_3SO_3]$ +25%Glucose) – with stirring.

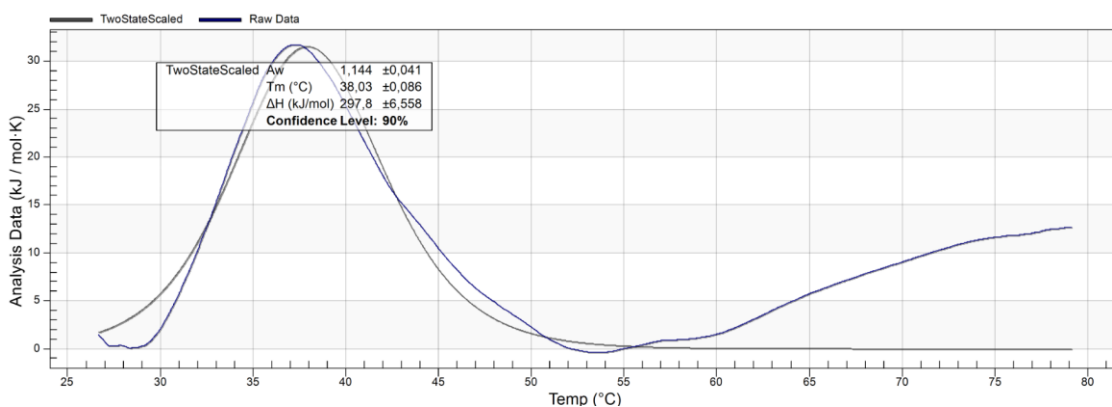


Figure 6. 30 Thermogram of Lys 1mg/mL in  $[C_4C_1Im][CF_3SO_3]$ -rich phase (30% $[C_4C_1Im][CF_3SO_3]$ +25%Glucose) – without stirring.

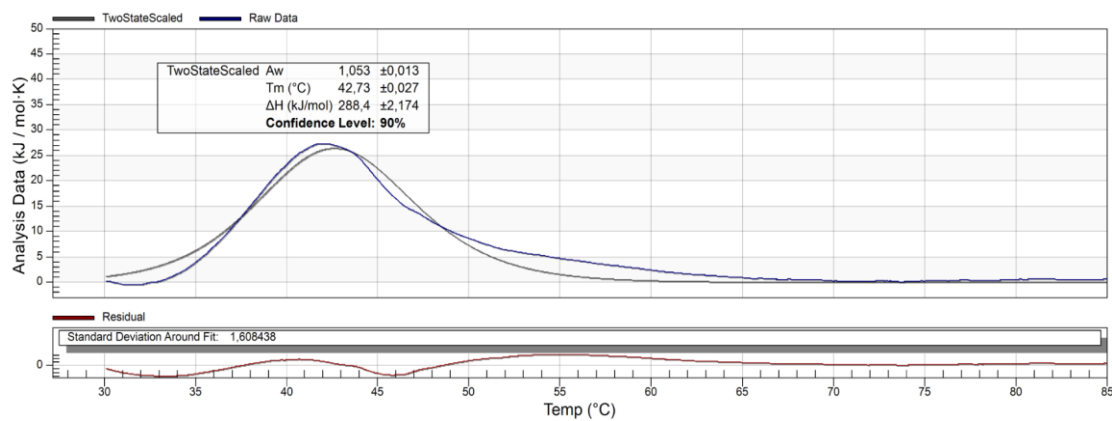


Figure 6. 31 Thermogram of Lys 1mg/mL in  $[C_2C_1Im][C_4F_9SO_3]$ -rich phase (30% $[C_2C_1Im][C_4F_9SO_3]$ +25%Glucose) – with stirring.

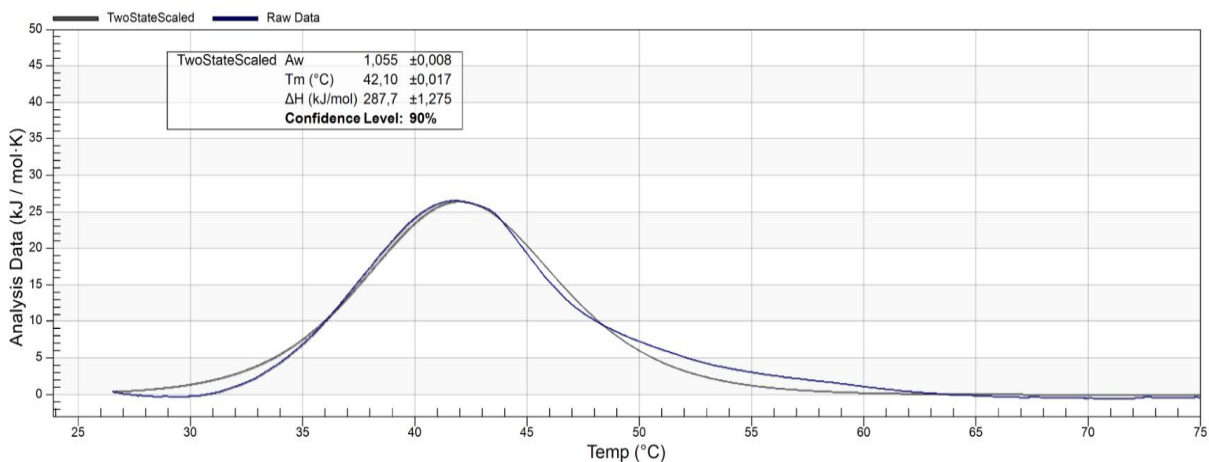


Figure 6. 32 Thermogram of Lys 1mg/mL in  $[C_2C_1Im][C_4F_9SO_3]$ -rich phase (30% $[C_2C_1Im][C_4F_9SO_3]$ +25%Glucose) – without stirring.

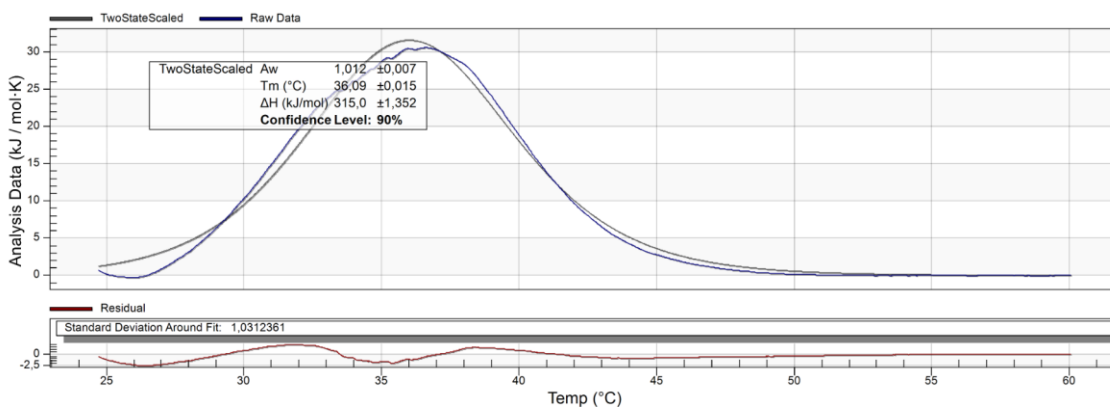


Figure 6. 33 Thermogram of partitioned Lys in  $[C_4C_1Im][CF_3SO_3]$ -rich phase (30% $[C_4C_1Im][CF_3SO_3]$ +25%Glucose) – without stirring.

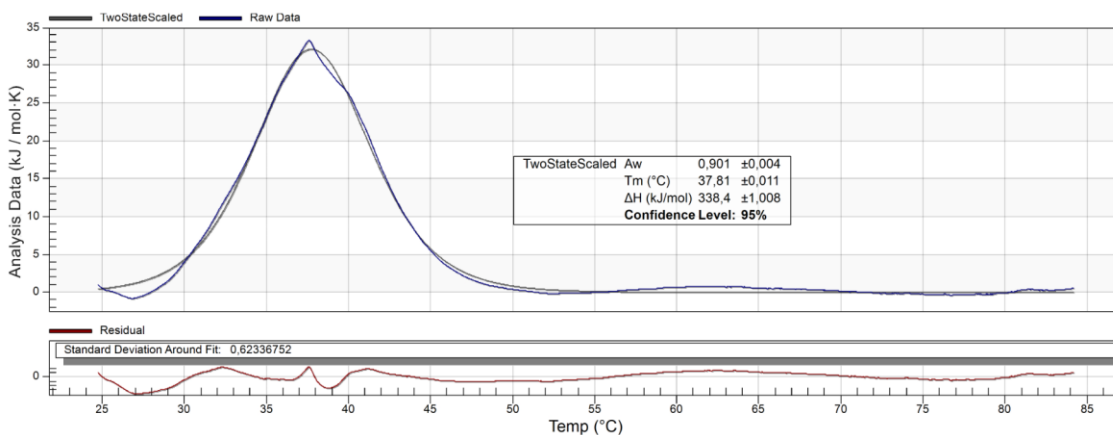


Figure 6. 34 Thermogram of partitioned Lys in  $[C_4C_1Im][CF_3SO_3]$ -rich phase (30% $[C_4C_1Im][CF_3SO_3]$ +25%Sucrose) – without stirring.

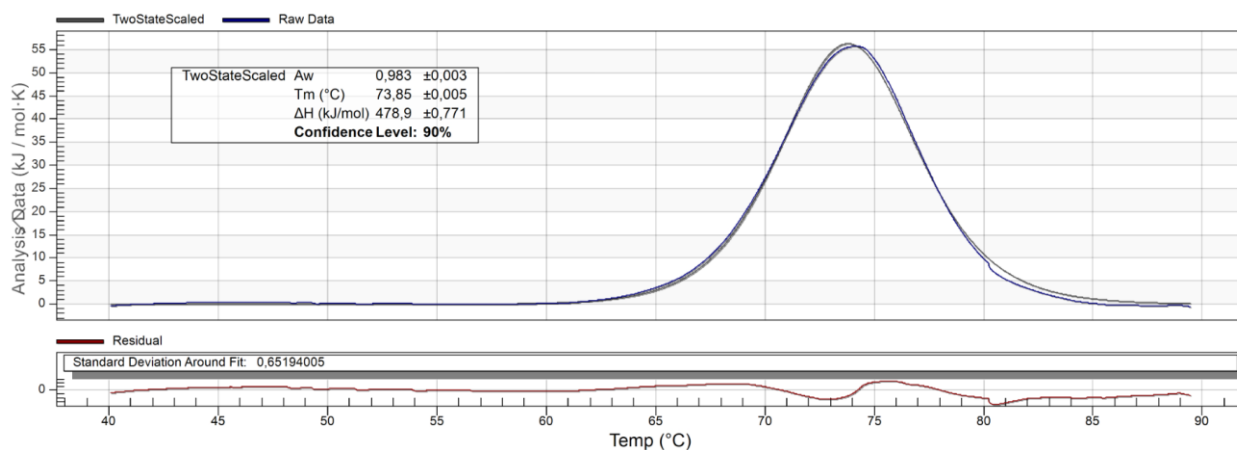


Figure 6. 35 Thermogram of Lys 3mg/mL in water.

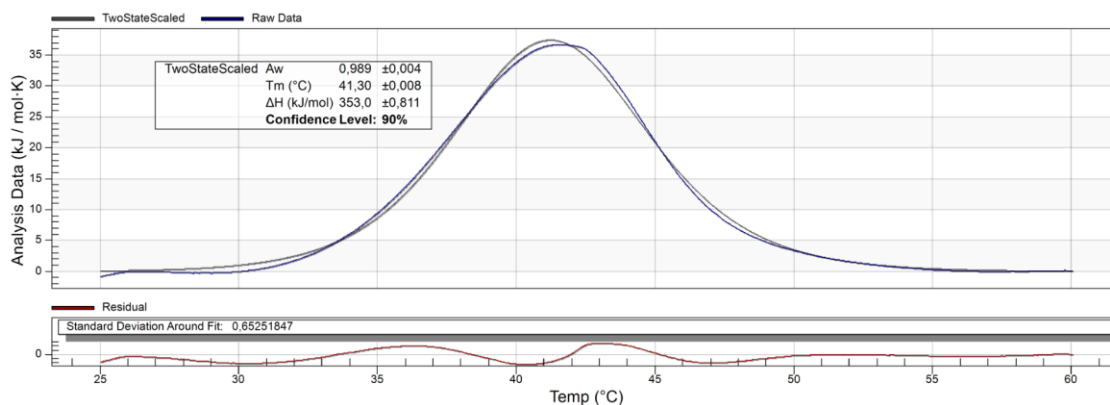


Figure 6. 36 Thermogram of partitioned Lys in  $[C_2C_1Im][C_4F_9SO_3]$ -rich phase (30%  $[C_2C_1Im][C_4F_9SO_3]$  + 25% Glucose) – without stirring.

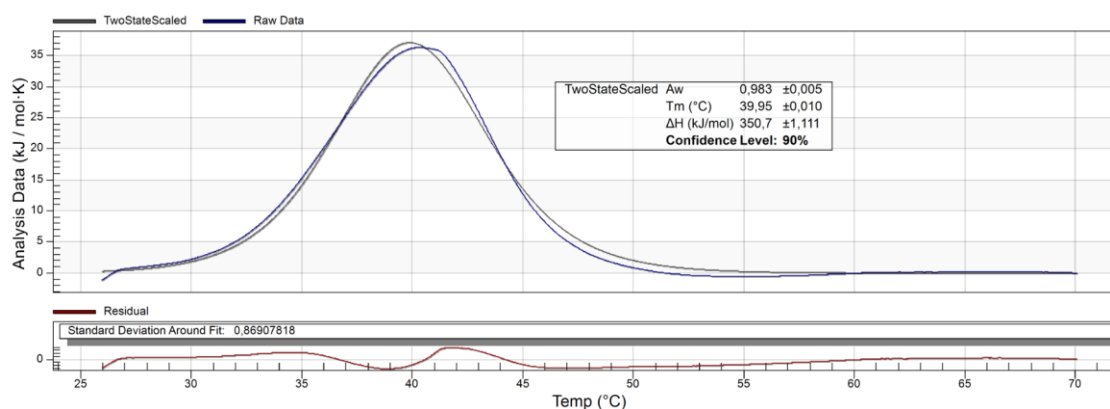


Figure 6. 37 Thermogram of partitioned Lys in  $[C_2C_1Im][C_4F_9SO_3]$ -rich phase (30%  $[C_2C_1Im][C_4F_9SO_3]$  + 25% Sucrose) – without stirring.